

FRACTIONATION REQUIREMENTS FOR PRODUCING ANHYDROUS AMMONIA
FROM AMMONIA-WATER VAPOR SYSTEMS

M. C. Fields

United States Steel Corporation
Applied Research Laboratory
Monroeville, Pennsylvania

In several proposed processes^{1, 2, 3}* for recovering ammonia from coke-oven gas, the ammonia is absorbed in an aqueous solution that is subsequently stripped of its absorbed ammonia. If the stripping operation is performed at the normal boiling point of the solution and if the absorbent used is nonvolatile, the vapors leaving the stripper will consist of ammonia and water at a pressure of 1 atmosphere. These vapors can then be fractionated to produce anhydrous ammonia. If the fractionation is performed at the original pressure of the vapor feed, the anhydrous ammonia leaving the top of the column would have to be condensed in a refrigerated condenser. The cost of refrigeration will in general make this process economically unattractive. Consequently, the anhydrous ammonia must be produced in a column operating at a pressure high enough to permit ordinary cooling water to be used to condense the ammonia. At 200 pounds per square inch gauge (psig), ammonia condenses at approximately 100 F. With 80 F cooling water, the ammonia leaving the top of a fractionator operating at 200 psig can be condensed in a condenser with a 10 F approach and a 10 F cooling-water rise. Since the bottoms of the fractionator will be essentially pure water, open steam would be used and, consequently, steam at approximately 200 psig could be used. (Steam at this pressure is available at many plants.) The fractionation of the vapor feeds, initially at a pressure of 1 atmosphere, in a column operating at 200 psig is complicated by the desire to utilize as much as possible of the latent heat already contained by the vapor but at the same time to avoid high vapor-compression costs. Several alternative methods of accomplishing the fractionation are possible. These are shown in Figures 1 through 4.

Method I

As shown in Figure 1 the vapor, originally saturated at 14.7 psia, is compressed directly into a fractionator operating at 200 psig to produce an anhydrous-ammonia overhead. The vapor leaving the compressor at 200 psig is assumed to be essentially saturated at that pressure.

Method II

As shown in Figure 2 the vapor, originally at 14.7 psia, is first compressed only to a pressure where it can be readily condensed, and the condensate is then pumped into a fractionator operating at 200 psig to produce an anhydrous-ammonia overhead. The condensate, pumped to 200 psig, is heated to its saturation temperature with the fractionator bottoms prior to entering the fractionator. It was chosen to compress the vapor to a pressure where the bubble point of its condensate is 100 F so that the vapor could be condensed with cooling water available at 80 F in a condenser with a 10 F approach and a 10 F cooling-water rise. As a limiting case of this method, the vapor can be totally condensed without any compression if it is lean enough. At a pressure of 1 atmosphere, a vapor containing 25 per cent ammonia can be totally condensed at about 100 F. Consequently, vapors containing 25 per cent ammonia or less would be totally condensed without any compression.

* See references.

Method III

As shown in Figure 3 the vapor is first partially condensed at atmospheric pressure, and the liquid and vapor portions are then pumped and compressed, respectively, into a fractionator operating at 200 psig to produce an anhydrous-ammonia overhead. The liquid portion, pumped to 200 psig, is heated to its saturation temperature with the fractionator bottoms prior to entering the fractionator. The vapor portion leaving the compressor at 200 psig is assumed to be essentially saturated at that pressure. It was chosen to partially condense the vapor to a point where the dew point of the vapor and the bubble point of the resulting condensate are 100 F so that the vapor could be partially condensed with cooling water available at 80 F in a condenser with a 10 F approach and a 10 F cooling-water rise. At a pressure of 1 atmosphere, a condensate containing 25 per cent ammonia has a bubble point of 100F. The vapor leaving the partial condenser will be in equilibrium with this condensate and will therefore contain 95.4 per cent ammonia. As one limiting case of this method, if the vapor contains 25 per cent ammonia or less, the partial condenser becomes a total condenser and no subsequent compression is required. Consequently, for feeds containing less than 25 per cent ammonia, this method degenerates to the same limiting case as did Method II. As the other limiting case of this method, if the vapor contains 95.4 per cent ammonia or more, no partial condensation will occur, and this method will become identical with Method I.

Method IV

Instead of totally condensing feeds containing less than 25 per cent ammonia, as would be done in Methods II and III, or simply compressing them into the fractionator, as would be done in Method I, these lean feeds can first be fed to a prefractionator operating at atmospheric pressure and enriched to a composition that can still be totally condensed with ordinary cooling water as shown in Figure 4. The condensed overhead leaving this first unit would then be pumped to 200 psig and heated to its saturation temperature with the water waste from the high-pressure fractionator. It would then enter the high-pressure fractionator to produce an anhydrous-ammonia overhead.

In all four methods, the vapor feeds at 1 atmosphere were assumed to be at their saturation temperature. Actually, the ammonia-water vapors arising from the stripping of an ammonia-absorbing solution will often be somewhat superheated with respect to their own dew point. However, the small amount of additional sensible heat will have very little effect upon the condenser and fractionator calculations. The results of calculations, which are to follow, were all based upon producing 1 ton per hour of anhydrous ammonia.

In analyzing the four fractionation methods described to ascertain in what range of feed composition each is most economical, only utility costs were considered and capital costs were ignored. This could be done for two reasons. First, the capital costs were relatively small compared with the utility costs. For example, the cost of the fractionating tower in terms of its depreciation and maintenance per year, did not amount to more than 5 per cent of the utility costs per year. Also, the capital costs involved in all of the different methods, especially in the ranges of feed compositions where the methods were competitive with each other, were roughly equal, and thus were not a significant factor in evaluating the different methods.

The power requirements for compressing the vapor feed, originally at 0 psig, into a fractionator at 200 psig producing one ton per hour of anhydrous ammonia are shown in Figure 5. Since the ammonia content of the feed is essentially 1 ton per hour at all feed compositions, the feed rate will increase and the power requirements will correspondingly rise as the feed becomes increasingly lean in ammonia.

Shown in Figure 6 are the power requirements for compressing the vapor feed, initially at 1 atmosphere, to a pressure where the bubble point of its condensate is 100 F, and the cooling-water duty for subsequently condensing the partially compressed vapor. As seen, the pressure to which the vapor must be compressed becomes greater as the ammonia content of the feed increases above 25 per cent ammonia. This factor causes the power requirement to increase as the feed becomes increasingly rich in ammonia. However, at the same time the feed rate decreases and this factor causes the power requirement to decrease. Consequently, the curve showing the horsepower requirements will go through a maximum as seen in the slide. Vapor feeds containing 25 per cent ammonia or less can be totally condensed at a pressure of 1 atmosphere and, hence, the horsepower requirements reduce to the negligibly small amounts needed to pump the condensate into the tower. The cooling-water duty for condensing the vapor decreases as the feed becomes increasingly rich in ammonia, owing to the decreasing feed rate. The cooling-water duty curve changes from a concave to a convex shape at a composition of approximately 85 per cent ammonia because of the very rapidly decreasing heat of condensation of ammonia-water vapors richer than 85 per cent ammonia.

Shown in Figure 7 is the cooling-water duty required to partially condense the vapor feed at atmospheric pressure to a temperature of 100 F (that is, to a condensate containing 25 per cent ammonia) and the power requirement for compressing the vapor portion leaving the partial condenser to a pressure of 200 psig. Consistent with what has been said earlier, the fraction of the feed leaving the partial condenser in the vapor state varies between 0 at a feed composition of 25 per cent ammonia and 1.0 at a feed composition of 95.4 per cent ammonia. Hence, as the feed composition increases beyond 25 per cent ammonia, an increasingly large fraction of the feed must be compressed, but at the same time the total feed rate is decreasing. Hence, the horsepower curve is convex and goes through a maximum as seen. The cooling-water duty decreases as the feed becomes increasingly rich in ammonia, both because the feed rate decreases and because for feeds richer than 25 per cent ammonia the fraction of the feed that is condensed also decreases with increasing ammonia concentration. The cooling-water duty is zero for a feed composition of 95.4 per cent ammonia, since at this composition none of the feed is condensed.

Shown in Figure 8 is a comparison of the utility requirements for sending the feed, which is initially a vapor at atmospheric pressure, to a fractionator operating at 200 psig by means of Methods I, II, and III. Method IV will be considered separately later. Method I, in which all the vapor is compressed from 0 to 200 psig, entails the greatest consumption of power, as would be expected. However, since in Method I the feed is sent to the fractionator in the vapor state, it will entail the lowest steam consumption in the fractionator. As explained earlier, Methods II and III have identical requirements for feeds containing less than 25 per cent ammonia. For feeds richer than 25 per cent ammonia, Figure 8 shows that Method III entails a smaller condenser duty than does Method II because in Method III only part, rather than all, of the feed is condensed. It is also clear from Figure 8 that Method III entails a smaller power consumption than does Method II. Method III entails the compression of a relatively small amount of vapor through a relatively large pressure ratio, and Method II entails the compression of a relatively large amount of vapor through a relatively small pressure ratio. That Method III should require a smaller power consumption than Method II is not evident from any prior considerations but is a consequence of the particular properties of the ammonia-water system.

With the feeds now at 200 psig and at different thermal states depending on the method used to elevate their pressure, it remains to calculate the utility requirements for fractionating them. All fractionation requirements were based on producing 1 ton per hour of anhydrous ammonia and a water waste containing not more than 0.5 per cent ammonia. The steam and condenser-duty requirements were calculated by the Ponchon-Savarit Method since the widely different molar latent heats of ammonia and water render the McCabe-Thiele Method inapplicable to this system.

Fractionation requirements are usually calculated by first selecting an optimum reflux ratio. Although this can always be done by a balance of capital and operating costs, a rule of thumb that is often used is that the optimum reflux ratio will be about 1.5 times the minimum reflux ratio. This rule was found to be a poor guide for the ammonia-water system. A better guide was to first select an optimum number of theoretical plates.

Because of the very favorable vapor-liquid equilibrium of the ammonia-water system, it is extremely easy to fractionate ammonia from ammonia-water feeds, and it was found that a tower containing about 10 theoretical plates would require but slightly more steam and condenser water than would an infinitely high tower. Therefore, by providing the tower with more than 10 theoretical plates very little could be saved on steam and cooling water. However, if the number of theoretical plates were reduced substantially below 10, the steam and cooling-water rates would begin to increase more quickly. For the purposes of this paper it is assumed that a tower containing 10 theoretical plates represents an optimum installation. Consequently, the steam and cooling-water requirements were obtained by the Ponchon-Savarit Method to correspond to a fractionator containing 10 theoretical plates. For any given application it is necessary to more accurately establish the optimum tower size.

Shown in Figure 9 are the steam and condenser-duty requirements for a 10-theoretical-plate fractionator, operating at 200 psig and producing 1 ton per hour of anhydrous ammonia and a water waste containing not more than 0.5 per cent ammonia. Anhydrous ammonia contains no more than 0.3 per cent water. For both all-liquid and all-vapor feeds, the steam rate and condenser duty decrease as the feed becomes richer in ammonia primarily because of the decreased amounts of feeds that need be handled. For an all-vapor feed, the condenser duty required is higher and the steam rate is lower than for a liquid feed, as would be expected. For a liquid feed, the steam rate and condenser duty do not approach zero as the feed composition approaches 100 per cent ammonia. This is because as long as any fractionation at all is accomplished the feed must be vaporized and recondensed. Of course, when the feed composition reaches 99.7 per cent ammonia, no fractionation would be needed and all requirements would drop discontinuously to zero. For a vapor feed, the steam rate approaches zero as the feed composition approaches 100 per cent ammonia, since the feed already enters the column in a vaporized state. However, the condenser duty for a vapor feed does not approach zero as the feed composition approaches 100 per cent ammonia since the vapor feed must always be condensed to produce liquid anhydrous ammonia. The mixed vapor-liquid feed line shown indicates the steam rate and condenser duty required to fractionate feeds containing the proportions of liquid and vapor leaving the partial condenser in Method III. For each over-all feed composition, the fraction of the feed that will leave the partial condenser in the vapor state has been shown in Figure 7. As explained earlier, and as shown, the mixed vapor-liquid feed will become an all-liquid feed at a feed composition of 25 per cent ammonia, and will become an all-vapor feed at a feed composition of 95.4 per cent ammonia.

From the utility requirements shown on the previous two slides, Figures 8 and 9, the utility costs can be computed, the following assumed utility rates being used:

Power at 1 cent per kilowatt-hour
Steam at 70 cents per thousand pounds
Cooling water at 2 cents per thousand gallons

These are average utility rates applicable to many plants.

The cooling-water rate is computed from the condenser duty on the basis of a cooling-water rise that will yield a 10 F approach in the condenser. Consequently, the allowable cooling-water rise in the column condenser will be 10 F. For feeds containing more than 25 per cent ammonia, the allowable cooling-water rise in the feed condenser will also be 10 F because of the manner in which these feeds are handled.

Feeds leaner than 25 per cent ammonia have a bubble point higher than 100 F and, therefore, can be condensed with 80 F cooling water in a condenser with a 10 F approach and a cooling-water rise greater than 10 F. For these lean feeds, the allowable cooling-water rise was based upon a 10 F approach in the condenser, provided that the outlet cooling-water temperature did not exceed 125 F.

Shown in Figure 10 are the utility costs for producing 1 ton per hour of anhydrous ammonia from a vapor feed, initially at atmospheric pressure, by means of Method I. The steam cost for the column and the cooling-water cost for the column condenser (curves 2 and 3) were computed from the vapor-feed curves shown on the previous figure. The power cost for the compressor (curve 1) was computed from the power requirements shown earlier, Figure 5, for compressing the vapor from 0 to 200 psig. All of the utility costs increase and hence the total utility cost increases as the feed becomes increasingly lean in ammonia, primarily because of the increasingly larger amount of feed that must be handled.

Shown in Figure 11 are the utility costs for producing 1 ton per hour of anhydrous ammonia from a vapor feed, initially at atmospheric pressure, by means of Method II. Feeds containing less than 25 per cent ammonia will have a bubble point higher than 100 F at atmospheric pressure and therefore can be totally condensed without compression. The cooling-water cost for the feed condenser (shown by curve 1) is lower for a feed containing 20 per cent ammonia than it is for a feed containing 25 per cent ammonia, because of the greater cooling-water temperature rise that is allowable for the leaner feed. As the feed composition becomes leaner than 20 per cent ammonia, the cooling-water cost for the feed condenser increases, because of the overpowering effect of the increasing feed rate. For feeds containing more than 25 per cent ammonia, the allowable cooling-water temperature rise in the feed condenser will remain constant, since the vapor is always compressed to a pressure where the bubble point of its condensate is 100 F. Hence, the cooling-water cost for the feed condenser gradually decreases as the ammonia content of the feed increases above 25 per cent ammonia. The steam cost for the column and the cooling-water cost for the column condenser (curves 4 and 3) were computed from the liquid feed lines on the slide showing the fractionation requirements, Figure 9. The power cost for the compressor (curve 2) was computed from the power requirements, shown earlier, Figure 6, for compressing the vapor from atmospheric pressure to a pressure where the bubble point of its condensate is 100 F. It is seen that for lean feeds the total utility cost increases primarily as a result of the increasing steam cost for the column rather than as a result of increasing power costs as in Method I. As the feed composition increases beyond 25 per cent ammonia, the power cost for compressing the vapor increases more quickly than the steam and cooling-water costs decrease, and therefore the total utility cost begins to increase. As the power cost begins to level out, the decreasing steam and cooling-water costs then cause the total utility cost to decrease. Hence, the total utility cost goes through a maximum at a feed composition of 45 per cent ammonia. Therefore, if the fractionation were performed as prescribed in Method II, it would cost more to fractionate a vapor feed containing 45 per cent ammonia than a vapor feed containing 20 per cent ammonia, both initially at atmospheric pressure. This leads to the surprising conclusion that it would be advantageous to dilute the feed containing 45 per cent ammonia to a feed containing 20 per cent ammonia in a direct condenser, totally condense it, and pump the condensate into the high-pressure fractionator. It is clear from Figure 11 that this means of operation will be more economical than Method II for feed compositions covering the extent of the dotted line shown, namely from about 20 to 75 per cent ammonia. If the fractionation of these feeds is accomplished by this dilution method, the total utility cost involved will remain approximately constant at about \$4 per ton of ammonia produced.

Shown in Figure 12 are utility costs for producing 1 ton per hour of anhydrous ammonia from a vapor feed, initially at atmospheric pressure, by means of Method III. Feeds containing less than 25 per cent ammonia can be totally condensed at atmospheric pressure and hence no subsequent compression is required. The cooling-water cost for the feed condenser given by curve 1 decreases, then increases, and finally decreases

again for generally the same reasons as given for Method II. The steam cost for the column and the cooling-water cost for the column condenser (curves 4 and 3) were computed from the mixed vapor-liquid feed curves shown in Figure 9. As the feed composition increases above 25 per cent ammonia, the feed rate decreases and the fraction of the feed that enters the fractionator as a vapor increases. Consequently, as the feed becomes increasingly rich in ammonia, the steam cost for the fractionator decreases more quickly than in Methods I and II and the cooling-water cost for the fractionator condenser decreases more slowly than in Methods I or II. In Methods I and II, the thermal state of the feed entering the fractionator did not vary with the feed composition as it does in Method III. The power cost for the compressor (curve 2) was computed from the power requirements, shown earlier, Figure 7, for compressing the vapor fraction leaving the partial condenser from 0 to 200 psig. As the feed composition increases above 25 per cent ammonia, the power cost for compressing the vapor increases. However, the power cost increases slowly enough so that the decreasing steam and cooling-water costs are not offset, and hence, the total utility cost does not exhibit a maximum in this range, but decreases slowly with increasing ammonia content in the feed.

It was seen from the previous figures that it is relatively expensive to fractionate a lean vapor, either because of the compression cost if the vapor is compressed into the fractionator, Figure 5, or because of the steam cost in the fractionator if the vapor is condensed and then pumped into the fractionator, Figure 9. In Method IV, the lean vapor is first sent to a prefractionator where it is enriched to a composition that can still be readily condensed with available cooling water. The overhead from this first column is then pumped into the high-pressure fractionator to produce the anhydrous ammonia. If the lean vapor feed is handled in this manner, some of the latent heat already contained by the vapor can be utilized in its enrichment without incurring any compression costs. Hence, it may be anticipated that for lean vapor feeds Method IV will prove to be most economical.

Shown in Table I are the utility requirements and costs for producing 1 ton per hour of anhydrous ammonia by means of Method IV, from a saturated vapor feed at atmospheric pressure containing 5 per cent ammonia.

Table I

Requirements for Producing Anhydrous Ammonia by Means of Method IV
From a Vapor Feed Containing 5% Ammonia

Basis: 1 ton per hour of anhydrous ammonia produced

Prefractionator:

Pressure: 0 psig
 Feed: Saturated vapor at 0 psig containing 5% ammonia
 Distillate: Ammonia-water solution containing 15% ammonia
 Waste: Water containing 0.2% ammonia

Main Fractionator:

Pressure: 200 psig
 Feed: Saturated ammonia-water solution containing 15% ammonia
 Distillate: Anhydrous ammonia
 Waste: Water containing 0.5% ammonia

Utility Requirements and Costs Per Ton of Anhydrous Ammonia Produced

	Condenser Duty, Millions of BTU	Cooling Water Cost, \$	Steam Rate, Thousands of lbs	Steam Cost, \$
Prefractionator	43.6	2.33	1.4	0.98
Main Fractionator	2.8	0.67	4.4	3.08

Total Utility Cost = \$7.06

The distillate composition of 15 per cent ammonia, chosen for the prefractionator, results in the best balance of utility costs between the prefractionator and the main fractionator. If the distillate composition were made richer than 15 per cent ammonia, the cooling-water cost for the prefractionator condenser would increase because of the smaller allowable cooling-water temperature rise that would result. If it were made leaner than 15 per cent ammonia, the steam cost for the main fractionator would increase sharply. As seen in the next figure, the total utility cost of \$7.06 per ton of ammonia, which results from handling the vapor feed containing 5 per cent ammonia by means of Method IV, is considerably less than would result from handling the same feed by any other method.

Shown in Figure 13 is a comparison of the total utility costs involved in producing 1 ton of anhydrous ammonia by each of the different methods considered. It is evident that for lean feeds a large economic incentive exists for prefractionating the feed as described in Method IV. The total utility cost that results from handling a feed containing 5 per cent ammonia by this method is \$7.06. If this feed were totally condensed and the condensate subsequently pumped into the high-pressure fractionator, as in Methods II and III, a total utility cost of \$10.80 would result. Compressing the feed directly into the high-pressure fractionator, as in Method I, would result in a much higher cost than is involved in either of the two previously mentioned methods. In Method IV the lean feed is enriched to 15 per cent ammonia. Consequently, when the feed composition reaches 15 per cent ammonia, Method IV reduces to simply condensing the feed and pumping the condensate into the high-pressure fractionator. As explained earlier, for feeds containing less than 25 per cent ammonia, Methods II and III reduce to totally condensing the feed and pumping the condensate into the high-pressure fractionator. Hence, at a feed composition of 15 per cent ammonia, Method IV will become identical with Methods II and III.

Figure 13 shows that for feeds containing more than 25 per cent ammonia, Method III is more economical than Method II. For feeds ranging in composition from about 25 to 75 per cent ammonia, it is more economical to first dilute the feed to about 20 per cent ammonia, totally condense it, and pump the condensate into the high-pressure fractionator than it is to handle the feed by means of Method II. However, as can be seen, this method of diluting a rich feed to a composition that can be totally condensed at atmospheric pressure is never more economical than partially condensing the feed and then compressing the vapor leaving the partial condenser as is done in Method III. As explained earlier, for feed compositions richer than 94.4 per cent ammonia, Method III is identical with Method I and the vapor is simply compressed into the high-pressure fractionator.

If utility rates, cooling-water temperature, and steam pressure are significantly different from those assumed in this paper, not only will the utility costs change but the preferred method for handling a feed of a given composition will also change. For example, if the fractionation is performed in a location where power costs are unusually high, the costs of Methods II and III will increase since both involve compressing the vapor. However, the cost of diluting the rich vapor to a composition that can be totally condensed at atmospheric pressure and pumping the condensate into the high-pressure fractionator will remain approximately constant at the value indicated by the horizontal line, Figure 13. Consequently, where power costs are high, it would be more economical, at least over some range of feed compositions, to dilute a rich feed to a composition at which it could be totally condensed rather than handling it by means of Method III. The same procedure would also be used if the available cooling-water temperature is unusually high, for it would become necessary to operate the fractionator at a pressure significantly higher than 200 psig to condense the anhydrous ammonia. Consequently, the compression costs involved in Methods II and III will increase, and it might be most economical to dilute a rich feed to a composition that could be totally condensed at atmospheric pressure.

Summary

For the cooling-water temperature, steam pressure, and utility rates chosen in this paper, the preferred methods of producing anhydrous ammonia from ammonia-water vapors initially at atmospheric pressure are as follows:

1. Feeds containing less than 15 per cent ammonia are first sent to a prefractionator operating at atmospheric pressure in which they are enriched to a 15 per cent ammonia overhead. The distillate from the prefractionator is then pumped into the main fractionator operating at 200 psig to produce anhydrous ammonia.

2. Feeds containing from 15 per cent ammonia to 25 per cent ammonia are totally condensed at atmospheric pressure, and the condensate is pumped into a fractionator operating at 200 psig to produce anhydrous ammonia.

3. Feeds containing from 25 per cent ammonia to 95 per cent ammonia are first partially condensed at atmospheric pressure to a temperature of 100 F. The condensate and vapor leaving the partial condenser are then pumped and compressed, respectively, into a fractionator operating at 200 psig to produce anhydrous ammonia.

4. Feeds richer than 95 per cent ammonia are compressed into a fractionator operating at 200 psig to produce anhydrous ammonia.

Literature Cited

1. Bahr, H., German Patent No. 741,222 (1943).
2. Bergfeld, L., German Patent No. 270,204 (1911).
3. Societe Industrielle et Financiere de Lens, French Patent No. 857,242 (1940).

METHOD II - COMPRESSION FOLLOWED BY CONDENSATION

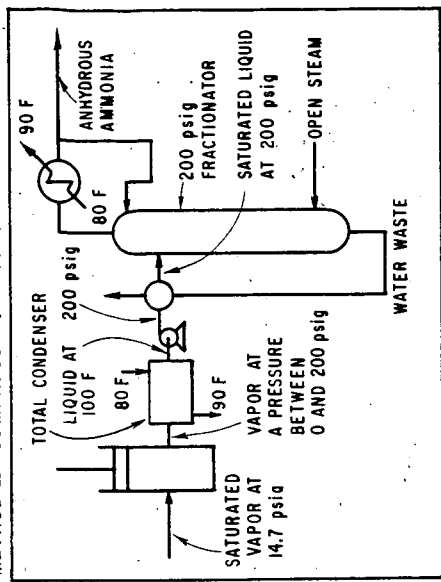


FIGURE 2

METHOD IV - PREFRACTIONATION

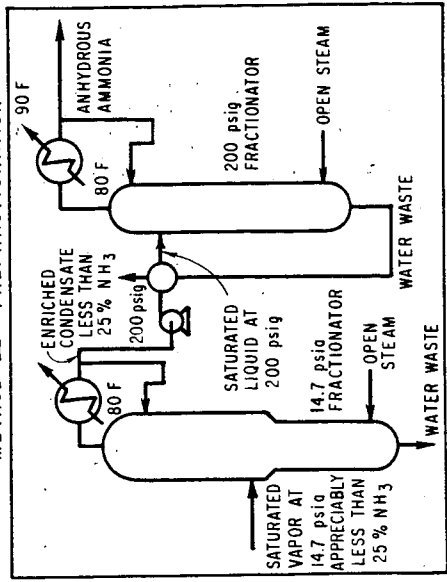


FIGURE 4

METHOD I - DIRECT COMPRESSION TO 200 psig

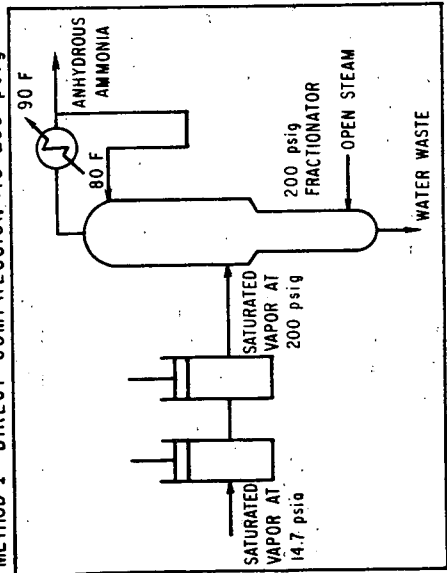


FIGURE 1

METHOD III - PARTIAL CONDENSATION FOLLOWED BY COMPRESSION

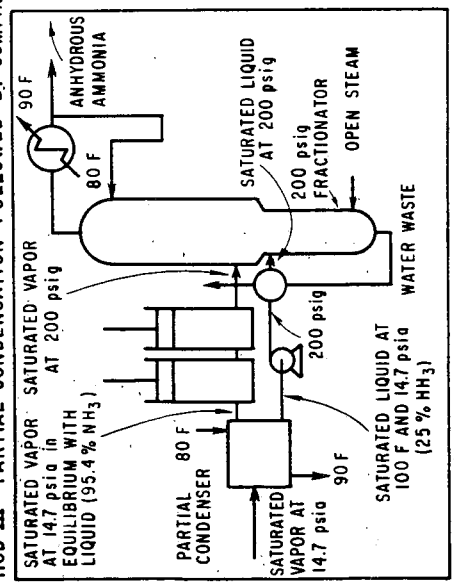


FIGURE 3

REQUIREMENTS FOR COMPRESSING ALL OF THE VAPOR INTO A 200 psig TOWER PRODUCING 1 TON/HR ANHYDROUS AMMONIA AS IS DONE IN METHOD I

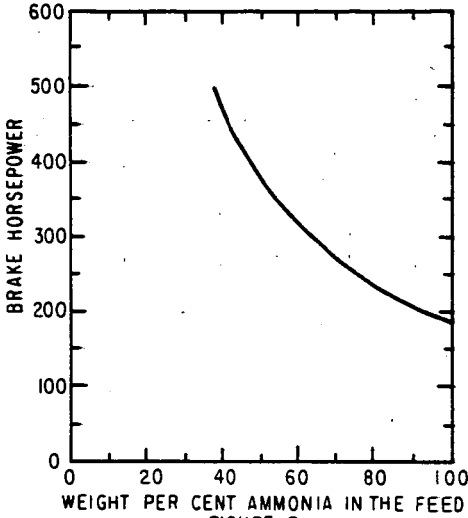


FIGURE 5

REQUIREMENTS FOR COMPRESSING THE VAPOR TO A PRESSURE WHERE ITS BUBBLE POINT IS 100 F AND THEN TOTALLY CONDENSING IT AS IS DONE IN METHOD II (BASIS: 1 TON/HR OF NH₃)

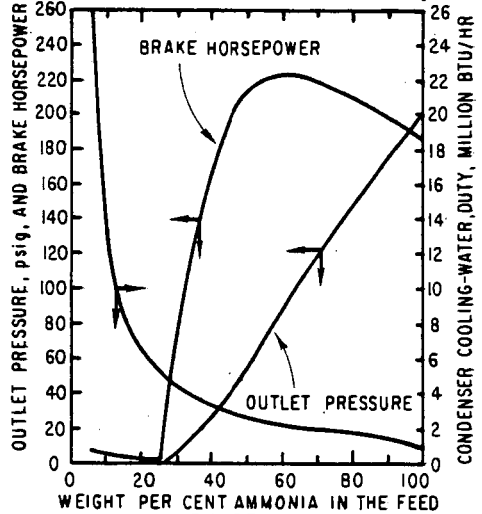


FIGURE 6

REQUIREMENTS FOR PARTIALLY CONDENSING THE VAPOR AT 1 ATM AND THEN COMPRESSING THE VAPOR PORTION INTO A 200 psig TOWER PRODUCING 1 TON/HR AMMONIA AS IS DONE IN METHOD III

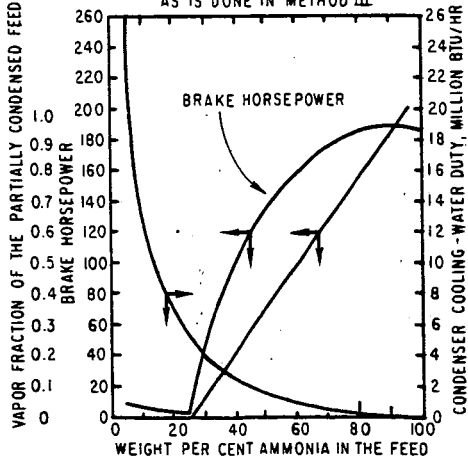


FIGURE 7

UTILITY REQUIREMENTS FOR SENDING THE FEED TO A FRACTIONATOR OPERATING AT 200 psig BY MEANS OF METHODS I, II, AND III

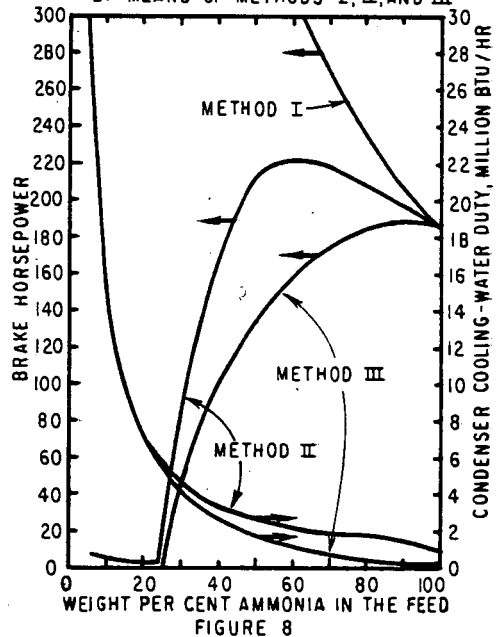


FIGURE 8

STEAM AND CONDENSER-DUTY REQUIREMENTS FOR A FRACTIONATOR AT 200 psig PRODUCING 1 TON PER HOUR ANHYDROUS AMMONIA AND A WATER WASTE CONTAINING NOT MORE THAN 0.5 PER CENT AMMONIA

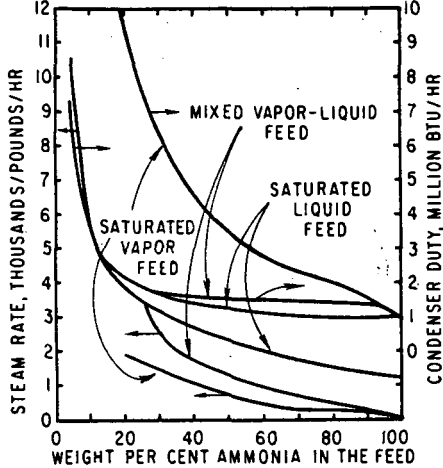


FIGURE 9

UTILITY COSTS FOR PRODUCING 1 TON/HR OF ANHYDROUS AMMONIA BY MEANS OF METHOD I
 ① POWER FOR COMPRESSOR
 ② STEAM FOR COLUMN
 ③ COOLING WATER FOR COLUMN CONDENSER

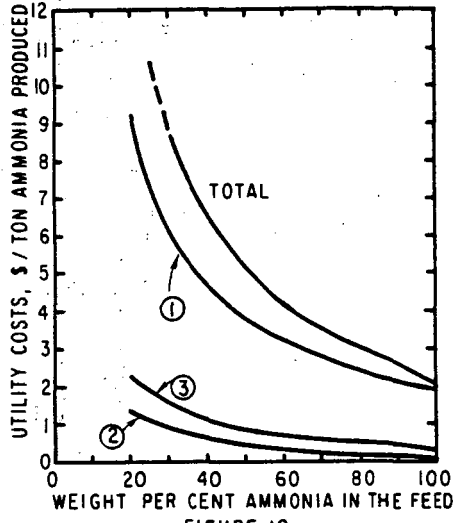


FIGURE 10

UTILITY COSTS FOR PRODUCING 1 TON/HR OF ANHYDROUS AMMONIA BY MEANS OF METHOD II

- ① COOLING WATER FOR FEED CONDENSER
- ② POWER FOR COMPRESSOR
- ③ COOLING WATER FOR COLUMN CONDENSER
- ④ STEAM FOR COLUMN

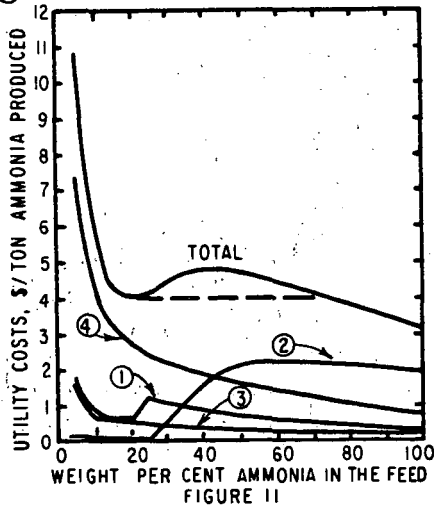


FIGURE 11

UTILITY COSTS FOR PRODUCING 1 TON/HR
ANHYDROUS AMMONIA BY MEANS OF METHOD III

- ① COOLING WATER FOR FEED PARTIAL CONDENSER
- ② POWER FOR COMPRESSOR
- ③ COOLING WATER FOR COLUMN CONDENSER
- ④ STEAM FOR COLUMN

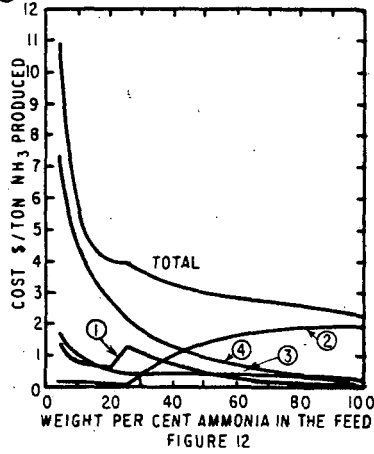


FIGURE 12

COMPARISON OF THE TOTAL UTILITY COSTS INVOLVED
IN PRODUCING ONE TON OF ANHYDROUS AMMONIA
FROM AN AMMONIA-WATER VAPOR FEED AT ATMOSPHERIC
PRESSURE BY MEANS OF METHODS I, II, III, AND IV

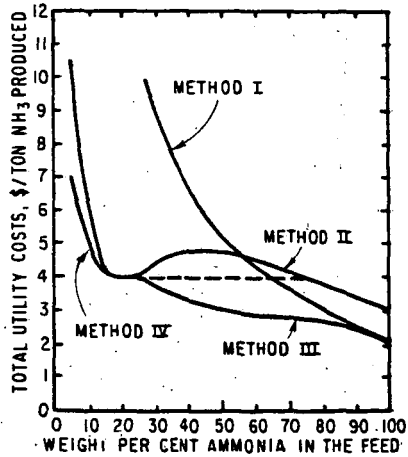


FIGURE 13

THE ROLE OF CORROSION TESTING IN THE COAL-CHEMICAL PLANT

R. J. Schmitt

United States Steel Corporation
Applied Research Laboratory
Monroeville, Pennsylvania

Introduction

It is a well-known fact that corrosion of plant equipment is costing the chemical producers millions of dollars annually. In the coal-chemical industry, as in any other industry today, it is imperative to minimize maintenance and replacement costs and to insure uninterrupted production to remain competitive. Although the high cost of corrosion cannot be entirely eliminated, it can be greatly reduced by the proper selection of constructional materials, by modifications in equipment design and operating procedure, and by the proper selection and application of protective coatings and inhibitors. However, the answer to a corrosion problem, whether it lies in replacement of the present materials of construction or in a modification in design, is usually not simple and cannot be readily ascertained without firsthand knowledge of the problem. This data can best be developed by conducting a well-planned corrosion-testing program.

Such a program can best be defined as one that will provide the most reliable data and the most convincing data from a given set of conditions. In planning a corrosion-testing program, both laboratory and plant tests should be considered. The laboratory test provides the closest control of the important variables and permits individual study of each variable. However, it is extremely difficult to duplicate in the laboratory the combination of effects, such as solution concentration, temperature, velocity, viscosity, that takes place under actual operating conditions in a chemical plant. The limited quantity of solution used in the laboratory test restricts the number and size of the materials in test. Further, unless the test solution is continuously renewed, it is difficult or impossible to maintain a constant concentration of known corrosive constituents in the solution, and thus the results may be erroneous. In a plant test, however, all the above variables are present. As a result, data obtained from plant tests with operating equipment are considered more reliable and are more convincing than laboratory data where plant conditions can only be approximated.

These remarks are not meant to suggest that laboratory data are misleading and have no place in a well-planned corrosion-testing program. On the contrary, laboratory tests can be used to screen a series of materials or inhibitors prior to being plant-tested, to provide data for comparison purposes, or to supplement plant data. In the development of new processes where previous corrosion experience is lacking or in plant corrosion problems where the equipment is inaccessible for corrosion testing, the corrosion engineer must often turn to laboratory data for guidance in selecting suitable constructional materials. When a new process is being developed and a pilot plant is to be constructed, corrosion tests should also be conducted in these facilities. Inasmuch as pilot facilities are often small, arrangements should be made early in the design stage to include adequate corrosion-testing locations. However, the data obtained from either laboratory or laboratory and pilot-plant studies should be used judiciously in selecting construction materials for a full-size piece of equipment.

Plant Corrosion-Testing Methods

In plant corrosion testing, various methods are utilized depending upon the objective. The tests most frequently used are those described below:

Corrosion-Specimen Test

The corrosion-specimen test is probably the best known and most widely used method in the coal-chemical industry. The test consists of obtaining cleaned and weighed specimens of various materials, including the materials in the piece of equipment to be tested, and exposing them in the liquid and vapor space of the operating unit for a given period of time. The test specimens are normally welded to obtain information on the effect of welding on the corrosion performance of the material, which is an important factor in choosing materials of construction for equipment. Moreover, in certain environments, it is often desirable to expose stressed specimens in the equipment to develop information on the susceptibility of the various construction materials to stress-corrosion cracking.

Although the specimens can be individually suspended in the unit, they are normally placed in a specimen holder and separated with insulating material to prevent direct contact except when galvanic effects are being studied. Figure 1 shows a typical corrosion-test rack and its various components. (Special types of rack may have to be designed for units difficult in accessibility.) Although it is usually necessary to shut down the operating unit to install or remove a test rack, retractable holders can be constructed to permit testing during normal operations. However, this method limits the number of materials that can be tested at one time. If the unit is inaccessible, the specimens can usually be installed in the related piping, though the data will not be as representative as data obtained from the actual operating unit. In testing in a pipeline, the specimens are mounted on a pipe plug and placed in a tee in the line. However, care must be taken to install the specimens parallel with the flow so as not to cause a restriction in the line. Figure 2 shows a mounted pipe-plug specimen and method of installation. In special cases, the materials to be evaluated can be obtained in pipe form, and short sections of each can be installed in the line. Much like the test specimens, these sections should be cleaned and weighed prior to exposure and should be insulated from each other.

After exposure, the test specimens are carefully cleaned and reweighed, and their corrosion rates calculated from the weight losses. Care should be taken to examine the specimens for local effects, such as pitting, grooving, and cracking. The data obtained from this test method will provide information on the expected service life of the unit, type of corrosion occurring, and suitable replacement materials.

The Electrical-Resistance Method

The electrical-resistance method is a direct means of measuring corrosion continuously and is used in the chemical industry to follow the progress of corrosion in operating equipment.¹* A special probe and meter are utilized in conducting these measurements. Figure 3 shows an electrical-resistance probe, and Figure 4 shows a portable meter and a typical installation. Several of these corrosion-monitoring devices are commercially available. In making measurements, the probe containing an element of the material to be tested is placed in the system under study and is then electrically connected to the meter. The meter measures the change in electrical resistance of the probe element as the cross-sectional area of the element is reduced by corrosion. The amount of corrosion can then be read directly from the meter in microinches penetration of the probe element.

* See References.

With the electrical-resistance method, corrosion data can be obtained in a few hours, whereas with weight-loss measurements data sometimes cannot be obtained for months because the removal of specimens is governed by plant operations. Unlike the use of corrosion-test racks, the electrical-resistance method does not require shutting down the operating unit to remove or change probe elements. The measurements are not affected by the accumulation of most corrosion products or sludge. However, the measurements are affected by corrosion products that carry current, such as sulfides. Like any test, this method also has its undesirable features in that it is limited to measuring a uniform type of corrosion and it is necessary to visually examine the probes to determine the presence of local forms of corrosion, such as pitting.

Probably the most widespread use of the electrical-resistance method is in the evaluation of corrosion-preventive measures, such as inhibitors. In addition, this method is especially useful for correlating corrosion with changes in operations.

Service Test

The service test is the most satisfactory method of corrosion testing. In this test, sections of the equipment to be tested are replaced with full-size experimental parts. Probably the most frequent use of this method is with heat exchangers and pumps, both of which are normally inaccessible for corrosion-rack testing. For example, in evaluating materials for replacing heat-exchanger tubes, full-size tubes constructed of various materials are placed in the tube bundle for testing. After a sufficient operating period (six months to one year), the tubes are removed from the exchanger and examined. In a test of this type, where large pieces of equipment are often handled, the examination of the equipment usually consists of a visual inspection. However, for some equipment—tubes, for instance—the thickness of the parts can be measured with a micrometer prior to and after exposure to determine change in dimensions as a result of corrosion.

Unlike the other methods previously mentioned, this method will readily detect local points of corrosion. Unfortunately, this method is often impractical and expensive.

Visual-Inspection Method

Visual inspection is probably the most common method of evaluating the performance of a piece of equipment. However, it usually requires a complete shut-down and clean-out of the unit. The data obtained from visual inspection plus ultrasonic measurements of wall thickness provide convincing information on the service life of a unit. As a result, this method is widely used by insurance and state inspectors in examining pressure-coded equipment and by maintenance personnel in conducting preventive corrosion programs.

Nondestructive Testing Method

In nondestructive testing, two of the more widely used pieces of equipment are the ultrasonic thickness gauge and the magnetic-particle inspection equipment for detecting surface discontinuities, such as cracks. The ultrasonic thickness gauge is an instrument for the nondestructive measurement of an unknown wall thickness from one side. This instrument utilizes the principle of ultrasonic resonance in measuring thickness. Several portable, battery-operated gauges are commercially available. Figure 5 shows the ultrasonic thickness gauge and method of application. This method is especially useful in determining the wall thickness of inaccessible equipment where visual inspection cannot be made. The magnetic-particle inspection method has been very useful on occasion in determining the integrity of high-pressure equipment.

Corrosion-Testing Applications

The corrosion-detection methods discussed above are the major plant tools which the corrosion engineer has to work with in his endeavor to control corrosion. Examples of how some of these methods have been used in solving specific corrosion problems in U. S. Steel's coal-chemical plants are given below. For each of the examples, a brief description of the process as it concerns certain pieces of plant equipment is given. Several additional examples of how corrosion testing has solved specific corrosion problems in coal-chemical plants have been presented by Larrabee and Mathay.²⁾

Corrosion-Rack Tests in Tar-Distillation Equipment

One area in the coal-chemical plant that has caused operators considerable corrosion trouble is the tar-distillation plant. In this operation, the tar removed from the coke-oven gas in the collecting mains is placed in decanters to permit separation of the flushing liquor and finely divided carbon that are carried along with the tar from the collecting mains. After decantation, the tar is washed and centrifuged to reduce the moisture and inorganic salt content of the tar. The tar leaving the centrifuge is then placed in storage tanks until further processing. Upon demand, the tar is pumped into a dehydrating flash drum, where it is further dehydrated and preheated to a high temperature. The tar leaving the flash drum enters the tar still (carbon-steel shell lined with AISI Type 316 stainless steel, with Type 316 internal parts), where it is fractionated into tar acid oils and pitch. The acid oil is further treated by distillation for the recovery of naphthalene and solvents.

Corrosion of the tar-distillation facilities is essentially controlled by the decantation, washing, and centrifuging operations. The agents in coal tar that are believed to be responsible for corrosion are the inorganic salts, ammonium chloride and ammonium thiocyanate.³⁾ The tar-handling operations minimize the concentration of these contaminants. Of the two corrosion constituents, ammonium chloride is the most aggressive. The individual effect of thiocyanate and chloride compounds in acid oil on the corrosion of carbon steel was studied in laboratory tests. The results of these tests, Table I, show that operating problems with the tar-handling facilities can lead to serious corrosion problems as a result of large quantities of these corrosive constituents entering the tar-distillation equipment.

Recently, at one of the coal-chemical plants where serious operating problems were encountered in the tar-handling system, extensive corrosion of distillation equipment occurred. Interior inspection of the primary naphthalene fractionator revealed that the carbon-steel shell and AISI Type 410 stainless-steel internals of the fractionator were corroding. (The function of the primary naphthalene fractionator is to concentrate the crude naphthalene in the acid oil received from the tar still.) The corrosion attack was most severe at the top of the column where ammonium thiocyanate and ammonium chloride were found to concentrate. Following the inspection, the top of the column was lined with cement. At the same time, corrosion-test racks containing various metals were placed in the unit to determine suitable replacement materials, and the unit was again placed into operation. The types and chemical composition of the test materials contained in the racks are shown in Table II. After six months of operation, the fractionator was shut down and the test racks were removed. The results of these tests, Table III, show that AISI Types 304 and 316 stainless steels and USS TENELON stainless steel were practically unattacked.

Visual inspection of the unit revealed that the corrosion of the shell and internals had progressed to the point where replacement was necessary. On the basis of the above results, the corroded unit was recently replaced with a new AISI Type 316L stainless-steel fractionator. The low-carbon-grade Type 316L stainless steel was used in the construction to obtain maximum corrosion resistance at the weld areas.

Reducing the carbon content of the low-carbon stainless steels to the solubility limit of about 0.02 per cent minimizes or prevents carbide precipitation in the heat-affected zone of the metal during welding. As a result, the low-carbon stainless steels are less susceptible to intergranular corrosion at the weld areas.

Service Test in Wash-Oil System

In another coal-chemical plant, 150 million gallons of river water are used daily for cooling purposes. Although the water is treated with lime to raise the pH from about 3.8 to about 4.5 (further treatment being uneconomical because the water is not recirculated), the carbon-steel condenser tubes in the wash-oil regenerating system of the plant are corroded seriously and fail after about four months of service. (Wash oil is used to absorb from the coke-oven gas those constituents having boiling points below 200 C, such as benzol, toluene, and xylol.) The wash-oil condenser receives wash-oil vapors from a Dowtherm heat exchanger, which partially condenses the oil vapors coming from the wash-oil still. As shown in Figure 6, the hot oil flows through the shell side of the wash-oil condenser and is cooled by river water flowing through the tubes. The temperature of the oil is about 350 F. The cooling water enters the condenser at about 80 F and leaves at about 180 F.

In an effort to reduce the high maintenance and replacement costs caused by the rapid failure of carbon-steel condenser tubes, a service test was initiated to determine the suitability of stainless-steel tubes in the wash-oil condenser.⁴⁾ Four AISI Type 304 stainless-steel tubes and four carbon-steel tubes were installed in the tube bundle of the condenser at the same time. After four months of exposure, the carbon-steel tubes failed because of severe pitting by the cooling water. After six months of exposure, two of the Type 304 tubes removed from the condenser were practically unattacked. Figure 7 shows a section cut from the center of each type of tube after the service test. (The marks on the interior surface of the Type 304 tube are fabrication marks.) The remaining two Type 304 tubes were removed after one year of exposure and were also found to be in excellent condition. Because of the excellent resistance of the Type 304 tubes to corrosion by the low pH river water, Type 304 tubes will be installed in the entire condenser. The use of Type 304 tubes should result in a substantial yearly savings through decreased maintenance costs.

Corrosion Monitoring of Foul-Gas Line

In the utilization of coke-oven gas as a fuel for the open hearth, soaking pits, and reheating furnaces, it is desirable to remove the sulfur from the gas as it constitutes an unwanted contaminant in steel. At one of the coal-chemical plants, a portion of the coke-oven gas is processed for the removal of sulfur and other contaminants prior to sending the gas to the open-hearth melting furnace. In this process, the coke-oven gas leaving the gas line enters an absorption tower, where the gas is scrubbed counter-currently with a sodium carbonate solution to remove hydrogen sulfide, hydrogen cyanide, carbon dioxide, and other contaminants. The desulfurized coke-oven gas leaves the top of the tower and is sent to the open-hearth furnace. The foul solution is removed from the bottom of the tower and pumped into a stripping column, where it is regenerated by steam distillation and recycled to the absorber. The foul gas leaving the top of the column is sent to the open-hearth shop, where it is used as fuel for the boilers. The service life of the carbon-steel line carrying the foul gas to the open-hearth boilers is usually about two years. A corroded portion of the pipe after two years of service is shown in Figure 8.

An electrical-resistance probe with a carbon-steel element was installed in the foul-gas line to ascertain the effect of operating variables on the rate of corrosion of the line. Corrosion readings with the resistance meter were taken over

a period of 15 days during which time the progress of corrosion was determined when (1) steam was being fed to the steam tracers, (2) steam was not being fed to the steam tracers and, (3) the line was being steamed out. A graph of penetration (microinches) of the probe element versus time, Figure 9, shows that an increase in corrosion takes place only during steam-out periods. The corrosion attack is believed to be the result of hydrogen sulfide, hydrogen cyanide, and thiocyanate attack in the presence of water. The corrosion rate of carbon steel based on the resistance readings for the first steam-out period was 964 mils per year and that for the second steam-out period was 526 mils per year. This investigation also showed that the use of steam tracers for maintaining temperatures higher than about 150.F (normal gas temperature) on the line seemed to have no effect on the corrosion rate of the line. As a result of the investigation, the number of steam-outs was reduced.

Summary

The examples cited above represent only a few of the corrosion studies conducted in the Corporation's coal-chemical plants to determine suitable materials of construction for withstanding the extremely corrosive environments normally encountered. To give some idea of the extent of corrosion testing within the Corporation's plants since 1954, over 3500 corrosion specimens have been exposed in about 150 process units. In this same period of time, detailed corrosion inspections have been conducted on 110 process units.

As a result of these corrosion studies, suitable materials have been determined for the replacement of 21 major operating units and 39 smaller units. In addition, the corrosion data have enabled the Corporation to assist customers in selecting materials for the construction of new chemical plants.

References

1. A. J. Freedman, E. S. Troscinski, and A. Dravnieks, "An Electrical Resistance Method of Corrosion Monitoring in Refinery Equipment," Corrosion, 14, No. 4, pp. 29-32 (April 1958).
2. C. P. Larrabee and W. L. Mathay, "Controlling Corrosion in Coal-Chemical Plants," Corrosion, 14, No. 4, pp. 37-40 (April 1958).
3. D. McNeill, "Causes and Prevention of Corrosion in Tar Stills," Corrosion Technology, November 1957, p. 385.
4. R. J. Schmitt, "Behavior of Carbon and Stainless Steels in Acid Waters," Corrosion, 14, No. 10, p. 15 (October 1958).

Table I
Corrosion Rate of Carbon Steel Exposed to Samples
of Tar Acid Oil at 220 C

Thiocyanate Concentration, grams per liter	Chloride Concentration, grams per liter	Corrosion Rate, mils per year	
		Vapor	Liquid
*	*	3	5
5	0	13	40
0	5	42	184

* Present in residual amounts.

Table II
Types and Composition of Test Materials
Exposed in Primary Naphthalene Fractionator

Material	Per Cent									
	C	Mn	P	S	Si	Cu	Ni	Cr	Mo	N
Carbon steel	0.18	0.50	0.930	0.03	0.043	0.05	0.03	0.02	*	*
AISI Type 410 stainless steel	0.06	0.48	0.022	0.005	0.55	*	0.32	12.2	0.03	*
AISI Type 201 stainless steel	0.10	6.0	0.038	0.015	0.40	*	5.4	16.7	*	0.15
AISI Type 304 stainless steel	0.08	1.2	0.022	0.014	0.51	*	9.0	18.5	*	*
AISI Type 316 stainless steel	0.06	1.5	0.03	0.014	0.46	0.23	13.4	17.8	2.3	*
USS TENELON stainless steel	0.08	14.2	0.024	0.008	0.79	*	0.29	16.6	*	0.32

* Not determined; present in residual amounts.

Table III
Corrosion-Rack Tests in Primary Naphthalene Fractionator

Material	Rack Location in Fractionator	Corrosion Rate, mils per year
Carbon Steel	Top	*
	Middle	106
AISI Type 410 stainless steel	Top	16
	Middle	1
AISI Type 304 stainless steel	Top	<0.1
	Middle	<0.1
AISI Type 316 stainless steel	Top	<0.1
	Middle	<0.1
USS TENELON stainless steel	Top	<0.1
	Middle	<0.1

* Specimen completely disintegrated.

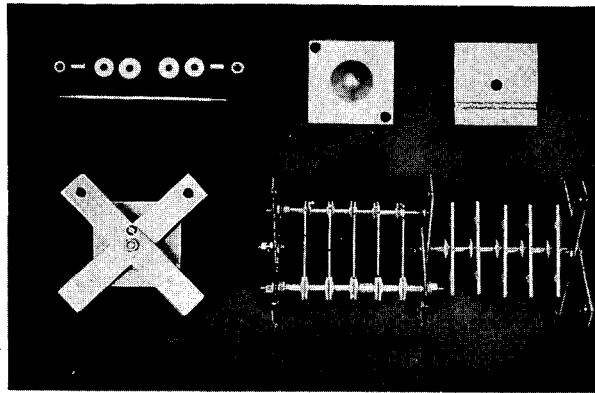


Figure 1. Corrosion-Test Rack and Component Parts.

Magnification: 0.125X

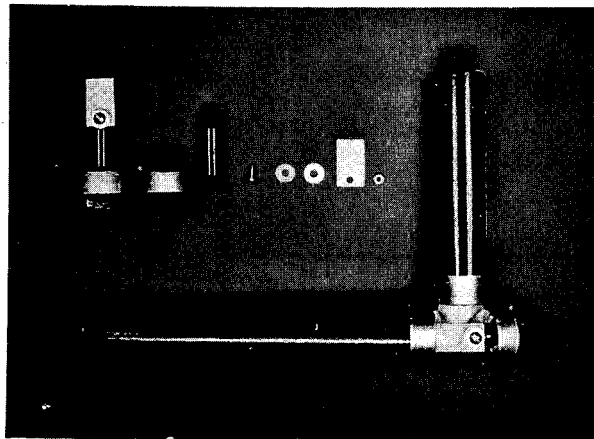


Figure 2. Mounted Pipe-Plug Specimen and Method of Installation.

Magnification: 0.125X

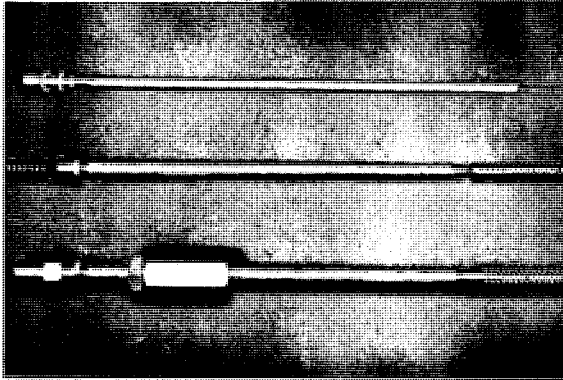


Figure 3. Electrical-Resistance Probe.

Magnification: 0.0625X



Figure 4. Portable Electrical-Resistance Meter and Typical Installation.

Magnification: 0.0625X

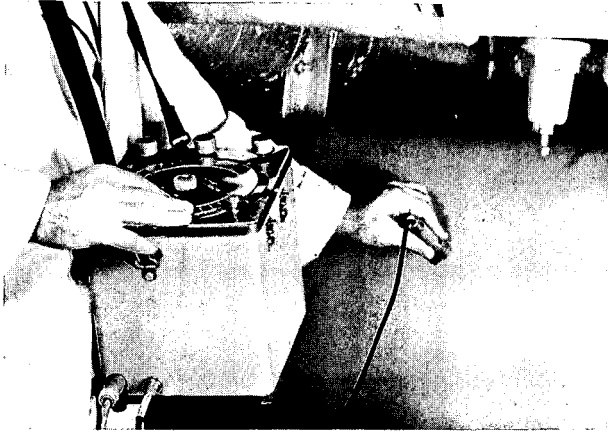


Figure 5. Ultrasonic Thickness Gauge and Method of Application.

Magnification: 0.125X

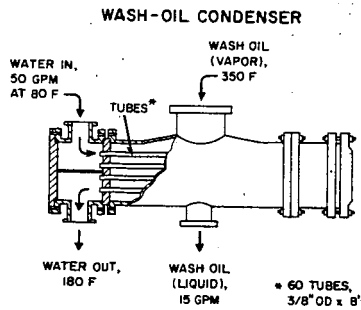


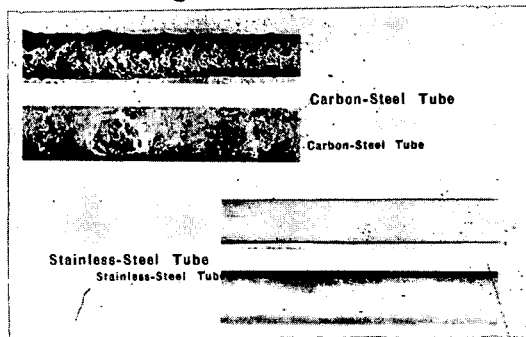
Figure 6.



FOUL-GAS LINE AFTER TWO YEARS OF SERVICE

Figure 7.

Magnification: 0.50X



TUBES AFTER EXPOSURE IN A WASH - OIL CONDENSER

Figure 8.

Magnification: 1X

CORROSION-PROBE MEASUREMENTS
IN FOUL-GAS LINE

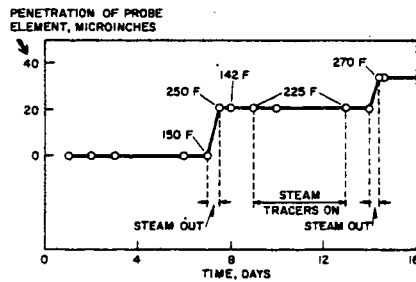


Figure 9.

NAPHTHALENE DESULFURIZATION WITH SODIUM

Donald A. Swalheim and C. J. Stapf, Jr.

E. I. du Pont de Nemours & Co., Inc.
Wilmington, Delaware

Improving the quality of coke oven naphthalene by treating the product with sodium to remove sulfur compounds and other impurities is of commercial importance to phthalic anhydride producers and other consumers of naphthalene. The treatment of naphthalene with sodium is disclosed in a patent issued in 1930 to G. Schroeter (U. S. Patent 1,763,410). Sodium has been used commercially to remove sulfur compounds, such as thionaphthenes, for a number of years. The available data, however, are inadequate to serve as the basis for designing a continuous process for large-scale operation. This study was undertaken to develop data on reaction rates and other factors essential in preparing preliminary design for a continuous process.

AMOUNT OF SODIUM REQUIRED FOR DESULFURIZATION

In the initial series of tests, crude coke oven naphthalene (74°C melting point) was treated with different amounts of sodium to determine the amount required to achieve essentially complete desulfurization under batch conditions. A 100 g. sample of the naphthalene was added to a 500-ml. round-bottom flask equipped with a heating mantle and reflux condenser. After the naphthalene had reached a temperature of about 210°C, the sodium was added. The mixture was maintained at the reflux temperature of about 217°C. during the reaction period. The contents were then rapidly distilled and the sodium-treated naphthalene was analyzed for sulfur using the Parr bomb method.

The results are given in Table I. In the first four experiments, the sodium used was in dispersion form; in the last three tests, the sodium was in 1/8-in. to 1/4-in. cubes. The results show that 2% by weight of sodium added as a dispersion is very effective in reducing the sulfur. The sulfur is reduced from 8000 ppm. to about 70 ppm. in 30 min. In 60 min., it is reduced to about 5 ppm. The poor results obtained with solid sodium can be attributed to the small surface area of sodium in direct contact with the naphthalene.

Additional tests were made to determine amounts of sodium required to desulfurize higher purity 78°C. naphthalene. Results obtained with 1% and 2% by weight of sodium as a dispersion are shown graphically in Figure 2. These tests were conducted at 187°C. as compared with the reflux temperature of 217°C. in the earlier experiments. The addition of 1% sodium, based on weight of crude naphthalene, reduces the sulfur content from 5000 ppm. to approximately 160 ppm. in 70 min. This is equivalent to removing 98.6% of the sulfur. The reduction in sulfur, as expected, was greater with 2% by weight of sodium.

INFLUENCE OF SODIUM PARTICLE SIZE ON DESULFURIZATION

Additional tests were made to obtain more data on the influence of the particle size of sodium. Crude naphthalene melting over the range of 74° - 78°C. serves as an ideal medium for dispersing sodium. The impurities or foreign components function as very effective dispersing agents. Dispersions containing 50% sodium/50% naphthalene were prepared by subjecting the mixture to high shear agitation with the temperature maintained at 110° - 120°C. The particle size was regulated by using different proportions of purified and crude naphthalene. Apparatus illustrated in Figure 1 was used for these tests. The samples were taken at selected intervals by applying a vacuum to withdraw the vapors from the reaction flask. The vapors were condensed in the sample bottle shown in the flask to the left.

The marked effect of the sodium particle size is illustrated by the data plotted in Figure 3. The reaction proceeds very rapidly with the 20-micron sodium dispersion. For example, the sulfur is reduced to 250 ppm. in 6 min. This is equivalent to removing 99.6% of the sulfur. A reaction period of 125 min., however, is required with the 150-micron sodium dispersion to reduce the sulfur to the same level.

CONTINUOUS DESULFURIZATION WITH OVERFLOW TYPE REACTOR

Data derived from batch-type experiments and reaction rate studies indicated that the sulfur should be reduced to a low concentration with a continuous feed, continuous overflow reactor having an average hold-up time of 3 hr. A series of tests was made by continuously feeding crude naphthalene and 2% by weight of sodium (added as a 50% dispersion in naphthalene) to a well-agitated reactor having an average hold-up time of 3 hr. A resin kettle of 1500 ml. capacity, of the type previously described in Figure 1, was used for this series of tests. The crude 74°C. naphthalene and the 50% sodium dispersion were fed into the reactor by gravity from graduated cylinders. Samples of the overflow product were collected at intervals and analyzed for sulfur.

The results given in Table II show that very effective desulfurization can be obtained with this type of continuous system.

CONCENTRATING THE RESIDUE FROM THE SODIUM-TREATED NAPHTHALENE

The sodium-treated naphthalene contains about 4% - 8% residue and high boiling fractions depending on the degree of purity of the crude naphthalene. Substantially all of the pure naphthalene content of the crude must be recovered for economic reasons. However, no data have been available on the heat transfer and physical characteristics of the mixture containing a relatively high percentage of residue.

The natural circulation evaporator used to boil off naphthalene from the mixture is shown in Figure 4. The rapid circulation is accomplished by applying the required heat in the exchanger indicated by (x). Naphthalene vapors pass overhead and are recovered from the condenser (y) shown on the left. The unit was operated until the mixture in the reboiler contained about 75% residue and 25% naphthalene. The heat transfer conditions in the heat exchanger were good under these conditions of high residue operation. With a properly designed, forced circulation unit, substantially all of the naphthalene could be recovered.

CHARACTERISTICS OF THE SLUDGE

All of the naphthalene from the 75% residue/25% naphthalene mixture obtained from the natural circulation reboiler just described was recovered by further evaporation in a distillation flask. The viscosity characteristics of the sludge after removing substantially all of the naphthalene are shown in Figure 5. The sludge upon cooling is very fluid at temperatures above 100°C. but the viscosity increases rapidly below this value. At room temperature, it may be described as semirigid in consistency.

COMMERCIAL EQUIPMENT FOR DESULFURIZATION

A wide variety of types of reactors for desulfurizing naphthalene can probably be considered in view of the rapid desulfurization rates achieved using fine particle size sodium dispersions. For example, the rate studies indicate that the hold-up time provided in a distillation column may, in some cases, be adequate. This presentation, however, is restricted to an evaporator type of reaction system. The major steps in the process are listed in Table III. The first step consists of preparing a 50% dispersion of sodium in crude naphthalene. The dispersion is mixed with the crude naphthalene feed which is then continuously fed to a desulfurization reaction vessel. High residue bottoms from this reactor are pumped to a second evaporator to recover the remaining naphthalene. The residue is discharged periodically from this vessel. The three major steps of the process are:

(A) Dispersing Liquid Sodium in Naphthalene

The basic equipment required for this step in the process is illustrated in Figure 6. The high-shear dispersion unit is charged with approximately equal parts of liquid sodium and crude naphthalene. Fine particle size dispersions are readily prepared by agitating the contents of the vessel for periods of 5-10 min. The dispersion is then discharged to a holding tank. A continuous feed from this tank is combined with the main naphthalene feed stream and introduced into the evaporator or desulfurization vessel.

(B) Evaporator-Type Desulfurization Reactor

The second step of the process, illustrated in Figure 7, is essentially a continuous flow system. The incoming feed (A) and the vaporized naphthalene (B) plus the side stream (C) going to the second evaporator are regulated to maintain approximately a 50% residue/50% naphthalene mixture in the reactor. The vessel is designed to provide an average product hold-up time of 3 hr. Through-put at this hold-up time with a 2500 gal. vessel is about 30 million lb./yr. of naphthalene, assuming 300 operating days. The mixture is pumped through the external heat exchanger at a rate of about 500 gal./min. which provides extremely turbulent mixing. Volume turnover in the reactor is approximately 18 times/hr. The bottoms from the reactor are pumped to a second smaller evaporator to recover the balance of the naphthalene. Assuming 5% residue including high boilers in the sodium-treated naphthalene, the bottoms flow rate is approximately one-tenth the incoming feed rate.

(C) Final Naphthalene Recovery and Residue Separation

The second evaporator shown in Figure 8 strips essentially all of the remaining naphthalene from the 50% naphthalene/50% residue mixture. It is operated on a semicontinuous basis. When the residue level in the evaporator approaches the capacity of the vessel, the feed from the first evaporator is shut off to permit discharging the vessel. With an 800-gal. capacity evaporator and a through-put rate of 30 million lb./yr., clean out will be required at approximately 8-hr. intervals.

The residue is fluid at the operating temperature and can be discharged by vacuum to a portable tank for conveyance to an incinerator. If the residue is transferred to a slag pile or other area for disposal, it is advisable to destroy small amounts of sodium in the mixture prior to discharging the residue from this evaporator. Although massive amounts of sodium will, under certain conditions, react rather violently with water, commercial experience has demonstrated that finely divided sodium mixed with inert material will react safely with superheated or dry steam in the presence of nitrogen and no hazards are involved. The reaction of sodium with steam to form caustic soda is completed in a matter of minutes.

CONCLUSIONS

Rapid reaction of the fine particle size sodium dispersions with the sulfur compounds present in crude coke oven grade naphthalene have been demonstrated. Basic data have been translated to preliminary design for a continuous process for desulfurizing coke oven grade naphthalene.

ACKNOWLEDGEMENT

We are indebted to H. F. Porter of Du Pont Engineering Department for his assistance in developing some of the basic design features of the process.

REFERENCE

1. Schroeter, G. (to Newport Manufacturing Co.) U. S. Patent 1,763,410 (June 10, 1930).

TABLE I
DESULFURIZATION OF NAPHTHALENE

<u>Run No.</u>	<u>Type Sodium Added</u>	<u>% Sodium Added</u>	<u>Treating Time, Min.</u>	<u>PPM. Sulfur After Treatment*</u>
1	Dispersion	2	30	50-70
2	Dispersion	2	60	5
3	Dispersion	3	30	10
4	Dispersion	4	30	Non-detectable
5	Solid	2	60	4900
6	Solid	3	60	4300
7	Solid	4	60	3900

* Sulfur Content of 74°-75°C Naphthalene Before Treatment-8000 ppm.

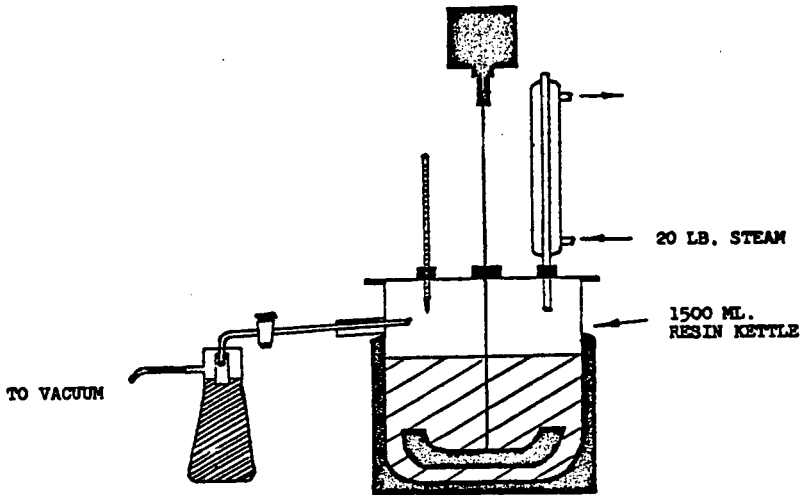
TABLE II
DESULFURIZATION WITH 3-HOUR AVERAGE HOLD UP TIME

<u>Reactor Temperature</u>	<u>Sulfur Content, ppm.</u>		<u>% Sulfur Removed</u>
	<u>Feed</u>	<u>Product</u>	
190°-200°C	3200-6200	30	99-99.8

TABLE III
PROCESSING STEPS IN DESULFURIZING

1. Dispersing the Liquid Sodium
2. Desulfurizing in an Evaporator Vessel
3. Recovery of Remaining Naphthalene
 - (A) Residue Separation

FIGURE 1



DESULFURIZATION APPARATUS

FIGURE 2

DESULFURIZATION RATES

78°C NAPHTHALENE
@ 187°C, 350 mm Hg

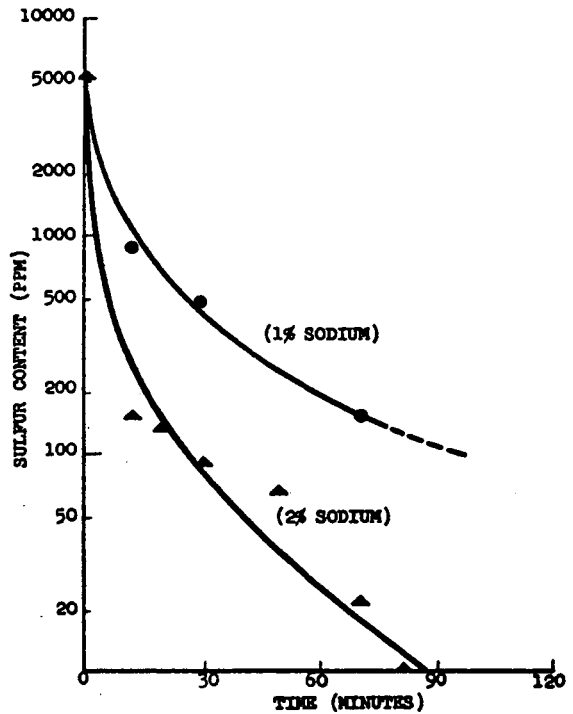


FIGURE 3

DESULFURIZATION RATES
WITH VARYING
SODIUM PARTICLE SIZE

78° NAPHTHALENE
TEMPERATURE 217°

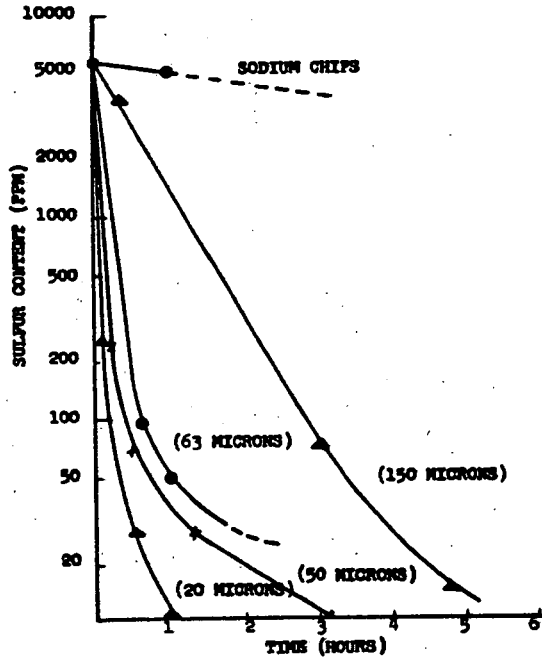
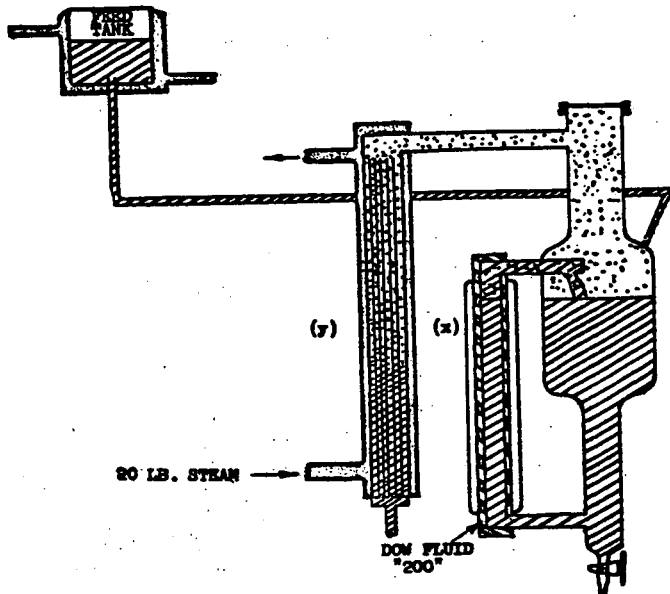


FIGURE 4



NATURAL CIRCULATION REBOILER

FIGURE 5

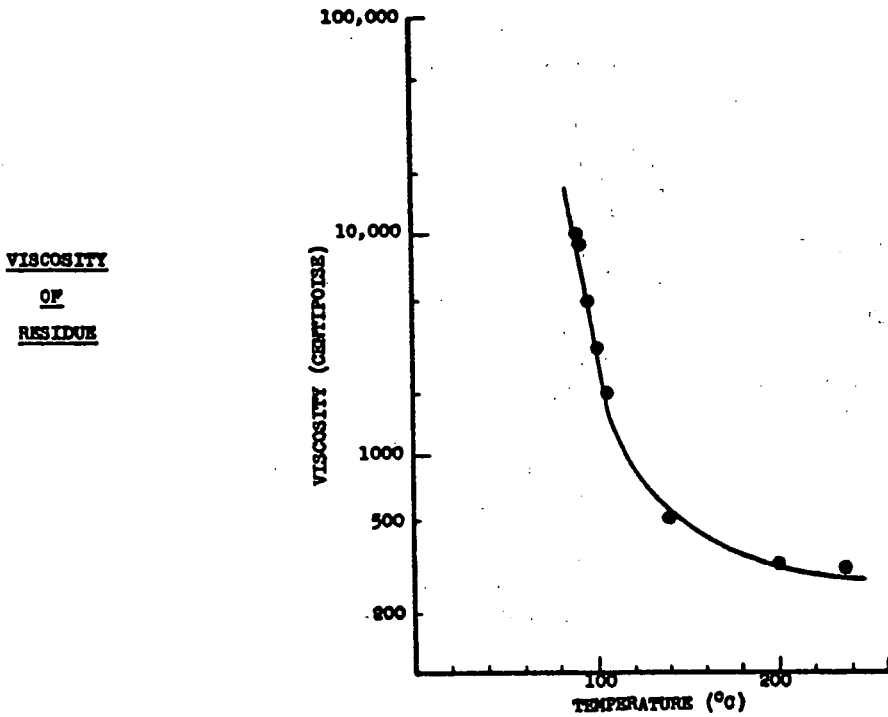
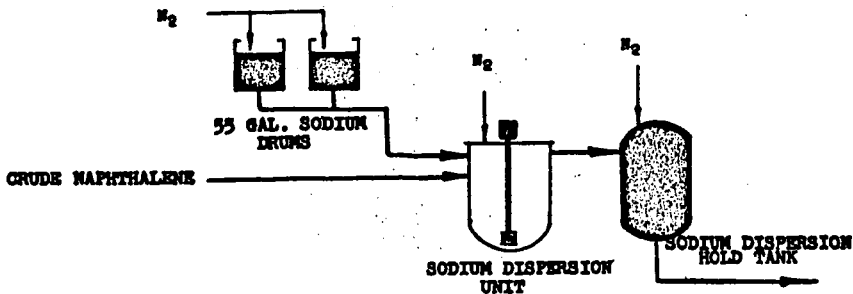


FIGURE 6



DISPERSING LIQUID SODIUM

FIGURE 7

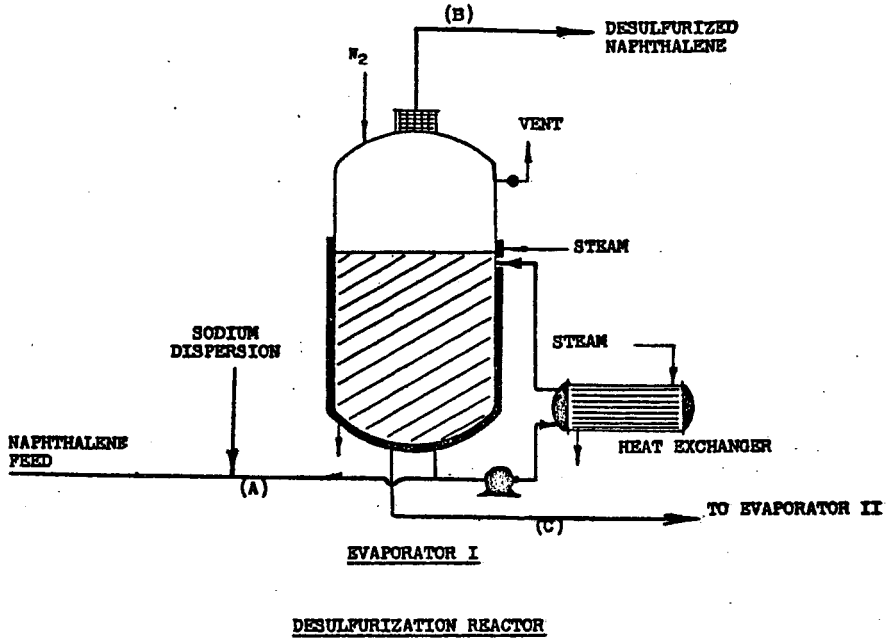
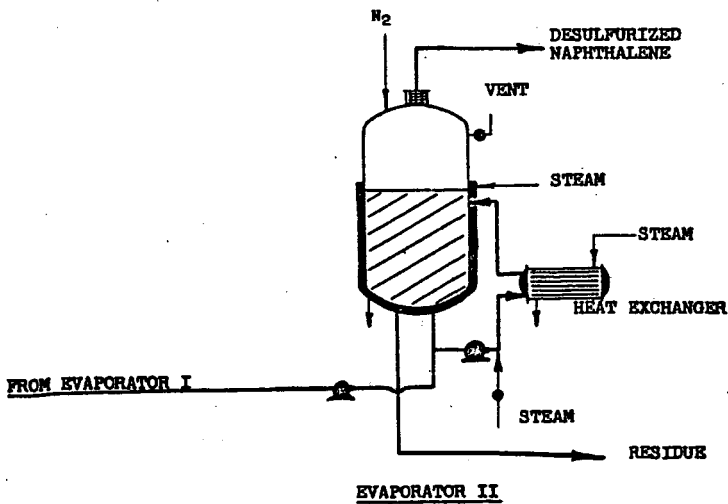


FIGURE 8



NAPHTHALENE RECOVERY AND RESIDUE SEPARATION

CHEMICALS FROM CARBAZOLE BY REDUCTIVE PROCESSES

Hans Dressler and Melvin E. Baum

Koppers Company, Inc.
Verona Research Center
Verona, Pennsylvania

Introduction: Carbazole was discovered in coal tar in 1872 (1). Synonyms for carbazole are dibenzopyrrole and diphenyleneimine. The numbering system used by Chemical Abstracts for the carbazole ring is shown in Figure 1.

(1) Graebe and Glaser, Ber., 5, 12 (1872).

Carbazole melts at 245.5°C. and sublimes readily. Its boiling point is 354°C./760 mm. It is sparingly soluble in most common solvents with the exception of acetone and pyridine. While most of the ring-substituted carbazole derivatives are also high melting, many N-substituted carbazole compounds melt below 100°C. Of course, all carbazole derivatives are high boilers.

The N-atom of carbazole is very weakly basic. Actually, the imino hydrogen is replaceable by alkali metals. Nevertheless, in aromatic substitution reactions the NH group exerts the same o, p-directing influence as in diphenylamine. Thus, in electrophilic substitution reactions, the 3- and 6- (i.e. p-) positions react primarily, with some o-substitution in the 1- or 8- positions.

In addition to being found in coal tar several good syntheses for making carbazole are also available. For example, the method of Tauber (2) involves the heating of 2,2'-diaminodiphenyl with a strong mineral acid to give excellent yields of carbazole (Figure 2).

(2) Tauber, Ber., 24, 197 (1891)

However, while synthesis will deliver a product of highest purity, it is believed that coal tar carbazole of 97% or better purity will always be cheaper than the synthetic product.

It is not intended to elaborate here on the methods of extracting carbazole from coal tar, but a brief general review may be useful. Dry coal tar contains 1-2% of carbazole. Of this amount, about 35% is industrially recoverable (3). Thus, the po-

(3) Lowry, ed., "Chemistry of Coal Utilization", J. Wiley & Sons, N. Y. 1945

tential U. S. capacity for coal tar carbazole is in excess of 50,000,000 lbs./yr. Generally, carbazole is recovered from coal tar by distillation and extraction. A coal tar distillate boiling at about 320-60°C., is allowed to cool whereupon crystalline solids deposit. These solids are recovered by centrifugation and contain 30-40% of anthracene, 20-25% of carbazole, and 10-40% of phenanthrene, their homologs, and impurities such as methyl fluorenes. Carbazole, anthracene, and phenanthrene can be isolated from this cake by fractional crystallization and/or extraction.

The commercial uses of carbazole have been mostly European developments. They include dyes such as Hydron Blue, pesticides, and vinylcarbazole polymers. In the U. S., the latter two have apparently never progressed beyond the pilot plant stage.

As a part of a wide-ranging utilization research program for the high boiling components of coal tar, the chemistry of carbazole was surveyed. These studies included reduction, oxidation, nitration-reduction, chlorination, alkylation, carboxylation, sulfonation, acetylation, pyridylethylation, and dye chemistry.

Scientifically and in their commercial prospects, the studies of the reduction of carbazole were perhaps the most fruitful. The present paper deals, for these reasons, with this aspect of carbazole chemistry.

In the past, the reduction of the carbazole nucleus by chemical agents or by catalytic hydrogenation has been difficult. Thus, compared with aromatics and certain other nitrogen heterocyclics such as acridine, indole, and phenylpyrrole, carbazole is much more resistant to catalytic hydrogenation. The first report (4) of the catalytic hydrogenation of carbazole claimed the formation of 2,3-diethylindole as the main product. However, none of the subsequent investigators were able to substantiate this claim. von Braun and Ritter (5) were actually unable to hydrogenate purified carbazole in the presence of a nickel catalyst at 260°C. and 450 psig., and obtained only fair yields of 9-methyl-1,2,3,4-tetrahydrocarbazole and 1,2,3,4,5,6,7,8-octahydro-9-methylcarbazole from 9-methylcarbazole. The perhydrogenation of carbazole in an organic solvent at 160-220°C. and 590-1200 psig., using a nickel catalyst, was reported

(4) Padoa and Chiaves, *Atti R. Accad. Lincei*, 16, 762 (1908); *Gazz. chim. ital.* 38, 236 (1903).

(5) v. Braun and Ritter, *Ber.*, 55, 3792 (1922).

in a 1930 German patent (6). The best data were obtained by Adkins and Coonradt (7) who hydrogenated carbazole in the presence of Raney nickel at 230°C. to obtain an 87%

(6) German pat. 514,822 (1930).

(7) Adkins and Coonradt, *J. Am. Chem. Soc.*, 63, 1563 (1941).

yield of dodecahydrocarbazole; when they used a copper chromite catalyst under these conditions, a 72% yield of 1,2,3,4-tetrahydrocarbazole was obtained. However, this procedure required rather high pressures (of 3600-4400 psig.) and highly purified materials.

Prior work on the chemical reduction of carbazole was limited to the sodium-alcohol system. In 1907, the preparation of 1,4-dihydrocarbazole from carbazole by this reagent was reported (8). Later it was shown that the product of this reaction is a mixture containing at least 50% of carbazole, tetrahydrocarbazole, plus unknowns (9). Surprisingly, a 1950 publication again claimed the isolation of 1,4-dihydrocarbazole from this mixture (10). 1,2,3,4-Tetrahydrocarbazole can indeed be prepared in fair yield by the reduction of carbazole with sodium and alcohol (11).

-
- (8) Schmidt and Schall, Ber., 40, 3225 (1907).
(9) Barclay, Campbell, and Gow, J. Chem. Soc., 1946, 997.
(10) Sanna, Gazz. chim. ital., 80, 572 (1950).
(11) Zanetti, Ber., 26, 2006 (1893).
-

The present paper concerns (1) a reinvestigation of the catalytic hydrogenation of carbazole, (2) a study of the chemical reduction of carbazole and derivatives with lithium metal in amine, and (3) some new N-substituted derivatives of carbazole and its hydrogenation products.

1) The Hydrogenation of Carbazole

Rhodium catalysts are effective for the hydrogenation of aromatic compounds and heterocyclics like pyrrole and pyridine at room temperature and atmospheric pressure while ruthenium catalysts are useful for the reduction of aromatic compounds at elevated temperature and pressure (12). The use of these catalysts for the hydrogenation of condensed heterocyclic ring systems has apparently been little explored.

-
- (12) Gilman and Cohn, in "Advances in Catalysis", IX, 733 (1957), Academic Press, Inc., New York, N. Y.
-

An investigation of the hydrogenation of carbazole revealed that 5% Rh-C and 5% Ru-C were about equally effective, with reduction of the carbazole ring beginning at about 100°C. and 500 psig. of hydrogen. Purification of materials was unnecessary. The use of a 5% Pd-C catalyst under similar conditions gave only about one fourth of the rate of hydrogenation realized with the rhodium or ruthenium catalysts. The conditions for obtaining optimum yields of either tetrahydro- or dodecahydrocarbazole are summarized in Table I. Thus, in the decalin medium the reduction of carbazole with a 5% Ru-C catalyst at 250 psig. of hydrogen and 250°C., when stopped at the pressure drop calculated for tetrahydrocarbazole, gave a 53% yield of tetrahydrocarbazole plus a 15% recovery of carbazole, the remainder of the product being higher hydrogenation products. The reduction of carbazole in decalin solution at 500 psig. and 200°C. in the presence of 5% Ru-C gave an 81% yield of dodecahydrocarbazole. Surprisingly, carbazole could be reduced in water suspension (pH 5.5) at 1000 psig. (320 psig. hydrogen partial pressure) and 200°C., using a 5% Rh-C catalyst, to obtain a 93% yield of dodecahydro-

carbazole. Both U.O.P. prereduced and stabilized nickel-on-kieselguhr and sponge nickel catalysts worked equally well under these conditions, to give 88-90% yields of dodecahydrocarbazole. In all of these systems the yields of tetrahydrocarbazole were only fair when the hydrogenation of carbazole was stopped at the theoretical hydrogen uptake for tetrahydrocarbazole. When carbazole was hydrogenated in an aqueous suspension, adjusted to pH 12 with potassium hydroxide, at 1000 psig. (320 psig. hydrogen partial pressure) and 250°C., the hydrogen uptake practically stopped at the tetrahydro stage and an 87% yield of 1,2,3,4-tetrahydrocarbazole could be isolated. The same experiment carried out in a water medium adjusted to pH 10 gave only a 67% yield of tetrahydrocarbazole.

As expected, 9-alkylcarbazoles were also easily reducible. For example, 9-methylcarbazole could be hydrogenated in decalin solution at 500 psig. of hydrogen and 150-200°C., using a 5% Pd-C catalyst, to give an 88% yield of N-methyldodecahydrocarbazole.

The facile perhydrogenation of ring-substituted carbazoles was demonstrated by the example of 3-amino-9-methylcarbazole (I). The hydrogenation of 0.135 m. of this compound in water containing 0.27 m. of hydrochloric acid in the presence of 5% Rh-C catalyst at 50-100°C. and 800-350 psig. gave a 72% yield of 3-amino-9-methyldodecahydrocarbazole (II, fig. 3).

It is known that partial hydrogenation of ring-substituted carbazoles is difficult to stop at a specific stage of reduction. In addition, the ring containing the substituent and/or the unsubstituted ring may be exclusively or simultaneously hydrogenated. The only such example investigated by us was 3-amino-carbazole (III) which gave a 38% yield of unchanged starting material and an 11% yield of 3-amino-1,2,3,4-tetrahydrocarbazole (IV) as the only identified product. The latter compound is structurally similar to the indole derivative tryptamine. 3-Amino-1,2,3,4-tetrahydrocarbazole was tested for its ability to inhibit (serotonin) monoamine oxidase and found to be moderately active but not as effective as Marsilid, amphetamine hydrazine, harmine, and harmaline for this purpose*.

* Private communication from Dr. Bernard Witkop, Chief, Laboratory of Chemistry, National Institute of Arthritis and Metabolic Diseases.

Tetrahydrocarbazole itself should be a versatile intermediate useful in fields such as dyes, pharmaceuticals, and plastics. For example, the monomer 9-vinyl-1,2,3,4-tetrahydrocarbazole is made in excellent yield by vinylating carbazole with acetylene (13).

(13) W. Reppe, Ann., 601, 133 (1956).

Dodecahydrocarbazole possesses antioxidant activity in gasoline and should have anticorrosive action. These combined properties may make dodecahydrocarbazole a useful low-cost additive to fuels and lubricants. Dodecahydrocarbazole should also be useful in dye chemistry as a component of certain dye salts.

2) The Reduction of Carbazole Compounds with Lithium in Amine

The chemical reduction of benzenoid rings to the tetrahydro (cyclohexene) and hexahydro (cyclohexane) stage by means of the lithium in amine reagent has been reported recently (14, 15). The reduction of carbazole compounds with this reagent was investigated (Figure 4). It was hoped that 1,4-dihydrocarbazole might be obtained by

(14) Benkeser, Robinson, Sauve, and Thomas, J. Am. Chem. Soc., 77, 3230 (1955).

(15) Reggel, Fridel, and Wender, J. Org. Chem., 22, 891 (1957).

1,4-addition of lithium to one of the benzenoid rings of carbazole. However, when carbazole dissolved in n-propylamine was reacted with 2 moles of lithium per mole of carbazole, a product of m.p. 137-45°C. was obtained which could not be purified by recrystallization. When 4 moles of lithium per mole of carbazole were employed for the reduction, a 90% yield of 1,2,3,4-tetrahydrocarbazole was obtained. The latter was resistant to further reduction by lithium in amine. This result was unexpected, since aromatic amines such as N-methylaniline have been readily reduced by this reagent (16).

(16) Benkeser, Lambert, Ryan, and Stoffey, J. Am. Chem. Soc., 80, 6573 (1958).

Presumably, tetrahydrocarbazole, which is more basic than carbazole, formed a N-lithium compound and was thus stabilized against further reduction. This presumption was strengthened by the reduction of 9-methylcarbazole to 9-methyl-1,2,3,4,10,11-cis-hexahydrocarbazole with 12 moles of lithium per mole of carbazole in n-propylamine in good yield. The intermediate 9-methyl-1,2,3,4-tetrahydrocarbazole no longer has a hydrogen atom on the nitrogen atom and was therefore reduced further. This is the first synthesis of a hexahydrocarbazole directly from carbazole. cis-Hexahydrocarbazole itself was also resistant to further reduction by lithium in amine, yielding an 82% recovery of hexahydrocarbazole.

The reduction of ring-substituted carbazoles was briefly investigated and proved to be more complex. Thus, the reduction of 3-aminocarbazole with lithium metal in ethylene diamine gave a 27% recovery of starting material as the only identified product. A similar reduction of carbazole-3-carboxylic acid gave a 24% yield of a product tentatively identified as 1,4-dihydrocarbazole-3-carboxylic acid plus a 35% yield of an unidentified nonacidic product.

3) Some New N-Substituted Carbazole Derivatives

The noncatalytic reaction of 2- and 4-vinylpyridines with nucleophilic reagents such as sodiomalonic ester, piperidine, diethylamine, and sodium bisulfite was first recognized by Doering and Weil (17). Subsequently, this reaction, using alkali metal or acid catalysts, was applied to aromatic amines such as N-methylaniline (18),

(17) Doering and Weil, J. Am. Chem. Soc., 69, 2461 (1947).

(18) Reich and Levine, J. Am. Chem. Soc., 77, 4913 (1955).

and nitrogen heterocyclics such as pyrrole (18) and indole (19). The literature mentions that diphenylamine, which is structurally similar to carbazole, could not be pyridylethylated (18).

(18) Reich and Levine, J. Am. Chem. Soc., 77, 4913 (1955).

(19) Gray and Archer, *ibid.*, 72, 3554 (1957).

Carbazole and the hydrocarbazoles, which had not been pyridylethylated before, have now been reacted with 2- and/or 4-vinylpyridine to give excellent to fair yields of the corresponding N-pyridylethylation products (Fig. 5 shows an example) as listed in Table II. Carbazole itself and 1,2,3,4-tetrahydrocarbazole, which are very weak bases, were reacted in pyridine solution with vinylpyridine in the presence of alkali metal catalysts. 1,2,3,4,10,11-cis-Hexahydrocarbazole and dodecahydrocarbazole, which are relatively strong bases, were pyridylethylated using acid catalysts. Pyridylethylated carbazole has fungicidal properties which will be reported in detail elsewhere.

Although dodecahydrocarbazole has been known for more than 30 years, only a few derivatives have been prepared from it. A survey of the reactions of dodecahydrocarbazole revealed that it undergoes, as expected, all the usual transformations of a secondary cycloaliphatic amine. The melting points of the solid derivatives were not too sharp which was not surprising since the dodecahydrocarbazole was a mixture of stereoisomers. The new derivatives of dodecahydrocarbazole are tabulated in Table III.

The potential uses of these derivatives lie in the areas of corrosion inhibitors, fungicides, solvents, antioxidants, plasticizers, textile chemicals, resin curing agents and catalysts, and ore flotation agents. For example, the nitrous salt of dodecahydrocarbazole was found to be a good vapor phase corrosion inhibitor; and 9-dodecoyldodecahydrocarbazole might find application as a plasticizer with mild antioxidant properties.

Acknowledgements: The authors wish to thank Dr. J. O'Brochta for continued guidance and Messrs. J. Martini and H. Hampson for their experimental assistance.

Experimental

All melting and boiling points are uncorrected.

Dodecahydrocarbazole. - A 1-gal. stainless steel autoclave (stirring-type) was charged with 167 g. (1.0 m.) of 97% carbazole, 85 g. of a prereduced, stabilized nickel-on-kieselguhr catalyst (55% Ni), and 1000 ml. of water. The autoclave was sealed, the mixture was stirred and heated to 200°C., at which temperature the autogeneous pressure was 630 psig. The autoclave was pressured to 1000 psig with hydrogen, and repressured to 1000 psig. whenever the pressure fell to 700 psig. After 6 hrs., no further pressure drop occurred. The catalyate

was filtered. The insolubles were extracted with 500 ml. of benzene. The benzene extract was then used to extract the filtrate. The organic phase was distilled through a 4-in. Vigreux column to give 157 g. (88% yield) of dodecahydrocarbazole, b.p. 124-5°C./10 mm. (20).

(20) Adkins and Coonradt, J. Am. Chem. Soc., 63, 1563 (1941), report b.p. 124-125°C./10 mm.

The other perhydrogenations of carbazole were carried out similarly. The amount of catalyst used in the case of 5% rhodium-on-carbon or 5% ruthenium-on-carbon was 2-5% by wt. of the carbazole charge.

1,2,3,4-Tetrahydrocarbazole by the Hydrogenation of Carbazole. - A 1-gal. autoclave, charged with 167 g. (1.0 m.) of carbazole, 1000 ml. of water adjusted to pH 12 with dilute potassium hydroxide, and 85 g. of a prereduced nickel-on-kieselguhr catalyst, was stirred and heated to 250°C. A pressure of 680 psig. was reached. The autoclave was then pressured to 1000 psig. with hydrogen. A fast reaction ensued. The autoclave was repressured to 1000 psig. with hydrogen when the pressure fell to 800 psig. In 60 min., the hydrogen absorption had practically stopped. The mixture was allowed to cool, the autoclave was vented, and the catalyzate was filtered. The insolubles were extracted with a 500-ml. and a 200-ml. portion of benzene. The combined benzene extract was shaken with three 200-ml. portions of 30% hydrochloric acid, in which carbazole is insoluble. Dilution of the combined acid extracts with water to give a 15% hydrochloric acid concentration precipitated tetrahydrocarbazole. The precipitate was filtered off, washed with water, a little ammonia, and again with water, then dried to give 134 g. (87% yield) of 1,2,3,4-tetrahydrocarbazole, m.p. 115-8°C.; after one recrystallization from 95% ethanol, m.p. 118-9°C. (21).

(21) Adkins and Coonradt, loc. cit., report m.p. 115-115.5°C.

3-Amino-9-methyldodecahydrocarbazole. A 1-gal. stirring autoclave was charged with 26.0 g. (0.135 m.) of 3-amino-9-methylcarbazole, 1.0 l. of water, 23.8 g. (0.27 m.) of concentrated hydrochloric acid, and 4.0 g. of 5% Rh-C catalyst. The mixture was hydrogenated at 50-100°C. at 800-350 psig. of hydrogen pressure during 4 hrs. after which time no further pressure drop was observed. The catalyzate was filtered through a Celite filter. The clear filtrate was boiled for a short time and filtered again to remove solids which had formed. The filtrate was concentrated to 160 ml. volume, made alkaline with 28% ammonium hydroxide, and extracted with two 100-ml. portions of ether. The extract was dried over anhydrous sodium sulfate, concentrated, and the residual oil was distilled through a 4-in. Vigreux column to give 20.0 g. (72% yield) of a colorless mobile liquid, b.p. 115-25°C./3 mm. Redistillation gave a heart cut of b.p. 115-9°C./3.5 mm.

Anal. Calcd. for $C_{13}H_{24}N_2$: Neutral equiv., 104; N, 13.4
Found: Neutral equiv., 108; N, 12.8

1,2,3,4-Tetrahydrocarbazole by Reduction of Carbazole with the Lithium in Amine Reagent. - To a solution of 8.35 g. (0.05 m.) of carbazole in 100 ml. of n-propylamine was added 1.46 g. (0.21 m.) of lithium ribbon in small pieces during 5 hrs. The mixture was stirred at room temperature overnight. Thereafter, 17 g. (0.32 m.) of ammonium chloride was added to the solution, the mixture was evaporated to dryness under vacuum, and the solid residue was taken up in 100 ml. of water. The resultant slurry was extracted with two 100-ml. portions of ether. The extract was washed with water and dried over anhydrous sodium sulfate. Evaporation of the ethereal filtrate to dryness gave 8.6 g. (100% yield) of solids, m.p. 115-19°C. One gram of this product was recrystallized from 5 ml. of cyclohexane to give 0.9 g. (90% yield) of tetrahydrocarbazole, m.p. 119-20°C.

A similar reduction of carbazole in ethylenediamine at 85-100° with lithium gave a 87% yield of tetrahydrocarbazole.

3-Amino-1,2,3,4-Tetrahydrocarbazole. - A solution of 36.4 g. (0.2 m.) of 3-aminocarbazole in 200 ml. (0.2 m.) of 1 N hydrochloric acid and 800 ml. of water was hydrogenated in a 1-gal. stirring autoclave in the presence of 3.0 g. of 5% Ru-C catalyst at 100°C. and 820 psig. of hydrogen for 12 hrs. The catalyze was then filtered to remove 17 g. of insolubles, i.e. a 38% recovery of 3-aminocarbazole (corrected for catalyst wt.) was made. Extraction of the insolubles with ethanol and concentration of the extract gave 3-aminocarbazole, m.p. 238-41°C. The aqueous filtrate was alkaline (pH 8) due to the formation of higher hydrogenated carbazoles. It was concentrated to 200 ml. volume, made strongly alkaline with ammonium hydroxide, and extracted with ether. The extract was evaporated to dryness to give 4.2 g. (11% yield) of solids, m.p. 116-70°C. After recrystallization from ethanol, m.p. 170-2°C. A sample was titrated in acetic acid with perchloric acid. The calculated neutralization equivalent for the title compound is based on the fact that tetrahydrocarbazole was found to be too weakly basic to be titratable.

Anal. Calcd for $C_{12}H_{14}N_2$: N. E. 186; Found, N. E. 184.

Since hexahydrocarbazole was titratable, the alternate structure, 3-aminohexahydrocarbazole $C_{12}H_{16}N_2$, would have a neutralization equivalent of 94. 6-Amino-tetrahydrocarbazole is eliminated on the basis of its m.p. 152°. The ultraviolet spectrum of the product was similar to that of tetrahydrocarbazole but different from that of hexahydrocarbazole (Table IV).

9-Methyl-1,2,3,4,10,11-cis-hexahydrocarbazole. - A solution of 9.1 g. (0.05 m.) of 9-methylcarbazole in 200 ml. of n-propylamine was treated with 4.3g. (0.62 m.) of lithium ribbon in small pieces during 5 hrs. at 25°C. After stirring for an additional 1.5 hrs., some unreacted lithium pieces were removed with forceps. Finally, 33.2 g. (0.62 m.) of ammonium chloride was added to the solution. The solvent was evaporated. The residue was taken up in water and extracted with two 100-ml. portions of ether. The extract was dried over Drierite, filtered, and the filtrate was evaporated to give 9.8 g. of residue. This crude product was distilled through a semimicro Vigreux column to give 6.5 g. (71% yield) of 9-methylhexahydrocarbazole, b.p. 125-35°C./1 mm., 98 mole % pure by nonaqueous titration with perchloric acid in acetic acid. An authentic sample of 9-methyl-1,2,3,4-tetrahydrocarbazole was too weakly basic to be titrated by this method.

Anal. Calcd. for $C_{13}H_{17}N$: Neutral. equiv., 187
Found: Neutral. equiv., 190

The ultraviolet spectrum of the product was similar to that of 1,2,3,4,10,11-cis-hexahydrocarbazole itself except that the absorption maxima were shifted to slightly higher wavelengths. This corroborates the proposed structure of the product further, since a similar slight shift to higher wavelength was observed in the ultraviolet spectra of 9-methyl-1,2,3,4,-tetrahydrocarbazole vs. 1,2,3,4-tetrahydrocarbazole. The comparative spectral data are given in Table IV.

Reduction of Carbazole-3-carboxylic Acid with Lithium in Amine. -

To a solution of 3.4 g. (0.016 m.) of carbazole-3-carboxylic acid in 100 g. of ethylamine was added at 25°C. during 40 min. 0.78 g. (0.112 m.) of lithium ribbon in small pieces. After stirring for 2 additional hrs. at 25°C., 5.95 g. (0.112 m.) of ammonium chloride was added. The mixture was evaporated to dryness under vacuum. The residue was digested in water and the mixture was extracted with ether. The extract was evaporated to dryness to give 1.8 g. of a nonacidic solid. This solid was distilled through a Bantamware column to give 1.2 g. (35 wt. % yield) of low-melting yellow solids, b.p. 220-70°C. (bath)/2 mm., which were not further investigated. The alkaline aqueous solution obtained above was acidified and extracted with ether. The ether extract was evaporated to dryness to give 0.8 g. (24 wt. % yield) of solids, m.p. 215-9°C; after vacuum sublimation, m.p. 220-1°C., colorless crystals. While carbazole-3-carboxylic acid has a -CO-absorption peak at 1660 cm^{-1} , the product showed -CO-absorption at 1685 cm^{-1} . This indicated that the carboxyl group of the product was in conjugation with a double bond (22) and that the product was probably 1,4-dihydrocarbazole-3-carboxylic acid.

(22) L. J. Ballamy, "The Infra-red Spectra of Complex Molecules", 2nd Ed., John Wiley & Sons, New York 1958, p. 168

Pyridylethylation of Carbazole and 1,2,3,4-Tetrahydrocarbazole. - A stirred mixture of 167 g. (1.0 m.) of carbazole, 115 g. (1.1 m.) of 2-vinylpyridine, 2.0 g. (0.05 m.) of small pieces of metallic potassium, and 1000 ml. of pyridine was refluxed for 3 hrs., then cooled to 60°C., and stirred for 0.5 hr. with 15 ml. of absolute ethanol. The solution was concentrated to ca. 250 ml. volume and poured into 2 l. of ice-water. An oil separated which solidified quickly. The solid was filtered off, washed with water, and air-dried to give 265 g. (98% yield) of crude product, m.p. 73-5°C. After recrystallization from 95% ethanol, m.p. 77-8°C., 99 mole % pure by nonaqueous titration with perchloric acid in acetic acid (only the pyridine N is basic enough to be picked up by this method).

Anal. Calcd. for $\text{C}_{18}\text{H}_{16}\text{N}_2$: Neutral. equiv., 272
Found: Neutral. equiv., 275

The infrared spectrum of the product showed no NH absorption peak, indicating the formation of a 9-substituted carbazole.

The reactions of carbazole with 4-vinyl pyridine and of 1,2,3,4-tetrahydrocarbazole with 2- and 4-vinylpyridine were carried out in similar fashion.

Pyridylethylation of 1,2,3,4,10,11-cis-Hexahydro- and Dodecahydrocarbazole. - A mixture of 17.3 g. (0.1 m.) of cis-hexahydrocarbazole, 10.5 g. (0.1 m.) of 2-vinylpyridine, 6.0 ml. (0.1 m.) of glacial acetic acid, and 50 ml. of methanol was stirred and refluxed for 8 hrs. The alcohol was then stripped off and the concentrate was poured over 500 g. of crushed ice. A sticky gum formed. The mixture was made alkaline by the addition of 100 ml. of 10% sodium hydroxide and extracted with two 250-ml. portions of ether. The combined extracts were dried over Drierite, filtered, and concentrated. The residue (27.0 g., 97% yield) was distilled through a 4-in. Vigreux column to give 22.4 g. (80% yield) of a fraction of b.p. 175-80°C./1 mm., 98 mole % pure 9-[omega-(2-pyridyl) ethyl] - 1,2,3,4,10,11-cis-hexahydrocarbazole by nonaqueous titration with perchloric acid in acetic acid (both nitrogen atoms are basic enough to be picked up by this method).

Anal. Calcd. for $C_{19}H_{23}N_2$: Neutral. equiv., 139.5
Found: Neutral. equiv., 142.4

Dodecahydrocarbazole was reacted with 4-vinylpyridine in the same manner, except that no solvent methanol was used.

Table I
Catalytic Hydrogenation of Carbazole

<u>Catalyst</u> ^{a)}	<u>Medium</u>	<u>Total Pressure (psig.)</u>	<u>Hydrogen Partial Pressure (Psig.)</u>	<u>Temp. °C.</u>	<u>Main Product</u> ^{b)}
5% Ru-C	Decalin	250	250	250	53% THC
5% Ru-C	"	500	500	200	81% DHC
5% Rh-C	Water (pH 5.5)	1000	380	200	93% DHC
U.O.P.-Ni	"	"	"	"	86% DHC
Sponge-Ni	"	"	"	"	90% DHC
U.O.P.-Ni	Water (pH 12)	"	320	250	87% THC
U.O.P.-Ni	Water (pH 10)	"	"	"	67% THC

a) Ru-C = Ruthenium on carbon; Rh-C = rhodium on carbon; Universal Oil Products Ni catalyst = Prerduced and stabilized nickel on kieselguhr (55% Ni).

b) THC = 1,2,3,4-tetrahydrocarbazole; DHC = dodecahydrocarbazole.

Table II

Pyridylethylation of Carbazole and Hydrocarbazoles

<u>Nucleophile^{a)}</u>	<u>Vinylpyridine (VP)</u>	<u>Catalyst</u>	<u>Solvent</u>	<u>% Yield of Adduct</u>	<u>Melting or Boiling Point, °C.</u>
Carbazole	2-VP	K	Pyridine	98	m. 77-8
"	4-VP	Na	"	97	m. 173-4
THC	2-VP	"	"	29	b. 194-201/3 mm.
"	4-VP	"	"	55	m. 83-4
HHC	2-VP	Acetic Acid	Methanol	80	b. 175-80/1 mm.
DHC	4-VP	"	None	65	b. 174-82/2 mm.

a) THC = 1,2,3,4-tetrahydrocarbazole; HHC = 1,2,3,4,10,11-cis-hexahydrocarbazole;
DHC = dodecahydrocarbazole

Table III

Derivatives of Dodecahydrocarbazole

Dodecahydrocarbazole Reacted With	Product ^{a)} (% Yield)	Physical Properties
Lauroyl Chloride	9-Dodecoyl DHC (87)	pale yellow oil, b.p. 247-52°C./3 mm.
KCN	DHC-9-carboxamide (74)	colorless crystals; m.p. 167-70°C. (f. EtOH)
Urea	" (88)	m.p. 180-2°C. (f. dil. EtOH)
CS ₂	N,N-(Perhydro-o,o'-biphenylene) dithiocarbamate (100)	almost colorless solid; m.p. 184-91°C. (f. EtOH)
HCOOCH ₃	8-Formyldodecahydrocarbazole (90)	colorless liquid, b.p. 157-9°C./4 mm.
CH ₂ = CH ₂ CN	9-(2-Cyanoethyl) DHC (89)	colorless oil, b.p. 157-61°C./2 mm.
Cyclohexanone	9-(1-Cyclohexenyl) DHC (62)	pale yellow oil, b.p. 155-60°C./1 mm.
CH ₂ O + alpha-methylstyrene	1-(9-dodecahydrocarbazolyl)-3-phenyl-butene-3 (12)	colorless liquid, b.p. 169-80°C./1 mm.
Succinic Anhydride	9-(3-Carboxypropionyl) DHC (68)	colorless liquid, m.p. 111-5°C.
Phthalic Anhydride	9-(2-Carboxybenzoyl) DHC (74)	colorless solid, m.p. 182-7°C.
Maleic Anhydride	9-(omega-Carboxyacrylyl) DHC (65)	colorless solid, m.p. 124-9°C.
HNO ₂	Nitrous salt of DHC (68)	colorless solid, m.p. 150-5°C.
CH ₃ COOH	Acetate of DHC (96)	colorless solid, m.p. 148-53°C.
BF ₃	BF ₃ Adduct of DHC (89)	colorless solid, m.p. 212-4°C.

a) DHC = dodecahydrocarbazole

Table IV
Comparative Ultraviolet Spectral Data

<u>Compound</u>	<u>λ max (EtOH)</u>	<u>log E</u>
1,2,3,4-Tetrahydrocarbazole	227.5, 283, 291	4.5, 3.9, 3.8
9-Methyl-1,2,3,4-tetrahydrocarbazole	230, 287, 293.4	4.6, 3.8, 3.8
3-Amino-1,2,3,4-tetrahydrocarbazole	225, 283	4.5, 3.8
1,2,3,4,10,11-cis-Hexahydrocarbazole	241, 292	3.9, 3.4
9-Methyl-1,2,3,4,10,11-cis-hexahydrocarbazole	244, 294-5	3.8, 3.3

Figure 1

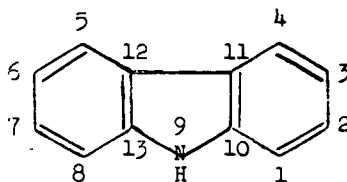


Figure 2

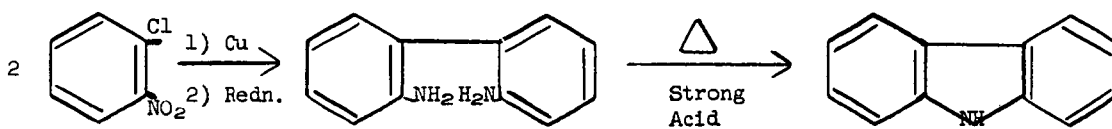


Figure 2

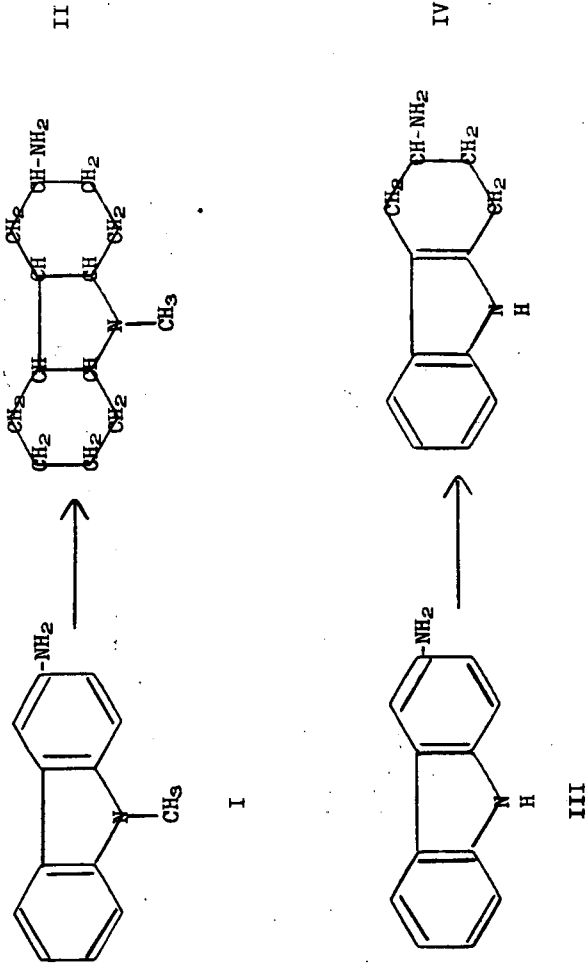


Figure 4

Lithium in Amine Reductions

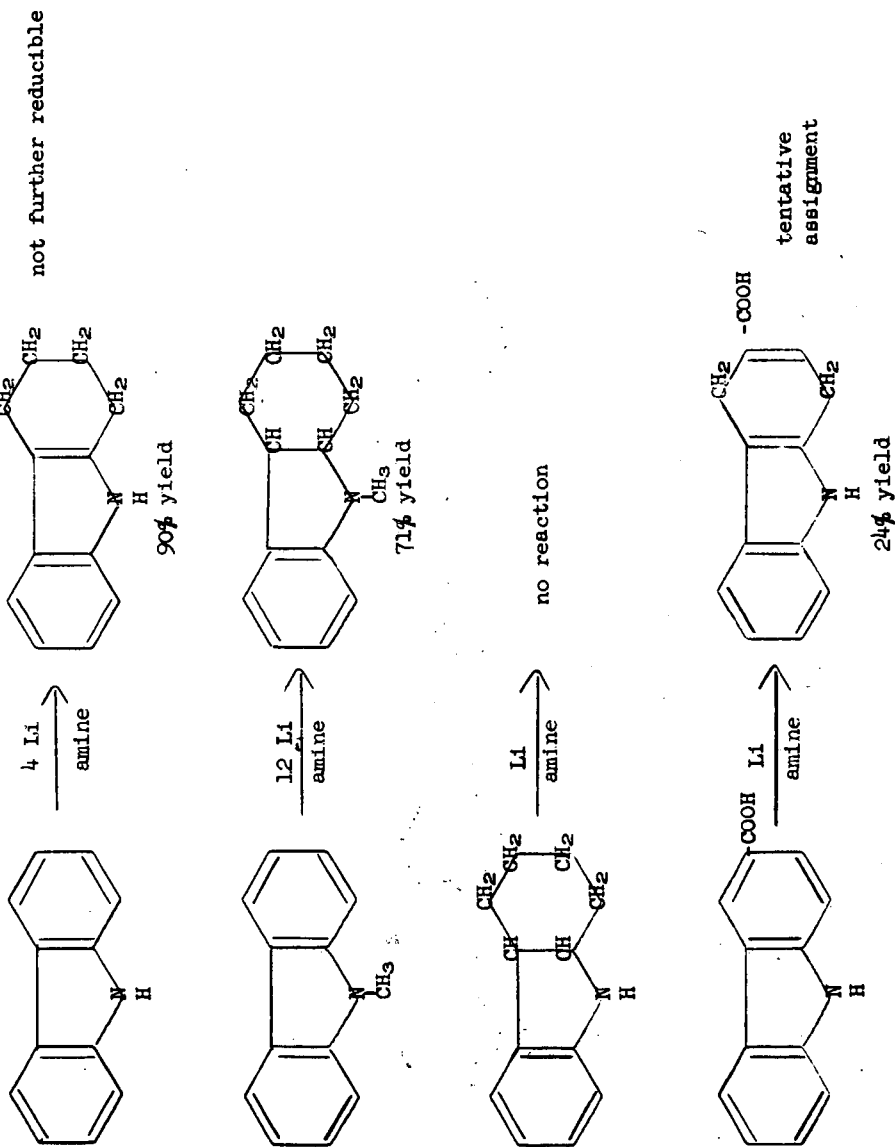
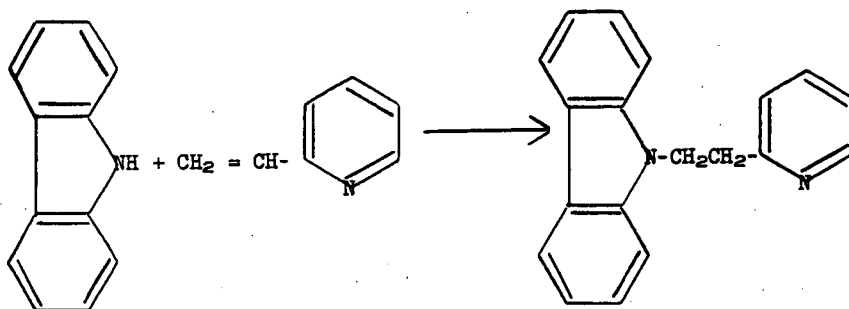


Figure 5



THE GAS-CHROMATOGRAPHIC ANALYSIS OF COKE-OVEN
BENZENE-TOLUENE-XYLENE (BTX),
BENZENE-TOLUENE (BT), AND BENZENE
FOR MINOR COMPONENTS

A. J. Miskalis

United States Steel Corporation
Applied Research Laboratory
Monroeville, Pennsylvania

Introduction

Rapid methods for analyzing coke-oven benzene-toluene-xylene (BTX), benzene-toluene (BT) and benzene fractions for minor components are necessary to supplement purification processes for improving the quality of the benzene, toluene, and xylene fractions of light oil. During the investigation of methods for removing sulfur-containing compounds and other impurities from BTX and BT fractions, it was suspected that catalyst poisoning and the formation of undesirable resins were caused at least in part by cyclopentadiene, which occurs in such fractions when they are first collected. Since cyclopentadiene dimerizes easily, a method of analyzing for both the monomer and the dimer was desired. Along with the investigation of purification processes, one of the recurring analytical problems in our laboratory is the determination of trace impurities in refined light-oil products. The cyclohexene, cyclohexane, and methylcyclohexane contents of benzene were of particular interest.

Colorimetric methods for detecting and determining cyclopentadiene (1,10,13) and dicyclopentadiene (6,13) have been reported. Methods in which a maleic anhydride reaction (3,9) is utilized have been published. The condensation reaction between cyclopentadiene and aldehydes or ketones to form highly colored fulvenes has been used for the quantitative determination of cyclopentadiene and dicyclopentadiene in hydrocarbon mixtures (7). Techniques that involve saponification (2) and bromination (5,12) have been investigated. Infrared (11) and ultraviolet (8,14) spectrophotometric techniques have been published for determining cyclopentadiene and dicyclopentadiene in hydrocarbon mixtures. Various procedures, including mass spectrometry and infrared spectroscopy, can be used to determine the paraffin content of aromatic hydrocarbons. The total paraffin content of benzene is obtained by the ASTM sulfonation procedure D851-47.

Most of these methods are complicated by difficulties associated with interfering compounds, lengthy analysis times and, in some instances, poor sensitivity. The ASTM method for paraffins is not applicable to the analysis of specific paraffins. Mass-spectrometric and infrared spectrophotometric methods are much too difficult, if not impossible, for use in the hydrocarbon concentration ranges of particular interest in this investigation.

The purpose of this paper is to describe the apparatus and materials used in developing gas-liquid chromatographic methods of analysis for determining (1) cyclopentadiene and dicyclopentadiene in BTX and BT fractions, and (2) cyclohexene, cyclohexane, and methylcyclohexane in benzene.

Experimental

Apparatus

The instrument used was the Perkin-Elmer Corporation Model 154-B Vapor Fractometer. A 0-10 millivolt recorder (Leeds-Northrup Co.) was used for the cyclopentadiene and dicyclopentadiene methods. For the cyclohexene, cyclohexane, and methylcyclohexane method, the same instrument was converted to a 0-1 millivolt recorder. Samples were introduced into the instrument through the liquid sample-handling valve by means of uncalibrated Perkin-Elmer capillary pipettes. Helium was used as the carrier gas. The columns and standard operating conditions for each method are listed in Table I.

Materials

The following reagents were used as standards. Phillips Petroleum Company Research Grade benzene was used in developing the methods for the analysis of cyclopentadiene and dicyclopentadiene in BTX and BT. A commercial benzene, containing a negligible amount of cyclohexane and methylcyclohexane as the only non-aromatic impurities, was used in developing the method for trace amounts of cyclohexene, cyclohexane, and methylcyclohexane in benzene. The dicyclopentadiene (95.6 wt % pure) was obtained from the Matheson Company. The cyclopentadiene was prepared by depolymerizing a portion of Matheson dicyclopentadiene, fractionating the depolymerized product, and recovering the cyclopentadiene fraction. The cyclopentadiene obtained by this method was 89.2 mole per cent pure, as determined by gas-liquid chromatography and mass spectrometry. The cyclohexene, cyclohexane, and methylcyclohexane were Phillips Petroleum Company Research Grade.

Procedure

Synthetic mixtures containing 0-2 weight per cent cyclopentadiene in benzene, 0-0.7 weight per cent dicyclopentadiene in benzene, and 0-0.5 weight per cent each of cyclohexene, cyclohexane, and methylcyclohexane in benzene were prepared. In the latter mixtures, the concentrations of the three components were varied independently, and dilutions of these mixtures were made, to provide solutions in which the concentrations of each component covered the three concentration ranges, 50-500, 5-50, and 0-5 parts per million (ppm).

All mixtures were chromatographed under the standard operating conditions. The gas-chromatographic data were corrected for purity of the standards, and calibration curves were prepared in which peak heights were related to concentration. The calibration curves were linear for all compounds in all concentration ranges investigated. In measuring the height of a peak, both in synthetic mixtures and in samples analyzed, the net height above the base line was always used.

With the peak-height and concentration data obtained in the investigation of the synthetic mixtures of cyclohexene, cyclohexane, and methylcyclohexane in benzene, equations were derived by the method of least squares; these equations were used to calculate the concentrations of cyclohexene, cyclohexane, and methylcyclohexane in benzene.

Results and Discussion

In the preliminary experimental work associated with the analysis of BTX and BT for cyclopentadiene, a 20-microliter sample of crude BTX was chromatographed under standard operating conditions. The resulting chromatogram, Figure 1,

in the range of interest (emergence time, 0 to 12 min), revealed one major peak and five minor peaks. When 20 microliters of a solution of approximately 0.5 weight per cent cyclopentadiene in benzene was chromatographed under identical conditions, the retention time for cyclopentadiene was very nearly equal to the retention time of peak number 1, Figure 1. The substance producing this peak in the chromatogram of the sample was tentatively identified as cyclopentadiene.

To confirm this tentative identification, the substance producing peak number 1, Figure 1, was trapped from the vent line of the gas chromatograph in a trap cooled in liquid nitrogen, and the material collected was analyzed by mass spectrometry. It was almost entirely cyclopentadiene. A very small concentration of an unidentified constituent was also detected. This impurity may have had a retention time similar to that of cyclopentadiene, but its concentration was so low that it could cause only negligible errors.

Not shown in Figure 1 is the remaining portion of the chromatogram (emergence time, 12 to 174 min), which revealed 11 additional peaks attributed to thiophene, toluene, the xylene isomers, dicyclopentadiene, and other unidentified constituents. These compounds were of no interest in the development of this method, except that they had to be removed from the column before another sample could be analyzed. Therefore, they were removed by back-flushing the column, a technique that reduces the time of analysis from 175 minutes (at standard operating conditions) to approximately 15 minutes. Only slight modifications of the flow system of the instrument and a few additional manipulations of controls are required.

Mass-spectrometric analysis of the cyclopentadiene used as a standard in this investigation indicated the presence of 10.1 mole per cent dicyclopentadiene. Because a pure cyclopentadiene standard was not available for comparison, it was not practicable to determine accurately the purity of the cyclopentadiene used. However, a reasonable estimate of the purity was deduced from the fact that the gas-liquid chromatogram of a 20-microliter sample of the cyclopentadiene standard revealed one major peak and eight minor peaks. None of the peaks represented the dicyclopentadiene in the sample because the retention time of this compound is much greater at the standard operating conditions than any constituent shown. No attempt was made to identify the minor peaks present in the chromatogram. However, if the thermal conductivities of the substances representing the minor peaks are assumed to be equal to that of cyclopentadiene, the combined unidentified impurities total 0.7 per cent. Consequently, the cyclopentadiene used as the standard for developing this method was assumed to be 89.2 mole per cent pure.

The average absolute error obtained in the analysis of a series of synthetic mixtures that contained 0 to 2 weight per cent cyclopentadiene was ± 0.01 weight per cent. The least detectable concentration of cyclopentadiene by the procedure described is 0.05 weight per cent.

In the preliminary experimental work associated with the analysis of BTX and BT for dicyclopentadiene, a 200-microliter portion of a silica-gel-treated BT was chromatographed under the standard operating conditions. The resulting chromatogram, Figure 2, revealed four major peaks and several minor peaks. Peak numbers 1, 2, 3, and 4 represent the benzene, toluene, xylenes, and unknown fractions of the sample. When a 200-microliter sample of a 1.4 weight per cent solution of dicyclopentadiene in benzene was chromatographed under the same conditions, the retention time for the dicyclopentadiene was very nearly equal to the retention

time of peak number 4, Figure 2. It appeared that this peak in the chromatogram of the sample was due, at least in part, to dicyclopentadiene.

This tentative identification was confirmed by the previously described gas-chromatographic mass-spectrometric analysis. The substance causing this peak in the chromatogram of the sample was mainly dicyclopentadiene with a very small proportion of a C₉ aromatic. The concentration of the C₉ aromatic was so small that any error it might cause would be negligible.

It was necessary to introduce a large quantity (200 microliters) of the sample into the instrument to obtain a measurable height for peak number 4. Although this peak appears to be relatively large in Figure 2, it was barely perceptible in the chromatogram of 200-microliter portions of several other BT samples examined.

The chromatogram of a 10-microliter sample of the Matheson dicyclopentadiene used as the standard in this determination displayed one major impurity peak. If the thermal conductivity of the substance causing this peak is assumed to be equal to that of the dicyclopentadiene, the Matheson dicyclopentadiene is 95.6 weight per cent pure. This value is based on the assumption that the major peak in the chromatogram is caused only by dicyclopentadiene. To confirm this assumption, this peak was trapped and analyzed by mass spectrometry. In addition to dicyclopentadiene, only traces of a C₉ aromatic were identified.

The method developed for determining dicyclopentadiene in BT was used to determine dicyclopentadiene in 18 samples in duplicate of crude BT or materials derived from it. The results of these analyses indicated that the average repeatability of the method is approximately 0.001 weight per cent over the range from 0 to 0.3 weight per cent dicyclopentadiene. The least detectable concentration of dicyclopentadiene by this method is 0.01 weight per cent. The time required for one measurement is approximately 10 minutes.

In the preliminary experimental work associated with the analysis of benzene for cyclohexene, cyclohexane, and methylcyclohexane, a 50-microliter portion of a sample of 1°-benzene was chromatographed under the standard operating conditions. The resulting chromatogram, Figure 3, revealed several peaks preceding the benzene peak. Tentative identification of the peaks was accomplished by chromatographing a portion of a synthetic blend of hydrocarbons in benzene and comparing the retention-time data of the synthetic blend with the retention-time data of the sample. Figure 4 illustrates the resolution of several hydrocarbons (Table II) obtained under the standard operating conditions.

To confirm the tentative identifications, the impurities of the sample of 1°-benzene were concentrated by progressive freezing, as described by Glick (4). This procedure was necessary because the impurities were in the ppm range. The concentrated impurities were chromatographed under the standard operating conditions, and the substances producing the unknown peaks were trapped as previously described and analyzed by mass spectrometry. By use of this technique, the major impurities were found to be n-heptane, cyclohexane, and methylcyclohexane (peaks no. 1, 2, and 3, respectively, of Figure 3). No cyclohexene was detected. The minor peaks shown in the chromatogram were attributed to small amounts of other hydrocarbon impurities.

Some difficulty was experienced in obtaining a paraffin-free benzene to be used as a standard in the preparation of synthetic mixtures. A commercial benzene was found that was almost completely paraffin-free. When a 500-microliter

portion of this benzene was chromatographed under operating conditions selected to give maximum sensitivity, the chromatogram, Figure 5, revealed two small peaks (peaks no. 1 and 2) preceding the benzene peak. These peaks were attributed to cyclohexane and methylcyclohexane, respectively, and their concentration was found to be approximately 2 ppm each.

The method developed for the determination of trace impurities in benzene was used to analyze several samples of benzene for cyclohexene, cyclohexane, and methylcyclohexane. The results of these analyses indicated that the average repeatability of the method is approximately 1 ppm over the range of 0 to 50 ppm and approximately 3 ppm over the range of 50 to 500 ppm for both cyclohexane and methylcyclohexane. No cyclohexene was detected in any samples analyzed. The lower limit of detection for each of the compounds was approximately 1 ppm. This value could probably be lowered by utilizing an amplifier to increase the signal from the detector. For the concentration ranges of 50-500, 5-50, and 0-5 ppm, the standard deviations for the respective compounds in the analysis of synthetic mixtures are shown in Table III.

Acknowledgements

The author wishes to thank C. F. Glick, who assisted in the development of the method for dicyclopentadiene in BTX and BT, and J. E. Friedline, who performed the mass-spectrometric analysis.

Literature Cited

- (1) Afanas'ev, B. N., Ind. Eng. Chem., Anal. Ed., 8, 15 (1936)
- (2) Bergmann, F., Japhe, H., Anal. Chem., 20, 146 (1948)
- (3) Birch, S. F., Scott, W. D., Ind. Eng. Chem., 24, 14 (1932)
- (4) Glick, C. F., Miskalis, A. J., Kessler, T. K., 136th National Meeting of the American Chemical Society, Atlantic City, New Jersey
- (5) Hammick, D. C., Langrish, D., J. Chem. Soc., 797 (1937)
- (6) Palfray, L., Sabetay, S., Kadrinoff, B., Ann. Chim. Anal. Chim. Appl., 23, 207 (1941); Chem. Zentr., 1942, 11, 2724
- (7) Powell, J. S., Edson, K. C., Fisher, E. L., Anal. Chem., 20, 213 (1948)
- (8) Powell, J. S., Edson, K. C., Ibid, 20, (1948)
- (9) Sefton, R., J. Soc. Chem. Ind., 64, 104 (1945)
- (10) Shuikin, N. I., Tulupov, V. A., Zhur. Obsheei Khim., 24, 2199 (1954)
- (11) Takeuchi, T., Tanaka, S., Coal Tar (Japan), 7, 356 (1955)
- (12) Tomicek, O., Blazek, A., Roubal, Z., Chem. Zvesti, 4, 479 (1950)
- (13) Uhrig, K., Lynch, E., Becker, H. C., Ind. Eng. Chem., Anal. Ed., 18, 550 (1946)
- (14) Vraný, M., Bohdanecký, M., Chem. Listy, 49, 936 (1955)

Table I

STANDARD OPERATING CONDITIONS

<u>Condition</u>	<u>Determination</u>		
	<u>Cyclopentadiene in BTX and BT</u>	<u>Dicyclopentadiene in BTX and BT</u>	<u>Cyclohexene, Cyclo- hexane, and Methyl- cyclohexane in Benzene</u>
Column	6 ft x 0.375 in. of o- and p- Benzylbiphenyls, 24% on Fisher Column Packing	12 ft x 0.25 in. of Dow Corning Silicone Stopcock Grease, 25% on Burrell Inert Carrier	20 ft x 0.25 in. of Paraplex U-148, 25% on Burrell Kromat-FB, and 14 ft x 0.25 in. of Paraplex G-54, 20% on Burrell Kromat-FB
Temperature (°C)	60	140	100
Pressure (psig)	5	25	20
Flow (ml/min)	210	330	50
Detector Voltage (volts)	8	8	8
Sample Size (µl)	20 (nominal)	200 (nominal)	50 (nominal) 500 (nominal)
Recorder Range (mv)	0-10	0-10	0-1

Table II

ABBREVIATED NOMENCLATURE OF C₅ TO C₈ HYDROCARBONS USED IN THE SYNTHETIC
BENZENE-PARAFFIN MIXTURE

<u>Compound</u>	<u>Abbreviated Nomenclature</u>
n-Pentane	n-P
2-Methylpentane	2-MP
n-Hexane	n-Hex
2,4-Dimethylpentane	2,4-DMP
Cyclopentane	CP
2-Methylhexane	2-MHex
3,3-Dimethylpentane	3,3-DMP
3-Methylhexane	3-MHex
Methylcyclopentane	MCP
2,3-Dimethylpentane	2,3-DMP
2,2,4-Trimethylpentane	2,2,4-TMP
3-Ethylpentane	3-EP
n-Heptane	n-Hep
1,1-Dimethylcyclopentane	1,1-DMCP
Cyclohexane	CHexane
2-Methylheptane	2-MHep
3-Methylheptane	3-MHep
Methylcyclohexane	MCH
n-Octane	n-Oct
Cyclohexene	CHexene

Table III

STANDARD DEVIATIONS OBTAINED IN THE ANALYSIS OF SYNTHETIC MIXTURES OF
CYCLOHEXENE, CYCLOHEXANE, AND METHYLCYCLOHEXANE IN BENZENE

<u>Concentration Range, ppm</u>	<u>Standard Deviations, ppm</u>		
	<u>Cyclohexene</u>	<u>Cyclohexane</u>	<u>Methylcyclohexane</u>
50-500	4.6	7.7	5.5
5-50	0.7	0.4	0.5
0-5	0.1	0.2	0.3

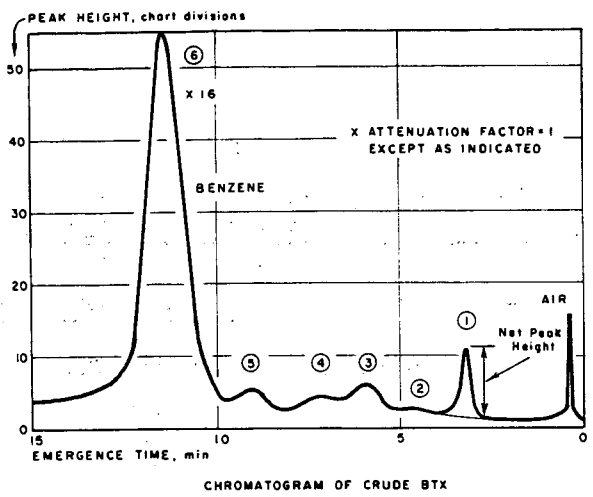


FIGURE 1

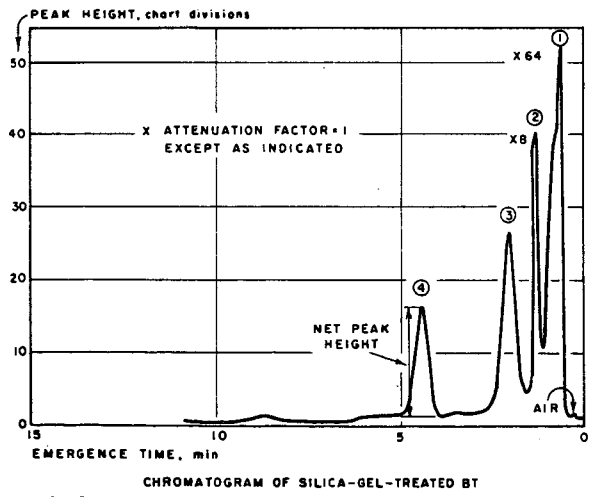
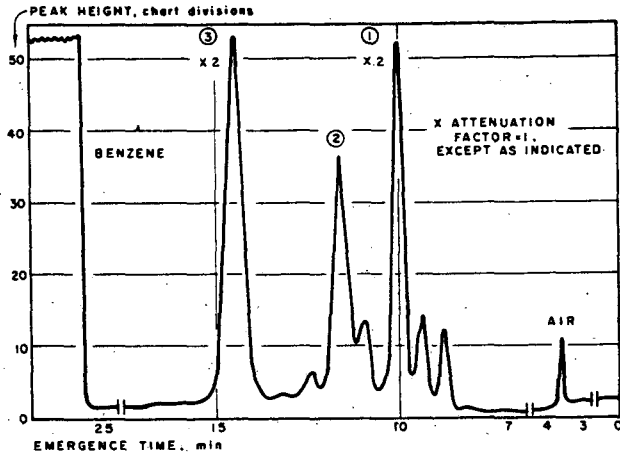
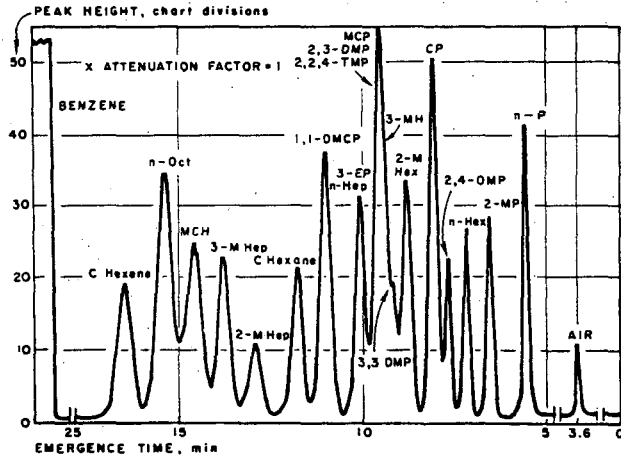


FIGURE 2



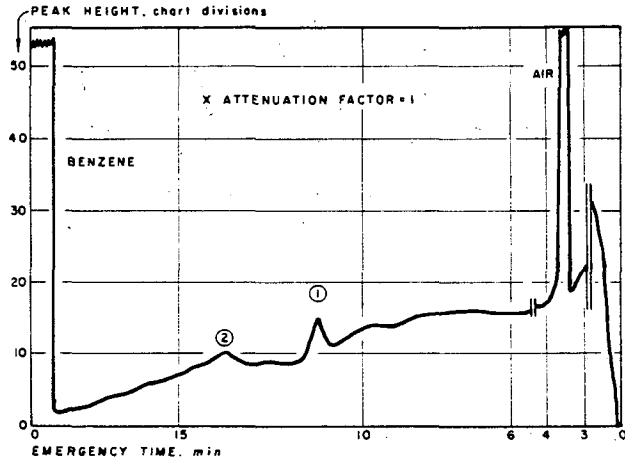
CHROMATOGRAM OF A 1° COKE-OVEN BENZENE

FIGURE 3



CHROMATOGRAM OF A SYNTHETIC MIXTURE OF HYDROCARBONS

FIGURE 4



CHROMATOGRAM OF 1° COKE-OVEN BENZENE USED AS A STANDARD
FIGURE 5

USE OF A STANTON THERMOBALANCE FOR MICROANALYSIS OF CREOSOTE

T. W. Smeal

United States Steel Corporation
Applied Research Laboratory
Monroeville, Pa.

Introduction

In the production of metallurgical coke by modern processes, the gases and tars driven from the coal are condensed to provide the raw material for a wide variety of coal chemicals. These coal chemicals, including millions of gallons of coal-tar creosote, are some of the important products of the United States Steel Corporation. As a major producer of coal-tar creosote, the Corporation has sought to learn more about the properties of creosote as a wood preservative.

One of the best methods for studying the chemistry of creosote as a wood preservative is to extract the residual creosote from wood that has been in service and for which a completely documented history is available. For analytical purposes, however, the amount of creosote that can be extracted from small core borings, sections of small test stakes, and other small specimens is not sufficient. Therefore the Applied Research Laboratory of the United States Steel Corporation initiated a search for a relatively simple method of characterizing very small samples (0.1 - 1.0 gram) to replace the Church-flask distillation, which requires a sample of 100 grams. The Church-flask distillation, which is accepted as the standard method for characterizing the composition of creosote, is fundamentally an evaporation method. Other apparatus that gives refined measurements of evaporation has been proposed by researchers at Allied Chemical Corporation and at Bell Telephone Laboratories.^{1,2}* These methods, however, were not well-adapted to our problem. It was logical to reason that since we were interested in the evaporation pattern of a small amount of volatile materials, a controlled-temperature recording balance would reveal the desired pattern. Such an instrument was available in the form of a thermobalance manufactured by the Stanton Instrument Company of London.

The Stanton Thermobalance

The Stanton thermobalance, Model TR-1 shown in Figure 1, is an analytical, continuously recording balance so constructed that the sample being weighed is supported within a tube furnace. The electrically heated furnace is constructed to operate throughout a range of 1000 centigrade degrees. The temperature is automatically raised during the weighing period by means of a program control motor. Although motors of different speeds are obtainable, the work reported here was done with a motor providing a constant rate of six degrees per minute temperature rise. The tube furnace, which contains baffles to reduce air movement, is two inches in diameter and has a hot zone two inches in depth. A platinum-rhodium thermocouple located near the furnace wall at the center of the hot zone actuates the temperature-recording pen. The furnace can be easily raised and lowered over the sample on the balance platform. The sample, itself, is contained in a small crucible supported on a rod attached to the weighing mechanism of the balance. A system of guide rods and counterweight keeps the furnace symmetrically aligned with the axis of the crucible.

* See References.

The balance mechanism is sensitive to one milligram and can record a weight change as great as 400 milligrams per minute to a maximum total weight change of 50 grams.

Use of the Thermobalance

Because the temperature-recorder thermocouple is located along the wall of the furnace rather than in the crucible, a crucible of high heat-conductivity must be used to minimize the unavoidable lag in temperature of the sample. We used a 10 cc platinum crucible conforming to Standard D-271 of the American Society for Testing Materials. Experimentation with various covers on the crucible revealed that the best correlation with existing standard was obtained when the crucible was used without a cover.

The Church-flask method of distillation that has been adopted as the standard method for creosote characterization by the American Wood-Preservers' Association (AWPA)³ and the American Society for Testing Materials (ASTM)⁴ is basically a vaporization method because there is no attempt at rectifying the vapors. The major difference in the results obtained by these two methods is caused by the difference in methods of measuring the temperature and weighing the distillate. The Church-flask method measures the temperature at a point slightly above the liquid surface, but the distillate is not weighed until it has been collected in a flask at the end of a side-arm condenser, a distance of 52 to 55 centimeters. The weight of the distillate collected at the end of the condenser is, therefore, considerably less than the weight loss of the sample. The discrepancy is the amount of vapor and condensate held up in the flask and in the condenser. The discrepancy is particularly great during the early portion of the distillation. The thermobalance, however, weighs the residue the instant the vapor leaves the surface of the sample in the crucible. The vapor loss, which is the difference in weight between the weight of the original sample and the weight of the residue, is plotted against a continuous record of temperature. The thermobalance results are not retarded and correspond more nearly to a true measure of evaporation. Plateaus or flats that are observed in the distillation pattern obtained by high-reflux distillation are not recorded by the thermobalance because there is no rectification of vapors, and the temperature is driven upward at a constant rate.

Experience has shown that for reliable results the sensitive thermobalance should be placed on an island site, preferably on a concrete floor, away from heat of direct sunlight, dampness, drafts and changes in temperature. There was also an indication that barometric pressure affected the results. Although this influence was not evaluated, it was believed that any adjustment of results would be insignificant relative to the interpretation of the data.

Developing the Procedure

The first step in developing a procedure was to determine the reproducibility of results with the thermobalance. To do this, seven vaporization patterns were made using replicate 0.5 gram samples of one creosote (Figure 2). The range of values show an acceptable level of reproducibility. Vaporization patterns made during any one day agreed more closely than replicate runs made on successive days. We believe that changes in barometric pressure, ambient temperature, and localized drafts account for a large part of the variation encountered.

The next step was to correlate the results obtained by use of the thermobalance with patterns obtained by use of a Church flask and by use of a Snyder 5-ball distillation column. Distillation through a five-ball column was chosen because it is rapid and because it is used by some researchers in the field of wood preservation. The Church-flask method is the accepted standard of the American Wood-Preservers' Association. The similarities and differences between the results of these methods are shown in Figure 3. The thermobalance results are observed to

fall between those of the other two methods. The data show that the differences between the results of the Church-flask method and thermobalance method are due primarily to the lag observed in the use of the Church-flask. Differences between the results of the five-ball column and thermobalance methods are attributed to the rapid rate of temperature rise (6 C per minute), which does not permit enough time for the low-boiling materials within the liquid to diffuse to the surface. It appears that the differences all occur below about 300 C, and all three methods agree reasonably well above this point.

The final step was to determine the ability of the thermobalance to detect differences in creosote composition. This was done by preparing thermobalance vaporization patterns of a fresh creosote and distillation residues from the same creosote after distillates to temperatures of 210, 235, 270, and 315 C had been removed with a five-ball column (Figure 4). This figure clearly shows the effects of removing the low-boiling fractions of creosote. It was reasonable to expect that the effects of any process changing the composition of the creosote could be determined by comparing vaporization patterns. Therefore, the thermobalance vaporization pattern of the chemically changed creosote was superimposed on a similar figure made with a sample of the original creosote. In addition, the thermobalance vaporization pattern provided more information than the Church or five-ball column distillation methods because a higher temperature was obtained with the thermobalance.

Application of the Method

To test the method on actual extracts from creosoted wood, a number of 3/4- by 3/4- by 30-inch stakes were withdrawn from field exposure plots. These stakes had been impregnated with a variety of creosotes and then exposed outdoors for periods of five and ten years, respectively. Each stake was sawn in sections as shown in Figure 5 so that indications of changes in the composition of creosote relative to its position within the stake could be obtained. These sections were shaved individually into fine chips. The residual creosote in each lot of chips was extracted with aromatic solvents. The solvents were then stripped from each extract by distillation under reduced pressure.

These samples of residual creosote were characterized by vaporization on the thermobalance, and the results were graphed. To interpret these graphs, the vaporization patterns were compared with patterns of the original creosotes and with patterns of creosote residues boiling above selected temperatures.

The thermobalance vaporization patterns for the residual creosotes, Figures 6 and 7, from a stake that had been in field test for ten years show that considerable losses of the more volatile compounds have occurred from all sections of the stake. It is noteworthy that the vaporization patterns for all sections fall closely to the vaporization curve obtained from creosote residue boiling above 315 C. The similarity among these curves indicates that much of the creosote boiling up to 315 C has been lost. This loss is known to occur by means of evaporation and migration. If the loss were solely by unhindered evaporation, the curves of the extract and of the control should be very close to each other. If downward migration of residual creosote occurs, then a concentration of high-boiling material can be expected in the lower portion of the stake. Such migration can be expected to appear as a net gain in preservative concentration at the lower end of the stake. This concentration was actually observed. Both below-ground sections retained about 0.08 gram of residual creosote per cubic centimeter of wood. The two sections above ground contained less than 0.05 gram per cubic centimeter.

Figure 6 shows, however, that there is considerable disparity between the vaporization curves of extracts from Section 1 and Section 2, both taken from below the groundline. What then can account for the apparent differences in composition of these extracts? We believe that soon after driving the test stake into the ground, some of the creosote begins to migrate downward through the porous cellular structure

of the wood. As it moves downward, a portion of the low-boiling volatile components are lost by evaporation from the surface of the stake. When the moving creosote approaches the moist groundline section, the downward migration is counteracted by the upward movement of moisture from the soil through the wick-like behavior of the stake. In the section of the stake just below the groundline, the net effect of these counter movements is such as to cause a concentration of creosote. This creosote by now is partially depleted of low-boiling volatile components, and has a high proportion of high-boiling relatively stable components. This concentration of high-boiling material is indicated by the relatively low position of the right end of the vaporization curve for the extract from Section 2.

If we convert the percentages of material boiling above 380 C to absolute amounts of that fraction remaining in the wood, it is found that the quantity of this fraction in Sections 3 and 4 is the same as was impregnated into the wood originally. Below ground, in Sections 1 and 2, the amount of this high-boiling fraction was about twice as great as in the freshly impregnated stake. This increase can result only from chemical changes in the creosote itself. These chemical changes are believed to result primarily from oxidation and polymerization reactions.

Figure 8 shows similar vaporization patterns for Sections 1 and 2 of a stake that had been in field test for only five years. These vaporization patterns lie between the control patterns for residues boiling above 235 and 270 C. Comparison with Figure 6 indicates that evaporation of the creosote has not progressed to the extent observed in the 10-year-old stake. Because the vaporization curves closely parallel the control curves, the chemical change is believed to be relatively small.

Summary

1. The Stanton Thermobalance can quickly and effectively characterize small (0.1 to 1.0 gram) samples of creosote.
2. The continuous vaporization pattern produced by the thermobalance is similar to that of both the Church-flask distillation (adopted by the AWPA and ASTM) and distillation through a five-ball column. The record of weight loss resulting from vaporization on the thermobalance is not retarded, as it is in a Church distillation, and thus is closer to a true measure of evaporation.
3. A method has been developed for estimating the extent of losses of creosote through evaporation.
4. A method has been developed for estimating the relative extent of chemical modifications that have occurred in wood in service during weathering.
5. Natural factors that are conducive to chemical modification of creosote appear to have their greatest effect at the ground line.

References

1. Stasse, H. L., "A Simple Fractional Distillation Test for Creosote," Proceedings, American Society for Testing Materials, 1954.
2. Leutritz, John, Jr., W. McMahon, and G. D. Deeg, "Relationship of Evaporation Pattern and Distillation Characteristics of Coal Tar Creosote," Proceedings, American Wood-Preservers' Association, 1959.
3. American Wood-Preservers' Association "Manual of Recommended Practice," Section A1-58, p 3.
4. American Society for Testing Materials "Standards," Part 4, pp 751-756 (1949).

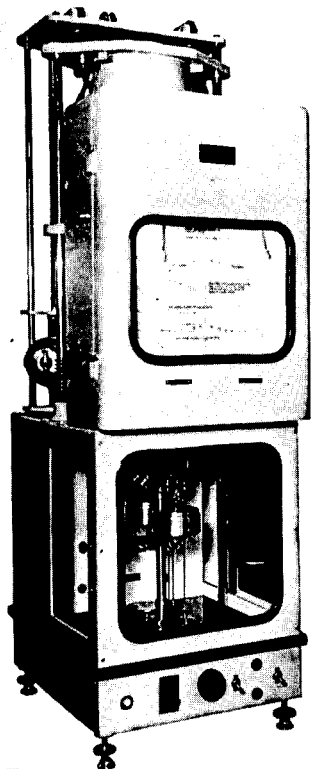


Figure 1. The Stanton Thermobalance.

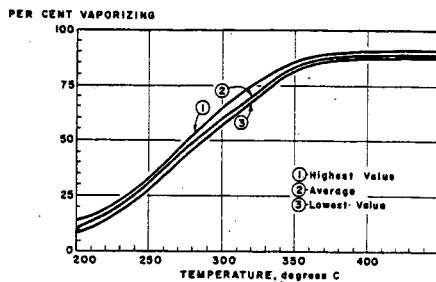


Figure 2. Range of Results From Seven Replicate Runs in Thermobalance.

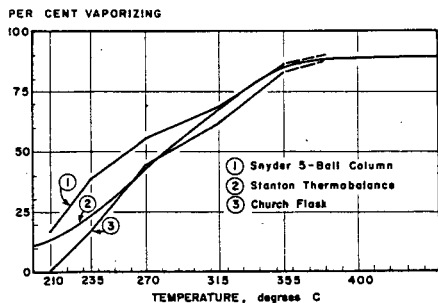


Figure 3. Characteristics of a Creosote Analyzed by Three Different Methods.

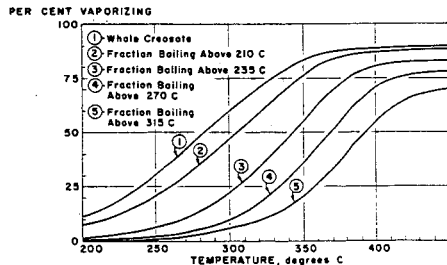


Figure 4. Vaporization Patterns From Whole Creosote and Four of Its Distillation Fractions.

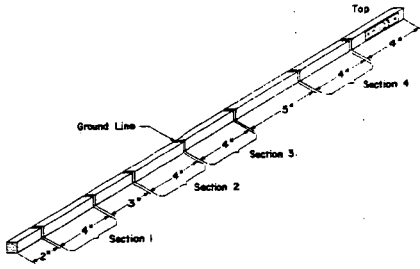


Figure 5. Position of Sections Cut From 3/4-Inch Square Stake for Extraction of Residual Creosote.

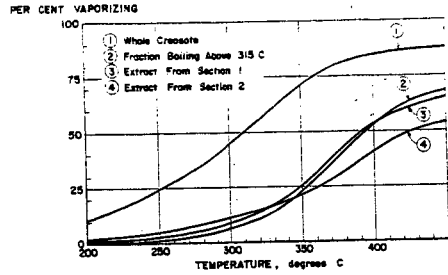


Figure 6. Changes in Creosote Resulting From Ten Years Exposure in Wood Below Ground.

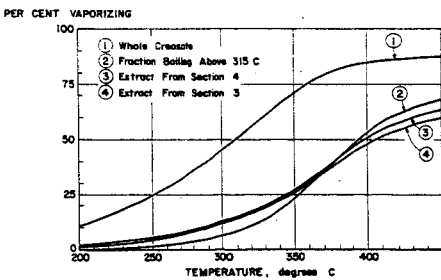


Figure 7. Changes in Creosote Resulting From Ten Years Exposure in Wood Above Ground.

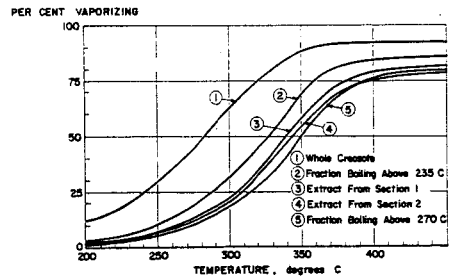


Figure 8. Changes in Creosote Resulting From Five Years Exposure in Wood Below Ground.

A RE-INVESTIGATION OF DENSIMETRIC METHODS OF RING ANALYSIS

Teh Fu Yen, J. Gordon Erdman, and William E. Hanson

Mellon Institute
Pittsburgh 13, Pennsylvania

For many years the chemist has sought a method whereby the average structural character of the molecules in a complex mixture might be determined. In general, two types of mixtures have received most attention. One has consisted of mixtures of compounds comprising a relatively narrow molecular weight range and where the average molecular weight could be obtained; examples are narrow boiling cuts from petroleum. The second has consisted of very complex systems, such as coals, where molecular weight could not be determined, and, indeed, where the concept of molecular weight might not be applicable.

Present studies in this laboratory have as their objective clarification of the structure of the asphaltic, non-hydrocarbon constituents of crude oil and of the presumably similar, but higher molecular weight, black, insoluble organic fraction of ancient sedimentary rocks. From the point of view of structural type analysis, these substances represent a situation somewhere between that of a low molecular weight hydrocarbon mixture and the macromolecular structure of coals.

The development of procedures applicable to mixtures of known low molecular weight and to coals has taken place concurrently, many investigators contributing. Vlughter, Waterman, and van Westen⁽¹⁾ were among the first to apply a system of ring analysis to complex hydrocarbon mixtures. van Nes and van Westen⁽²⁾ continued the study, developing the n-d-M method primarily for petroleum oils. Using refractive index, density, and elementary analysis, van Krevelen⁽³⁾, van Krevelen and Chermin⁽⁴⁾, and van Krevelen and Schuyer⁽⁵⁾ developed a somewhat similar method of statistical analysis, applicable to coals and other substances where molecular weight could not be obtained. Smith⁽⁶⁾ and Montgomery and Boyd⁽⁷⁾ elaborated on both methods to obtain further structural parameters, testing the methods using data for a variety of pure hydrocarbon compounds as recorded by the American Petroleum Institute Research Project 42. Good agreement was obtained with respect to paraffins and naphthenes, but discrepancies were observed for the aromatics, particularly those consisting of fused rings. Dryden⁽⁸⁾, working with coals, compared structural information derived from x-ray, nuclear magnetic resonance, and infrared data with comparable information calculated from the densimetric method of van Krevelen and found that agreement usually was poor.

Since the non-hydrocarbon constituents of the asphaltic fraction of crude oils and the insoluble organic residues obtained from ancient sediments, as well as of refinery asphalts, are believed to contain both aliphatic and aromatic fused ring groups, a re-investigation of the densimetric methods of ring analysis was considered justified.

- (1) J. Inst. Petrol. Tech., 18, 735 (1932); Ibid., 21, 661 (1935).
- (2) "Aspect of the Constitution of Mineral Oils," Elsevier, New York, 1951.
- (3) Brenn. Chem., 34, 167 (1953).
- (4) Fuel, 33, 79 (1954).
- (5) "Coal Science," Elsevier, New York, 1957.
- (6) Ohio State Univ. Bull., 152, 1 (1953).
- (7) Anal. Chem., 31, 1290 (1959).
- (8) Fuel, 37, 444 (1958).

For mixed aliphatic-aromatic compounds or mixtures thereof where the molecular weight could be determined, the following equations have been proposed by van Krevelen:

$$(1) \quad \frac{M}{\rho} = \sum_i n_i V_i - K_M$$

where:

$$(2) \quad K_M = V_R R$$

M = molecular weight of the compound or mixture,

ρ = the density,

n_i = the number of the i th atomic species,

V_i = Traube's atomic volumes,

K_M = molar volume contraction,

V_R = molar volume contraction per ring,

R = number of rings.

For aliphatic compounds or mixtures, K_M is approximately zero.

To cope with substances such as coal where molecular weight is very high or cannot be determined, the equation was converted to the form:

$$(3) \quad \frac{1200}{\%C \cdot \rho} = \sum_i \frac{n_i V_i}{C} - V_R \frac{R}{C}$$

where %C is the per cent carbon obtained by elementary analysis and C is the number of carbon atoms in the structural unit.

To calculate the average number of rings per molecule, R, from equations (1) and (2) or the number of carbons per ring, C/R, from equation (3), it is necessary to evaluate V_R . Using three reference substances, namely, cellulose where R = 0, polystyrene where R = 1, and graphite where R = ∞ van Krevelen and Chermin derived the empirical relation:

$$(4) \quad V_R = 9.1 - 3.6 \frac{H}{C}$$

where H is the number of hydrogen atoms.

Relations (1) and (3) thus become:

$$(5) \quad R = \frac{9.9C + 3.1 H + \dots - \frac{M}{\rho}}{9.1 - 3.6 \frac{H}{C}}$$

and

$$(6) \quad \frac{C}{R} = \frac{9.1 - 3.6 \frac{H}{C}}{9.9 + 3.1 \frac{H}{C} + \dots - \frac{1200}{\%C \cdot \rho}}$$

Equation (6) was used to calculate the number of carbons per ring for a native asphaltene prepared in this laboratory from a Lagunillas crude oil and for two carbon blacks studied by Kuroda⁽⁹⁾. In Table I, Part A, the values obtained (underlined) are compared with values derived from infrared, nuclear magnetic resonance, and x-ray data. The numerical results indicate that the values of C/R calculated by means of equation (6) are too low.

(9) J. Colloid Sci., 12, 496 (1957).

Testing of equation (5) with compounds of known structure indicated that the expression for V_R , equation (4), probably was in error. That this relationship was empirical and disputable was recognized, of course, by van Krevelen. Rather than being a function of H/C , V_R appeared to be a constant for systems comprising three or more fused rings. To test the theoretical implications of this conclusion, an attempt has been made to derive from basic assumptions an expression for V_R .

In order to treat the problem of a condensed ring aromatic system, i.e., of a hexagonal network in two dimensions, it is necessary to assume some sort of model. A number of models are possible, e.g., a circle, exemplified by coronene; a square, by anthrodianthrene; a triangle, by perinaphthindene; and a rectangle, by perylene. For all these models, however, the number of rings can be expressed as a function of the number of aromatic carbon atoms and the number of aromatic hydrogen atoms by the equation:

$$(7) \quad R = 1 + \frac{C_A - H_A}{2}$$

where:

$$(8) \quad H_A = p C_A^{1/2} - q$$

In the latter equation the values of p and q vary with the model. Of the various possible models, the rectangular was selected for development of an expression for V_R .

If an aromatic cluster is designated as $[m, n]$ according to the method of Coulson⁽¹⁰⁾ where m denotes the number of biphenyl type rings, i.e., along the x axis, and n the number of naphthalene type rings, i.e., along the y axis, then:

$$(9) \quad H_A = 2(2m + n)$$

$$(10) \quad C_A = 2m(2n + 1)$$

and the number of rings as:

$$(11) \quad R = 2mn - m - n + 1$$

Now, solving equation (11) in terms of H_A and C_A , equation (7) is obtained. Since long chains of condensed aromatic rings are seldom encountered in stable molecules, the simplified approximation is made that:

$$(12) \quad m \ll n$$

Now, H_A can be expressed in terms of C_A and after simplifying,

$$(13) \quad H_A = 3C_A^{1/2} - 3/2$$

or

$$(14) \quad R = 0.5 C_A - 1.5 C_A^{1/2} + 1.75$$

If the general equation (1) is applied to an aromatic cluster and the terms transposed,

$$(1a) \quad K_M = \sum_I n_i V_i - M/\rho_A$$

Substituting Traube's values for $\sum_I n_i V_i$ and the value of M :

$$(15) \quad K_M = 9.9C_A + 3.1H_A - (12C_A + H_A)\rho_A^{-1}$$

(10) "Proceedings of the Conference on Carbon," held at the University of Buffalo, Symposium Publication Division, Pergamon Press, New York, 1958.

To proceed further, it is necessary to evaluate ρ_A in terms of C_A . This step has been achieved through the following derivation -

In the case of a two-dimensional hexagonal net the area of the equilateral triangle formed by joining the centers of three adjacent rings can be expressed as:

$$(16) \quad \Delta = \frac{\sqrt{3}}{4} \cdot a^2$$

If the net is comprised of aromatic carbon atoms, a is the bond distance and Δ the area occupied by one carbon atom. For a system consisting of uniformly stacked sheets, the minimum interlayer distance is 3.34 Å and hence the maximum density, 2.28 g./cm.³.

Now it can be seen from Figure 1 that for aromatic hydrocarbons the density can be related to the number of carbon atoms by means of the equation:

$$(17) \quad \frac{2.28}{\rho} - 1 = a C_A^b$$

Although this equation is considered empirical at present, there appears to be theoretical evidence to support it. The plotted points in the figure represent nine aromatic hydrocarbons of known structure and the two carbon blacks cited in Table I, Part A. From the resulting straight line, the intercept, a , and the slope, b , can be evaluated as follows:

$$\begin{aligned} a &= 3.15 \\ b &= -0.5 \end{aligned}$$

and equation (17) becomes:

$$(18) \quad \rho_A^{-1} = 0.44 + 1.38 C_A^{-1/2}$$

With an expression for ρ_A in terms of C_A , it is possible to continue development of the relationship expressed by equation (15). Substituting the values of H_A for equation (13) and ρ_A from equation (18), and dropping the small $C_A^{-1/2}$ term, equation (15) becomes:

$$(19) \quad K_M = 4.6 - 8.6 C_A^{1/2} - 8.1$$

The final objective is to eliminate C_A by combining equation (19) with equation (14) and to substitute the resulting value of K_M in the general equation (1). Owing to the form of equations (19) and (14), a general solution for K_M in terms of R is difficult. Accordingly, the operation was accomplished graphically in Figure 2 by substituting arbitrary values of C_A into the equations and solving for R and K_M . The plotted points represent actual values for ten polynuclear aromatic hydrocarbons. The curve will be seen to be a straight line at large values of R but to become slightly concave upward at low R and does not quite pass through the origin. The slight curvature and failure to pass through the origin, of course, are not consistent with condition that K_M must be zero at R equal to zero. This is merely the result of the simplifying approximations that have been made.

The foregoing derivation shows that the assumption of V_R equal to a constant is entirely reasonable. To obtain the value of the constant, it is necessary only to replace the derived curve by its limiting slope.

Hence:

$$(20) \quad V_R = \frac{K_M}{R} = 9.2$$

Similar derivations based on the circular, square, and triangular models lead to equations for H_A differing only slightly from that for the rectangular model, equation (13), as follows:

$$(21) \quad \text{round} \quad H_A = 2.46 C_A^{1/2}$$

$$(22) \quad \text{square} \quad H_A = 2.82 C_A^{1/2} - 2$$

$$(23) \quad \text{triangular} \quad H_A = 3 C_A^{1/2} - 1$$

As can be seen, all these equations yield curves closely approximating that shown in Figure 2 for the rectangular model, thus confirming the generality of the conclusion that V_R should be a constant. Whatever the model chosen, the numerical value of the constant is the same.

On the basis of the above results, it is proposed that the following equations be used for substances containing condensed ring systems:

$$(24) \quad R = 0.11 (9.9 C + 3.1 H + \dots - \frac{M}{\rho})$$

where molecular weight can be determined and by:

$$(25) \quad \frac{C}{R} = \frac{9.2}{9.9 + 3.1 H/C + \dots - \frac{1200}{\rho C \cdot \rho}}$$

for substances where molecular weight cannot be determined.

In Table I, Part B, are presented new values of C/R for the petroleum asphaltene and carbon blacks, cited in Table I, Part A, this time calculated by means of equation (25). Referring to Part A, it will be seen that the values are in better agreement with the values derived from infrared, nuclear magnetic resonance, and x-ray than the values calculated by means of van Krevelen's equation (6).

In Table I, Part C, the values of C/R calculated by the two alternate methods are listed for the above asphaltene and for two others prepared from crude oils of widely different geographic origin. Values of density and elementary analysis are provided for comparison. It will be seen that the values of C/R computed by the method of van Krevelen and Chermin and by the modified method derived in this paper deviate not only in absolute value but also in trend. Further, it is interesting to note that the values of C/R calculated by the modified method do not vary as much with density and elementary analysis as do the values obtained by means of the van Krevelen equation, nor is there a direct correlation with density or the percentage of any single element.

In Tables II and III, equation (24) has been used to calculate values of R for a variety of compounds of known structure, using density values from the literature and values of C , H , etc., from the formulas. The compounds in Table II are unsubstituted aromatic hydrocarbons containing condensed ring systems. The compounds in Table III in many instances contain hetero elements and range from

aliphatic to cyclic systems containing substituted saturated and aromatic ring systems. The good agreement between the calculated R values and those indicated by the formulas is evident. It is concluded, therefore, that equation (25) will be dependable when applied to complex substances such as asphaltic fractions of crude oils and the black insoluble organic fraction of ancient sedimentary rocks.

Acknowledgment

This work was sponsored by the Gulf Research & Development Company as a part of the research program of the Multiple Fellowship on Petroleum.

Table I
Values of C/R for
A Native Petroleum Asphaltene and Two Commercial Carbon Blacks

Part A
 Comparison of the
 Values Calculated by Means of the van Krevelen and Chermin Equation (6)
 with
 Values Obtained from Other Physical Measurements

<u>Substance</u>	<u>Data From</u>	<u>Method</u>	<u>C/R Calculated</u>
Asphaltene (Lagunillas)	infrared spectroscopy ¹	absorbance of the C-H stretching proton type area	5.7
	nuclear magnetic resonance ¹		5.5
	x-ray ¹	(γ) and (002) bands	5.9
	x-ray ¹	(10) and (11) bands	4.2
	density-elementary analysis ¹	densimetric (van Krevelen and Chermin) Equation (6)	3.5
Royal Spectra	x-ray ²	(10) band	2.9 ³
	density - H/C approximated from X-ray L _a values ²	densimetric Equation (6)	2.1
Statex B	x-ray ²	(10) band	2.6 ³
	density - H/C approximated from x-ray L _a values ²	densimetric Equation (6)	2.1

Part B
 Values Calculated by Means of Equation (25) Derived by the Authors

<u>Substance</u>	<u>Data From</u>	<u>C/R Calculated</u>
Asphaltene (Lagunillas)	density-elementary analysis	6.2
Royal Spectra	density - H/C approximated from x-ray L _a values ²	2.5
Statex B	density - H/C approximated from x-ray L _a values ²	2.3

Part C
 Density, Elementary Analysis, and Values of C/R for Three Asphaltenes
 Prepared from Crude Oils of Widely Different Geographic Origin

<u>Field</u>	<u>Location</u>	<u>Helium Density ρ</u>	<u>Elementary Analysis Per Cent</u>					<u>C/R Calculated by Means of Equation</u>	
			<u>C</u>	<u>H</u>	<u>O*</u>	<u>N</u>	<u>S</u>	<u>(6)</u>	<u>(25)</u>
Lagunillas	Western Venezuela	1.158	84.2	7.9	1.6	2.0	4.8	3.46	6.24
Wafra	Neutral Territory (Middle East)	1.164	81.8	8.1	1.5	1.0	7.8	3.14	5.90
Baxterville	Mississippi U.S.A.	1.172	84.5	7.4	1.7	0.8	5.6	3.62	6.19

¹ Measurements made in this laboratory.

² Taken from the work of Kuroda, H., J. Colloid Sci., 12, 496 (1957).

³ Calculated assuming all the carbons are contained in a condensed aromatic sheet.

* Direct determinations

Table II
Calculation of R for
Compounds Consisting of Condensed Aromatic Ring Systems

Compound	Formula	Molecular Weight M	Density ρ	K_M	Rings per Molecule, R	
					Theoretical From Formula	Calculated by Equation (24)
naphthalene	$C_{10}H_8$	128	1.152 ⁴	12.7	2	1.4
anthracene	$C_{14}H_{10}$	178	1.25 ¹	27.2	3	3.0
fluorene	$C_{13}H_{10}$	166	1.203 ²	21.7	3*	2.4
triphenylene	$C_{18}H_{12}$	228	1.302 ¹	40.3	4	4.4
chrysene	$C_{18}H_{12}$	228	1.274 ¹	36.2	4	4.0
perylene	$C_{20}H_{12}$	252	1.35 ¹	48.5	5	5.3
anthanthrene	$C_{22}H_{12}$	276	1.39 ³	56.4	6	6.2
coronene	$C_{24}H_{12}$	300	1.377 ⁴	57.0	7	6.3
ovalene	$C_{32}H_{14}$	398	1.477 ⁵	90.7	10	10.0
circumanthracene	$C_{40}H_{16}$	496	1.52 ⁶	119	13	13.1

* Contains one five-membered ring.

1. "The Merck Index of Chemicals and Drugs," 6th Ed., Merck and Co., Inc., Rahway, New Jersey, 1952.
2. Lange, N.L., "Handbook of Chemistry," 9th Ed., Handbook Publishers, Sandusky, Ohio, 1956.
3. J. G. White, J. Chem. Soc., 1948, 1398.
4. J. M. Robertson and J. G. White, Nature, 154, 605 (1944).
5. D. M. Donaldson and J. M. Robertson, Proc. Roy. Soc., A220, 157 (1953).
6. E. Clar, et al., J. Chem. Soc., 1956, 3876.

Table III
Calculation of R for
Compounds of Varying Structure and Elementary Composition

Compound	Formula	Molecular Weight M	Density ρ	Rings per Molecule	
				Theoretical From Formula	Calculated by Equation (24)
d-tartaric acid	$C_4H_6O_6$	150	1.759 ¹	0	0
hexachloroethane	C_2Cl_6	237	2.09 ²	0	0
borneol	$C_{10}H_{18}O$	154	1.011 ²	1	0.7
p-hydroxybenzoic acid	$C_7H_6O_3$	138	1.46 ²	1	0.5
anthraquinone	$C_{14}H_8O_2$	208	1.43 ²	3	2.8
α -naphthylphenylmethane	$C_{17}H_{14}$	218	1.165 ³	3	2.7
papaverine	$C_{20}H_{21}NO_4$	339	1.337 ⁴	3	2.8
rosin	$C_{20}H_{29}O_2$	302	1.095 ⁵	3	2.5
laudanine	$C_{20}H_{25}NO_4$	243	1.26 ²	3	2.1
α -progesterone	$C_{21}H_{30}O_2$	314	1.166 ²	4	4.2
20-methylcholanthrene	$C_{21}H_{16}$	268	1.28 ²	5	4.2
strychnine	$C_{21}H_{22}N_2O_2$	334	1.359 ⁴	5	4.5

1. Bailey, T., "Bailey's Chemists' Pocket Book," 20th Ed., E. and F. N. Spon., Ltd., London, 1948.
2. "The Merck Index of Chemicals and Drugs," 6th Ed., Merck and Co., Inc., Rahway, New Jersey, 1952.
3. Egloff, G., "Physical Constants of Hydrocarbons," Vol. 4, Reinhold Publishing Corp., New York, 1947.
4. Hodgman, C. D., et al., "Handbook of Chemistry and Physics," 41st Ed., Chemical Rubber Publishing Company, Cleveland, 1959.
5. Simonds, H. R., et al., "Handbook of Plastics," 2nd Ed., D. Van Nostrand Company, Inc., New York, 1949.

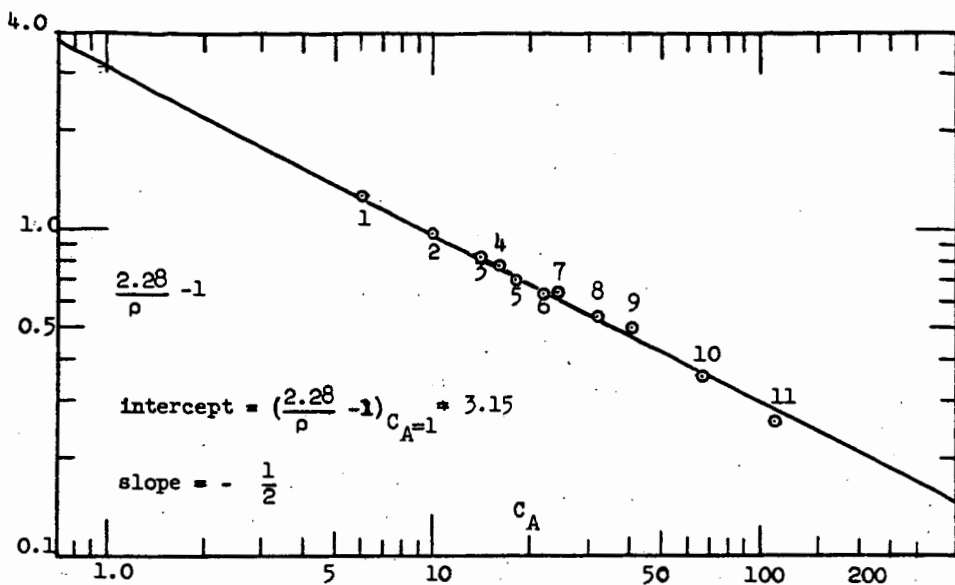


Figure 1
Relation of Density to Aromatic Carbon Number

- | | | | |
|----------------------|--------------------|----------------|-------------|
| (1) Benzene | (2) Naphthalene | (3) Anthracene | (4) Pyrene |
| (5) Triphenylene | (6) Anthanthrene | (7) Coronene | (8) Ovalene |
| (9) Circumanthracene | (10) Royal Spectra | (11) Statex B | |

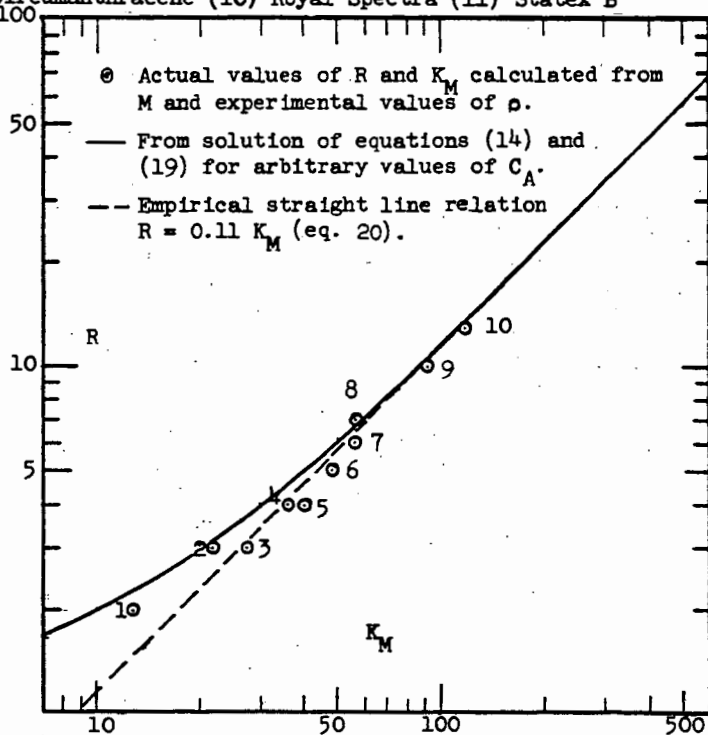


Figure 2
Relation of Molar Volume Contraction and Ring Number

- | | | |
|-----------------------|------------------|--------------|
| (1) Naphthalene | (2) Anthracene | (3) Fluorene |
| (4) Chrysene | (5) Triphenylene | (6) Perylene |
| (7) Anthanthrene | (8) Coronene | (9) Ovalene |
| (10) Circumanthracene | | |

CATALYTIC STEAM REFORMING OF LIGHT LIQUID HYDROCARBONS

J. C. Yarze and T. E. Lockertie

The M. W. Kellogg Company
Research and Development Department
Jersey City, New Jersey

Introduction

In the chemical process industry, catalytic steam-hydrocarbon reforming of natural gas or propane is widely employed to produce ammonia synthesis gas, high-purity hydrogen, and hydrogen-carbon monoxide mixtures for chemical synthesis. Currently, synthetic ammonia plants based on natural gas reforming account for 70-80 per cent of all ammonia produced in the United States, and a large percentage of domestic synthetic methanol production is derived from steam-hydrocarbon reforming.

The manufactured gas industry also employs steam-hydrocarbon reforming in the production of low-Btu carrier gas. Several continuous reforming units employing natural gas or propane feedstocks and steam-air oxidizing mixtures have been built in the United States. In a typical application, carrier gas and natural gas are blended to provide a mixture with the heating value, specific gravity, and hydrogen content required for satisfactory performance in customers' appliances. In Europe and Asia, carrier gas from steam-hydrocarbon reforming is commonly enriched with light hydrocarbons and diluted with inerts to about 0.5 specific gravity and 400-500 Btu higher heating value. The resulting mixture is used as a supplement or replacement for coke oven-carburetted water gas mixtures.

Steam-natural gas or steam-propane reforming techniques employed in producing ammonia synthesis gas, Fischer-Tropsch synthesis gas, hydrogen, and carrier gas have been described elsewhere /2,3,4,5,8/. In these and other applications of conventional fired-tube reforming furnaces, certain similarities are apparent. Feedstocks require careful desulfurization prior to conversion if temporary poisoning of nickel reforming catalyst and shutdowns for catalyst regeneration are to be avoided. Within the catalyst tubes, conversion of the original steam-hydrocarbon mixture occurs via highly endothermic chemical reactions yielding a product containing hydrogen, carbon monoxide, carbon dioxide, and small amounts of methane. When injection of air to the reformer is practiced, nitrogen becomes an additional component of the product. At the tube outlet, where gas temperatures of 1550°F may be obtained, product distribution is largely governed by equilibrium considerations. The water gas shift reaction



is found to be at equilibrium in reformer effluent, while the steam-methane reaction



attains a close approach to equilibrium.

Deposition of carbon on catalyst located near the tube inlet can be an operational problem in fired-tube reformers. Avoidance of carbon deposition is required to ensure long periods of continuous operation and prevent severe catalyst spalling. Freedom from carbon deposition is obtained by employing active catalysts

at high temperatures, and by using more than stoichiometric quantities of steam. Relative amounts of steam and hydrocarbon in the original mixture are conveniently specified by the steam-carbon ratio, moles steam per feedstock carbon atom. Selection of the optimum steam-carbon ratio is an important function of reformer design. Sufficient excess steam must be employed to prevent costly shutdowns and resulting lost production. However, a plant designed for an excessively high steam-carbon ratio also results in high manufacturing costs, since both investment and operating costs increase with increasing steam-carbon ratio.

Although continued growth of reforming capacity based on natural gas and propane feedstocks is predicted, an increased interest in utilizing heavier feedstocks has recently been indicated. In this paper, results of pilot plant and exploratory reforming tests on light liquid hydrocarbons are described and related to the known behavior of natural gas and propane. Particular consideration is given to the economically important steam-carbon ratio variable.

Pilot Plant Experiments

A. Apparatus and Methods

A vertically mounted 1-inch reformer heated by a conventional electrical resistance furnace was used for screening of variables and determination of operability limits at 20-125 psig reforming pressure. The reactor consisted of a 57-3/4 inch length of 1-inch Inconel pipe. A catalyst support tray at the tube outlet and an axial thermowell extending the length of the reactor were provided. Attached to the upper or inlet end was a 2-inch welding-neck flange. The inner diameter of the flange provided surface for falling-film evaporation of water, and the annulus formed by the inner diameter of the flange and the outer diameter of the tube afforded volume for hydrocarbon vaporization and mixing of vaporized water and hydrocarbon. A preheater assembly, 28 inches of 316 stainless steel bar stock welded to a 2-inch blind flange, fitted snugly into the reactor, with 0.003 inches radial clearance. The flange and bar stock were suitably tapped for inlet connections and the axial thermowell, and the bar stock was threaded to provide heat transfer area. A stainless steel ring closure was employed. Catalyst bed depth was 30 inches.

In operation, water and hydrocarbon were pressured from calibrated feed tanks with nitrogen. Flow rates were controlled by small air-operated valves responding to pressure drops across hypodermic needle orifices. Water and hydrocarbon metered to the reactor inlet were vaporized in the falling-film evaporator section of the reactor, preheated by downward passage through the preheater spiral, and contacted with catalyst. Furnace windings opposite the vaporization, preheat, and reaction sections of the reactor were automatically controlled. Reaction products were cooled by indirect exchange, and unreacted water separated. Product gases flowed through a back-pressure regulator maintaining unit pressure to a wet-test meter, sampling manifold, and vent. Periodic samples were analyzed by mass spectrometer. Pressure drop across the catalyst bed was continuously measured by a differential pressure cell with a range of 0-100 inches of water.

In all experimental studies made in the 1-inch unit, 1/8 inch extrusions of commercial steam-hydrocarbon reforming catalyst were utilized to maintain a reasonable relationship between reactor diameter and catalyst size. The particular catalyst employed was a pre-shrunk preparation which contains 20-25 per cent by weight nickel (as NiO) uniformly distributed throughout each pellet. Fresh catalyst, containing 0.49 per cent by weight sulfur, was either pretreated extensively at high temperature with a steam-hydrogen mixture, or used in extended reforming runs at high steam-carbon ratios, until the catalyst sulfur content was reduced to 0.003-0.005 per cent by weight. Extensive pretreatment was mandatory, since unreliable results were obtained with catalysts containing as little as 0.01 per cent by weight sulfur.

Feedstocks employed were of 99+ mole per cent purity, containing a maximum of 5 parts per million sulfur by weight. Catalysts discharged after extended contact with feedstocks containing 5 parts per million sulfur uniformly analyzed 0.003-0.005 per cent by weight sulfur, indicating that the sulfur content of the catalyst was substantially constant during test periods.

After catalyst pretreatment, feedstocks were reformed in a series of 12 or 24 hour experiments conducted at progressively lower steam-carbon ratios. Testing was continued until an increase in reactor pressure drop was indicated by the differential pressure cell. A measurable increase in pressure drop was taken as evidence of carbon formation in the catalyst bed at the particular steam-carbon ratio employed.

B. Experimental Results

For orientation, the reforming characteristics of 99.7 mol per cent cylinder propane were initially investigated, employing the technique described above. Typical experimental data obtained at 125 psig reforming pressure and substantially commercial temperatures and hydrocarbon space velocities are presented in Table 1. Tests made at steam-carbon ratios ranging from 3.77 to 1.51 were completed without evidence of carbon deposition. At 1.35 steam-carbon ratio, catalyst activity gradually declined during 24 hours of operation, and reactor pressure drop increased about 0.4 inches per hour. This behavior was interpreted as arising from deposition of carbon on the catalyst. Additional data from tests made without nitrogen diluent and a correlation relating rate of pressure drop increase to steam deficiency indicate that 1.50 moles of steam per carbon atom are required for operability at 125 psig when reforming propane.

Wet product gas analyses permit calculation of apparent gas temperatures at the tube outlet, assuming that the water gas shift and steam-methane reactions are at equilibrium in the product. Results of these calculations are presented in Table 1. The assumption of equilibrium for either reaction gives outlet temperatures which are generally in reasonable agreement with the measured outlet temperature. In larger pilot plants, the steam-methane reaction is usually further removed from equilibrium. The close approach of the steam-methane reaction to equilibrium at the outlet of the 1-inch unit reflects the high activity of 1/8-inch catalyst pellets relative to commercial-sized pellets when both are employed at the same hydrocarbon space velocity.

A similar operability study was made on ASTM grade n-heptane, a representative light liquid hydrocarbon reforming feedstock. Results of these tests are also presented in Table 1. At 20 psig reforming pressure and commercial temperatures and hydrocarbon space velocities, reactor pressure drop did not increase during test periods at 3.03 steam-carbon ratio and higher. At 2.53 steam-carbon ratio, reactor pressure drop increased 0.4 inches per hour during 12 hours of steady operation. Additional tests confirm that, at 20 psig, about 3.0 moles of steam per carbon atom are required to prevent carbon deposition when reforming n-heptane.

Product gas ratios and calculated outlet temperatures obtained when reforming n-heptane closely resemble results obtained using propane feedstock. Except that higher steam-carbon ratios are required for operability, the reforming characteristics of n-heptane appeared to be fundamentally similar to those of propane.

C. Effect of Hydrocarbon Molecular Weight on Operability

Operability limits determined for propane and n-heptane in this study can be compared with operability data from the literature /7/ to provide an estimate of the relationship between hydrocarbon molecular weight and minimum operable steam-carbon ratio at several reforming pressures. In Figure 1, published data obtained

in a 5-inch tube at essentially atmospheric pressure are compared with data from this study. A single relationship appears to represent both sets of data adequately. Required steam-carbon ratio is shown to increase logarithmically with increasing molecular weight at several pressures. The rate of increase is moderate, operability limits ranging from 1.1 steam-carbon ratio for natural gas or methane to 3.0 steam-carbon ratio for n-heptane.

While agreement between the two sets of data may be partly fortuitous, owing to differences in feedstock purity, catalysts, and operating conditions, additional studies in the 1-inch pilot plant tend to confirm the relationship shown in Figure 1. When reforming olefin-free and sulfur-free hydrocarbons, reforming pressures ranging from 20 to 125 psig are found to have no significant effect on minimum steam-carbon ratio.

Study of Reforming Variables in Glassware

A. Apparatus and Methods

Since pilot plant tests indicated no major effect of pressure on minimum steam-carbon ratios when reforming olefin-free and sulfur-free hydrocarbons, the study of light liquid hydrocarbon reforming was continued in glassware at atmospheric pressure to further clarify the influence of reactor and feedstock variables on operability. Reactions of steam-hydrocarbon mixtures were studied over various commercial reforming catalysts at several temperatures and steam-carbon ratios in a conventional 1-inch diameter quartz reactor heated by an electrical resistance furnace. A 2-inch bed of catalyst was employed so that, in effect, the top portion of a full catalyst charge in the 1-inch pilot plant was being studied, this being the critical zone for carbon formation.

In operation, hydrocarbon feedstock was introduced from a pressured container and vaporized. Flow rate to the glass unit was measured by calibrated rotameters. Steam-carbon ratio was controlled by gas saturation. A metered stream of vaporized feedstock, saturated to the desired steam-carbon ratio, was preheated by rapid passage through an annulus formed by the inner tube wall and snugly fitted quartz plug, and contacted with catalyst. Reactor effluent was rapidly removed from the reaction zone through 3-millimeter tubing, cooled to condense unreacted steam, measured in a wet-test meter, and vented. Periodic product gas samples were withdrawn and analyzed by mass spectrometer. Feedstock conversion was varied by altering hydrocarbon space velocity at constant steam-carbon ratio and temperature. At the completion of each test, the catalyst charge was analyzed for carbon by combustion and absorption of carbon dioxide. Previously cited limitations on catalyst and feedstock sulfur contents were observed. While the apparatus and technique employed are not ideally suited for kinetic measurements, they permit very efficient screening of variables for large effects on operability and product distribution.

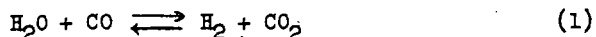
Before any reforming experiments were made, the catalyst space was filled with quartz chips, and steam-hydrocarbon mixtures passed through the unit at various combinations of temperature and contact time. In this way, temperature-contact time combinations sufficient to cause thermal cracking were determined for all feedstocks. Subsequent reforming tests were then carried out at conditions where precracking of feedstock could not occur, thus ensuring that catalytic reactions alone were being investigated.

In the tests to be described, two commercial catalysts were employed. Catalyst A is an impregnated type, containing about 5 per cent nickel (as NiO) on alumina. Catalyst B is the compounded preparation previously used for studies in the 1-inch pilot plant.

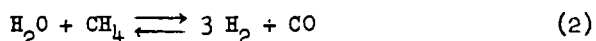
B. Experimental Results

Typical data obtained when reforming 99.7 mole per cent n-butane to partial conversion at 1075°F or 1275°F and 3.0 steam-carbon ratio are presented in Table 2. At all conversion levels, dry product gases are observed to consist almost entirely of conventional reformed products and unreacted feedstock. Various olefinic and paraffinic butane decomposition products are present at low concentrations in all product gas samples. Methane, a final product in commercial reforming operations, is not detected in gases produced at low conversions of feedstock. These characteristic features of partially reformed gases are confirmed by other studies employing different temperatures, steam-carbon ratios, and catalysts.

Product ratios corresponding to equilibrium constants for the water gas shift reaction



and steam-methane reaction

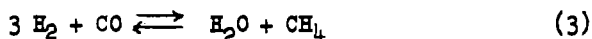


have been calculated and are reported in Table 2. At 1275°F, the water gas shift equilibrium constant is approximately 1.61. Shift constants calculated from experimental data obtained with compounded Catalyst B show a strong dependency on the extent of n-butane conversion. At conversions below 10 per cent, the shift reaction is far removed from equilibrium. However, in the range of 10-30 per cent n-butane conversion, equilibrium is rapidly approached, while at still higher conversions, equilibrium constants appear to scatter about the equilibrium value. At 1075°F, where the shift equilibrium constant is approximately 2.85, a parallel trend is evident from data obtained using Catalyst B. Data obtained with impregnated Catalyst A at 1275°F, indicate a much slower approach to equilibrium than with Catalyst B. However, the reproducibility of this apparent difference in catalyst activity for the shift reaction has not been determined. In general, all data in Table 2 indicate that the water gas shift reaction rapidly proceeds towards equilibrium in the presence of nickel reforming catalysts. Similar conclusions are made in a published study on natural gas reforming /6/.

The equilibrium constant for the steam-methane reaction at 1275°F is approximately 9.5. Calculated steam-methane equilibrium constants in Table 2 indicate that the approach to equilibrium over both Catalysts A and B, is very slow for this reaction, even at high n-butane conversions. This result is in agreement with commercial steam-hydrocarbon reforming results, where equilibrium is approached but not attained at much higher contact times than were employed in this study.

Methane production is further analyzed in Table 2 as a function of n-butane conversion at 1075°F or 1275°F and 3.0 steam-carbon ratio. In Figure 2, tabulated mole ratios of methane produced to n-butane converted are plotted against conversion and extrapolated towards zero conversion to determine if methane is a primary reaction product. As Figure 2 indicates, methane is produced only when the conversion of n-butane exceeds about 15 per cent. The relationship obtained appears to be essentially independent of catalyst type or temperature. Thus, methane is not a primary product of steam-butane reforming, and does not arise directly from catalytic decomposition of feedstock.

Consideration of other possible reactions yielding methane indicates that methane is probably formed by the methanation reaction



which is catalyzed by nickel at conditions similar to those employed in reforming. Production of methane is limited by the steam-methane back-reaction, since methane molecules can disappear by successfully competing with unreacted n-butane for active reforming sites on the catalyst.

Analyses of discharged catalysts indicate that, at steady state conditions, detectable amounts of carbon are always present on active catalysts. In general, carbon contents are higher at the lower reforming temperatures. Compounded Catalyst B contains less carbon than impregnated Catalyst A after comparable periods of exposure to steam hydrocarbon mixtures. The temperature dependency of catalyst carbon content is illustrated specifically in Table 3, where carbon levels are compared for runs made with Catalyst B at nominally constant conversion, constant steam-carbon ratio, and 900°F, 1100°F and 1300°F. Although absolute values for carbon content may be specific for the apparatus and conditions employed, these analyses indicate that carbon content decreases almost exponentially with increasing temperature.

All data from tests on n-butane have been evaluated to determine the apparent kinetics of n-butane disappearance. While the data are not sufficiently precise for a detailed kinetic analysis, the rate of butane disappearance appears to be approximately proportional to n-butane concentration for the temperatures, steam-carbon ratios, and catalysts studied. The apparent first order reaction rate constant increases exponentially with temperature. First order kinetics have also been shown to apply in natural gas reforming /1/. A comparison of rate constants for butane disappearance by steam-hydrocarbon reforming and by thermal cracking indicates that the reforming reaction is roughly 100 times faster at the same temperature, thus confirming that thermal cracking is not a major reaction in reforming.

Discussion

Information developed from partial conversion and pilot plant studies permits some reasonable speculation on the individual chemical reactions occurring in steam-hydrocarbon reforming. The overall conversion of paraffin hydrocarbons and steam to reformed products is indicated as occurring through a complex series of consecutive and competing reactions. Hydrocarbon molecules diffuse to the catalyst surface, are adsorbed, and undergo catalytic cracking-dehydrogenation reactions which yield strongly adsorbed olefinic fragments. Further dehydrogenation-polymerization reactions occur, leading to formation of coke or carbon on the catalyst. The sum of these consecutive steps is an overall reaction in which feedstock molecules are converted to carbon on the catalyst at a rate proportional to feedstock concentration.

Carbon deposits are continuously removed from the catalyst by a competing reaction involving steam. Adsorbed steam molecules react with deposited carbon to form hydrogen and carbon monoxide or carbon dioxide. These products, hydrogen evolved in the cracking-dehydrogenation-polymerization step, and steam also participate in methanation and water gas shift side reactions. In addition, a portion of the methane produced by methanation is continuously reformed through a sequence similar to that followed by the original feedstock.

This qualitative mechanism is helpful in rationalizing the behavior of reforming units, since it predicts that net carbon formation and inoperability result when the rate of feedstock decomposition exceeds the rate of carbon removal by the steam-carbon ratio. Operable reforming units are thus characterized by equal rates of carbon formation and removal at all points in the catalyst bed. Any change in conditions which induces a relative increase in the rate of carbon removal from the catalyst will accordingly favor operability. Major operating variables capable of altering this relative rate are temperature and steam-carbon ratio. An

increase in catalyst bed temperature will, in general, favor the attainment of operability. Although the rates of reactions producing and removing carbon both appear to increase exponentially with temperature, the steam-carbon reaction rate apparently increases at a relatively greater rate, as demonstrated by catalyst carbon analyses. With all other reactor variables held constant, an increase in catalyst temperature will therefore increase the relative rate at which carbon is removed from catalyst at all points within the bed, or lower the equilibrium carbon content of catalyst.

An increase in steam-carbon ratio will also favor the attainment of operability by reducing the rate of hydrocarbon decomposition. When reforming n-butane, for example, an increase in steam-carbon ratio from 2.0 to 3.0 reduces butane concentration in the feedstock from 0.111 to 0.0796 mol fraction, a decrease of about 31 per cent. Thus the initial rate of butane decomposition to carbon near the tube inlet is decreased about 31 per cent. The corresponding slight increase in steam concentration, from 0.889 to 0.922 mol fraction, does not appear to greatly influence the rate of carbon-removing reactions. Small increases in steam concentration can therefore strongly influence the relative rates of carbon laydown and removal on catalyst located near the bed inlet.

These observations are consistent with operating experience in pilot plants and commercial units. Carbon deposition generally occurs near the tube inlet where catalyst temperatures are low; in this critical zone, the steam-carbon reaction proceeds slowly relative to decomposition. The effectiveness of increased steam-carbon ratio in suppressing carbon formation in the critical zone is well known.

The relationship between paraffin hydrocarbon molecular weight and minimum steam-carbon ratio presented in Figure 1 may also be a consequence of changes in the relative rates of competing reactions producing and removing carbon. Experience suggests that, at the same temperature and steam-carbon ratio, n-butane is catalytically decomposed to carbon more rapidly than methane. If the rate of reaction between steam and carbon is similar in both cases, net carbon formation or inoperability will be favored for the heavier feedstock. To attain an equal degree of operability, additional steam will be required to reduce the rate of n-butane decomposition to carbon. Hence n-butane will require a higher minimum steam-carbon ratio than methane to balance carbon production and removal. The relationship shown in Figure 1 may therefore arise from a regular increase in the rate of catalytic decomposition to carbon with increasing feedstock molecular weight.

Conclusions

Pilot plant tests demonstrate that presently available steam-hydrocarbon reforming catalysts can be used successfully with light liquid hydrocarbon feedstocks. The similarity of behavior and results noted in tests with propane and n-heptane indicate that light liquid hydrocarbons and currently reformed feedstocks follow a similar reaction path. Partial conversion experiments suggest a mechanism involving simultaneous catalytic conversion of feedstock to carbon and catalytic removal of carbon by the steam-carbon reaction. Water gas shift, methanation, and steam-methane reforming side reactions are additionally indicated as occurring on the catalyst. The qualitative mechanism presented appears to rationalize some observed effects of reforming temperature and steam-carbon ratio on operability.

Table 3
EFFECT OF REFORMING TEMPERATURE ON CARBON
CONTENTS OF DISCHARGED CATALYSTS

Temperature, °F.	900	1100	1300
Carbon on Catalyst, Wt. %	1.34	0.46	0.12

REFERENCES

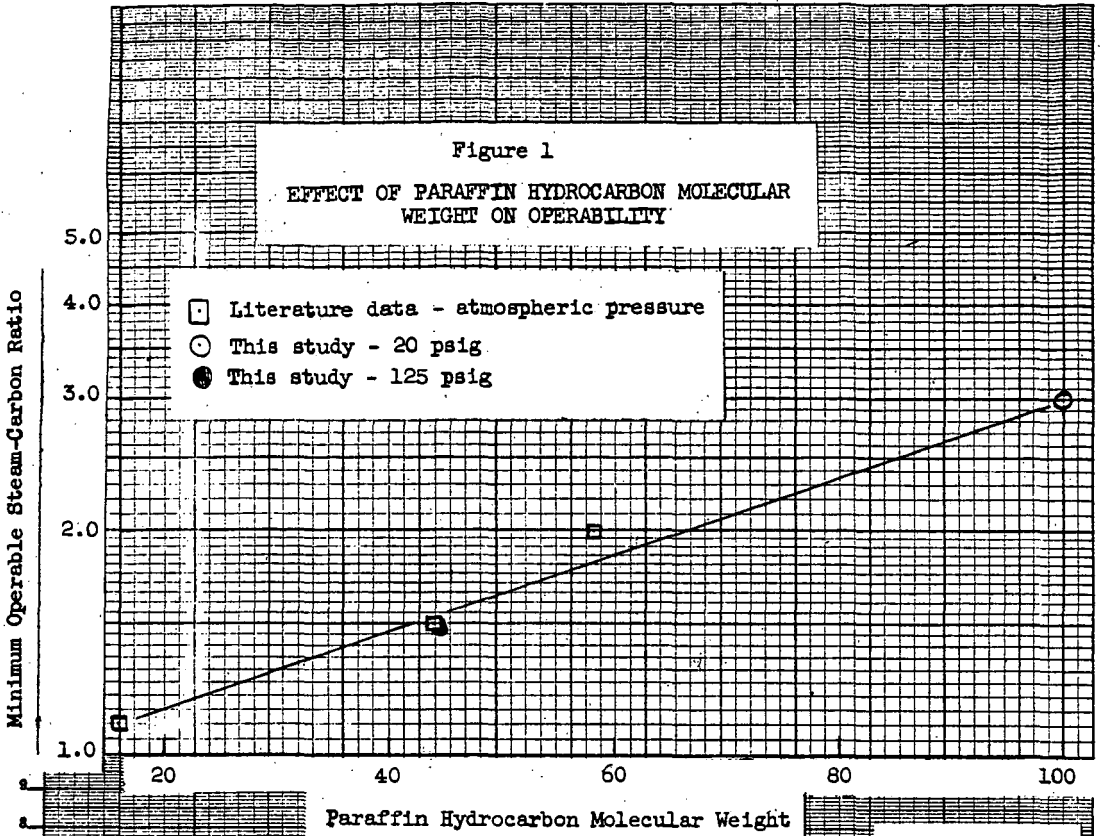
1. Akers, W.W. and Camp, D.P., "Kinetics of the Methane-Steam Reaction", A.I.Ch.E. Journal 1, 471-475 (1955).
2. Aron, "Kellogg Ammonia Process", Pet. Ref. 33, 3, 150 (1954).
3. Barnes, J.M. and Berger, E.S. "Eastern Utility Installs Catalytic Reforming Units", Gas 33, 39-42 (1957) December.
4. Eickmeyer, A.G. and Marshall, W.H., Jr., "Ammonia Synthesis - Gas Generation by Pressure Reforming of Natural Gas", Chem. Eng. Progr. 51, 418-421 (1955).
5. Reitmeier, R.E., Atwood, K., Bennett, H.A., Jr., and Baugh, H.M., "Production of Synthesis Gas by Reacting Light Hydrocarbons with Steam and Carbon Dioxide", Ind. Eng. Chem. 40, 620-626 (1948).
6. Riesz, C.H., Dirksen, H.A., and Pleticka, W.J., "Improvement of Nickel Cracking Catalysts", Institute of Gas Technology Research Bulletin No. 20, (1952) October.
7. Riesz, C.H., Jurie, P.C., Tsaros, C.L., and Pettyjohn, E.S., "Pilot Plant Catalytic Gasification of Hydrocarbons", Institute of Gas Technology Research Bulletin No. 6 (1953) July.
8. Updegraff, N.C., "Need Hydrogen? Examine This Process", Pet. Ref. 38, 9, 175-178 (1959).

Table 1

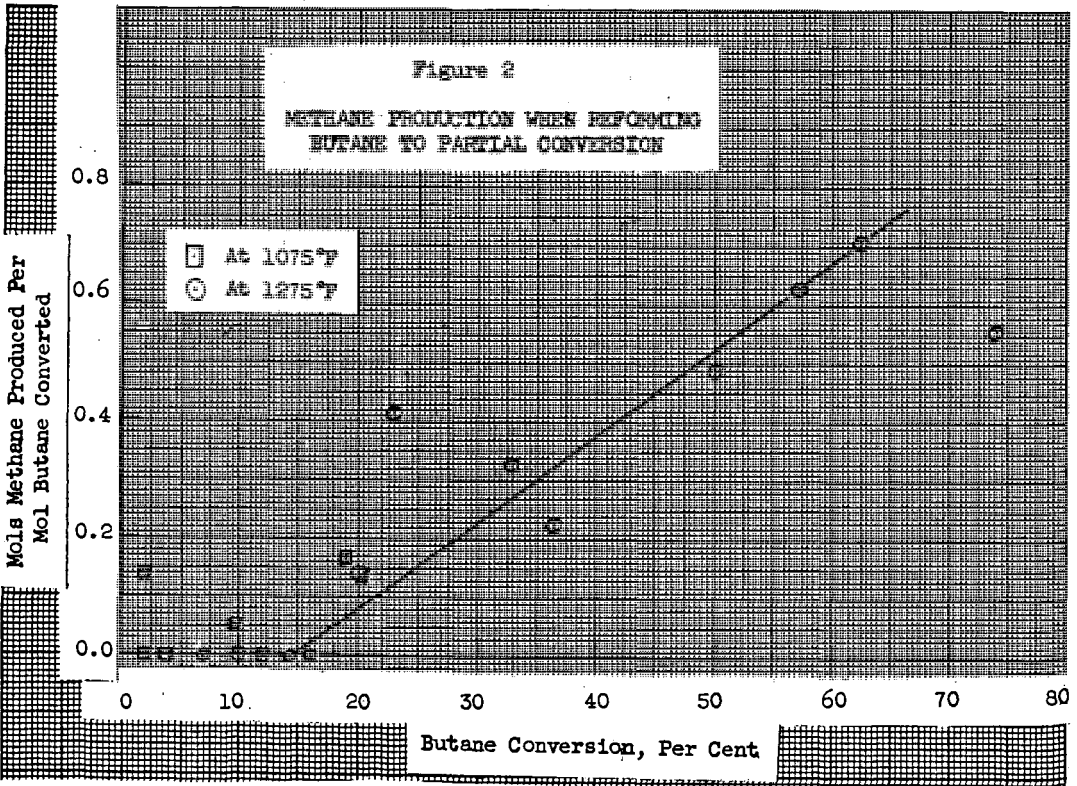
RESULTS OF PILOT PLANT REFORMING TESTS ON PROPANE AND HEPTANE

Feedstock	C ₃ H ₈				n-C ₇ H ₁₆							
	20	24	24	24	24	24	12	22-1/4	12	12		
Test Duration, hr	3.77	2.85	2.28	1.83	1.51	1.36	8.35	6.41	3.98	3.89	3.03	2.53
Steam-Carbon Ratio, moles steam per carbon atom	710	640	670	650	685	650	720	730	810	805	795	805
Reactor Inlet Temperature, °F	1450	1430	1440	1445	1440	1455	1455	1445	1450	1435	1400	1400
Reactor Outlet Temperature, °F	126	125	126	125	126	125	20	21	20	20	20	20
Rate of Reactor Δp Increase, in. water per hr	0.0	0.0	0.0	0.0	0.0	0.4	0.0	0.0	0.0	0.0	0.0	0.4
Dry Product Gas Analysis, mole %												
CO	12.2	14.1	15.0	19.1	19.3	19.8	7.3	9.2	14.4	14.6	15.9	18.9
CO ₂	10.7	9.6	7.7	5.6	5.1	4.3	18.2	17.0	12.7	12.4	10.7	9.4
H ₂	64.0	61.2	59.6	56.7	57.2	57.0	74.5	73.8	72.9	73.0	73.3	71.6
CH ₄	1.3	3.7	3.9	2.9	4.7	4.5/2/	-	-	-	-	0.1	0.1
N ₂ /1/	11.8	11.4	13.8	15.7	13.7	14.4	-	-	-	-	0.1	0.1
Atomic Balances, %												
C	104.3	101.7	102.0	102.0	100.7	100.0	101.4	95.1	96.3	95.3	96.5	98.2
H	100.2	98.3	99.5	94.3	93.8	97.3	106.2	99.5	97.1	96.3	105.6	101.2
O	99.5	100.8	95.9	96.9	91.5	91.2	106.0	99.9	98.3	94.1	101.7	98.0
N	103.2	87.9	109.8	120.3	99.4	99.7	-	-	-	-	-	-
Outlet Temperature Calc. from Water Gas Shift Constant, °F	1490	1500	1495	1545	1515	-	1450	1440	1520	1515	1420	1455
Outlet Temperature Calc. from Steam-Methane Constant, °F	1470	1435	1460	1390	1510	-	-	-	-	-	-	-

1/1 Nitrogen diluent from feedstock.
 2/ At start of test period. Severe catalyst deactivation was noted during test.



FILE NO. E-3116
JCY:LA 11/12/59



TRANSFER OF HEAT FROM HELIUM AT HIGH TEMPERATURES--
PHYSICAL CHARACTERISTICS OF CERAMIC HEAT EXCHANGERS

Stanley C. Browning* and John J. S. Sebastian

Morgantown Coal Research Center
Bureau of Mines, U. S. Department of the Interior
Morgantown, W. Va.

Preliminary cost studies indicate that it should be economically possible to use nuclear energy as process heat for certain endothermic reactions. The Federal Bureau of Mines' interest at present is utilizing heat from the fission of nuclear fuels to gasify coals with steam to produce synthesis gas. Of primary concern in the study of the use of nuclear heat for gasification of coal and for other industrial purposes is the problem of effective transfer of heat from the gas-cooled nuclear reactor-core to a reaction chamber where the endothermic reaction takes place. In order to remove the heat from the coolant-gas, it is necessary to design a heat exchanger capable of performance at temperatures much in excess of those ordinarily encountered in heat exchange equipment. Heat exchangers constructed of available metals will not withstand prolonged use at high temperatures. This suggests the investigation of certain ceramic materials capable of withstanding high temperatures and other severe conditions of corrosion and erosion.

Much data are available in the literature on heat transfer by forced convection to and from gases. Summaries of previous work have been published by McAdams (15) and others (8, 11). Most of the existing experimental data, however, refer primarily to heat exchange in metal tubes, and do not extend into the range of higher temperatures in which interest has increased in many current engineering applications.

An experimental investigation was undertaken at the Morgantown Coal Research Center of the Bureau of Mines, U. S. Department of the Interior, Morgantown, W. Va., to obtain heat-transfer information over a wide range of surface and fluid temperatures, with helium as the heat-transfer medium. As part of this broad program, an investigation was made of the transfer of heat from helium (flowing through smooth tubes) to the tubular surfaces of a vitreous alumina heat exchanger. The effects of such variables as tube-wall temperature and inlet helium temperature were investigated. The feasibility of the use of ceramic materials in a heat exchanger and some of the factors involved in the design and fabrication of a ceramic exchanger were also studied.

In most of the forms of heat-exchange apparatus based on forced convection the velocity of the fluid is maintained at a sufficiently high level to assure a turbulent flow. In this investigation, however, it was not possible to attain turbulent flow because of the low density of helium at atmospheric pressure and the increasing viscosities of gases with temperature. The pressure could not be increased above atmospheric as it was necessary to hold the helium loss from the system within practical limits. Consequently, this investigation was conducted in the lower laminar flow region at atmospheric pressure.

*Present address, Glen L. Martin Co., Baltimore, Md.

Complete mathematical solution is known for only a relatively few cases of heat transfer. Since this problem involves so many variables, a mathematical expression for the transfer of heat through the fluid film is usually developed by the method of dimensional analysis. Attempts to solve the Fourier-Poisson equation have met with little success, mainly because of the hydrodynamic problem that must be solved simultaneously. The completed solutions of the Fourier-Poisson equation depend on convenient assumptions concerning the motion of the fluid.

Drew (6) eliminates most of the proposed solutions and lists only three for the case of a jacketed tube or pipe, i.e. those of Graetz, Leveque and Russell. Several investigators (4, 7, 16) evaluated Graetz' results for the conduction of heat in fluids moving in laminar flow. Other equations (5, 13, 14, 18) derived for the calculation of the Nusselt number from the velocity distribution vary in form due to the various assumptions used in deriving them.

For laminar flow, McAdams (15, 19) recommends an empirical expression for calculating the inside-film heat-transfer coefficient:

$$\left(\frac{h}{Cv\phi}\right)\left(\frac{C\mu}{k}\right)^{2/3}\left(\frac{\mu_w}{\mu}\right)^{0.14} = 1.86\left(\frac{D}{L}\right)^{1/3}\left(\frac{Dvc}{\mu}\right)^{-2/3} \quad (1)$$

This relationship applies for Reynolds numbers below 2100, but it would give incorrect heat-transfer coefficients for very low "Re" numbers.

Theoretical formulas, such as those of Graetz, for heat transfer to fluids in viscous flow in tubes, do not take into consideration the effects of the radial temperature gradient on the axial and radial components of velocity. Because of the temperature coefficient of viscosity, a radial viscosity gradient results that affects the distribution of velocities considerably compared to that prevailing in isothermal flow. This presents a problem of deciding where, and at what temperature, the physical properties of the fluid should be evaluated. Colburn (4) obtained good correlation of data on heat transfer by employing film properties, but had to supplement his correlation by introducing a viscosity correction ratio.

Sieder and Tate (19) simplified calculations by basing their correlations on main stream properties. To express the interaction of the viscosity gradient on the velocity distribution, they included in the usual correlation of dimensionless numbers an additional dimensionless group, μ_a/μ_w , i.e., the ratio of the viscosity at the average helium temperature to that at the wall temperature.

The correlations heretofore discussed were made at relatively low temperatures; only limited data exists for heat transfer at higher temperatures. Zellnik and Churchill (20) obtained data for the transfer of heat from air in turbulent flow inside a tube for temperatures of 480 - 2000°F. and flow rates corresponding to Reynolds numbers from 4500 to 22,500. Others (10) have published some data on heating air inside a tube with wall temperatures up to 2950°F. More recently, Ramey, Henderson and Smith (17) determined heat-transfer coefficients for air flowing in a 2-inch pipe at temperatures of 500 - 1200°F., with gas-to-wall temperature differences of 300 to 1000°F., and Reynolds numbers from 2000 to 20,000. Their results include data on steam over a range of Reynolds numbers from 5000 to 60,000.

However, all these high-temperature heat-transfer studies pertain to turbulent flow. The data pertaining to turbulent flow at high temperatures deviated from those relating to low-temperatures when correlated by the proposed theoretical equations.

Apparatus and Procedure

A schematic diagram of the apparatus used for our study of heat transfer at high temperatures, is shown in Figure 1. Helium was recycled in a closed circuit by

means of a rotary positive-displacement blower. The helium from the pump was passed through a surge tank and heated to the desired temperature in a resistance-type electric furnace. This temperature was measured by a shielded thermocouple placed in a mixing chamber located between the outlet of the furnace and the inlet to the "test-section", i.e., that part of the train in which the tested heat exchanger is inserted. The helium temperature was measured also at the outlet from the test-section before entering the cooler. The helium cooled to room temperature was passed through two parallel-connected calibrated rotameters to measure the rate of flow of the heat transfer medium through the closed circuit. The test-section, shielded thermocouples, and adjoining tubing were thermally insulated. Additional helium to replace that which leaked from the system was supplied through a pressure-regulator. The flow rate of this "make-up" gas was indicated by a calibrated rotameter.

Compressed air was supplied as heat receiving medium to the annulus of the test-exchanger. The wall temperature of the inner tube of the test-exchanger was regulated by changing the rate of flow of the air through the annular space. High tube-wall temperatures were obtained by preheating this air in a commercial electric resistance furnace. The direction of flow of gases in the exchanger could be altered from concurrent to countercurrent, or vice-versa, simply by switching the inlet and outlet valves for the air or any other cooling fluid used as heat absorbers. The temperature of the cooling air was measured at the inlet and outlet of the heat exchanger; its flow-rate was measured by a calibrated rotameter.

A test-exchanger made of vitreous alumina, with a length-to-diameter ratio of 60, was used (Figure 2). The vitreous alumina inner tubing was surrounded by a larger diameter tube of the same material, and the cooling air was passed through the annular jacket thus formed. Tube wall temperatures were measured by means of (Pt)-(Pt+10 percent Rh) thermocouples located at ten different points along the tube length. Each thermocouple was placed in a slot cut halfway through the tube wall and covered over with alumina cement. The thermocouples were connected by means of a selector switch to a potentiometer.

The physical properties of the helium were computed by extrapolation of available published data. The thermal conductivity and viscosity data were taken from the results of work done at the National Bureau of Standards by Hilsenrath and Touloukian (9). The specific heat of helium at constant pressure (l) was taken as 1.24 B.t.u./ $(lb)(^{\circ}F.)$. This value agreed with that calculated from the Prandtl numbers and viscosity and thermal conductivity data of Hilsenrath and Touloukian and was assumed constant, since the specific heat of helium does not vary with temperature.

Experimental Results and their Evaluation

The average temperature of the helium ("hot gas"), T_a , was taken as the average of the inlet, T_1 , and outlet, T_0 , temperatures. Each of these temperatures was measured by a "shielded thermocouple" arrangement through which the hot helium had passed and was thoroughly mixed.

Average inside tube-wall temperatures were determined for various flow rates of helium and cooling air; typical results are illustrated for counterflow of gases in Figure 3, and for parallel flow in Figure 4. The rate of heat transfer (Q), the helium flow rate (V), average wall temperature (t_w), and the helium temperature at the inlet (T_1) are shown as parameters. The curves obtained are typical temperature distribution curves; similar trends were obtained for other conditions of flow and gas temperatures.

The average wall temperatures of the inner tube of the test-exchanger were obtained by measuring the area under curves similar to those in Figures 3 and 4 and dividing it by the length of the heat-transfer area. Thermocouples embedded in the tube wall were assumed to measure the temperature of the inside surface of

the tube. The fact that the calculated temperature gradients through the wall were found to be negligible, less than 3°F., justifies the assumption. The average inside-film heat-transfer coefficient (h_i) was obtained from the experimental data by the relation:

$$h_i = \frac{WC (T_i - T_o)}{A (t_w - T_a)} \quad (2)$$

As pointed out previously, the usual method of correlating experimental data on heat transfer by forced convection is being employed by determining the effects of significant variables on the rate of heat transfer and combining these variables into an empirical equation by means of dimensional analysis. The equation obtained by this method is:

$$\frac{h_i D}{k} = K \left(\frac{DW}{\mu} \right)^m \left(\frac{C\mu}{k} \right)^n \left(\frac{L}{D} \right)^p \quad (3)$$

where K is a constant and m , n and p are exponential constants. McAdams (15) suggested a simpler form of this equation, derived by assuming that m , n and p are equal:

$$\frac{h_i D}{k} = K \left(\frac{L}{\pi} \frac{WC}{kL} \right)^a \quad (4)$$

The experimental data obtained in this investigation were correlated by use of both types of equations. However, Equation (3) gave a better representation of the data from our ceramic heat exchanger for the L/D ratios employed. To establish a more general equation valid for any L/D ratio, additional investigation is necessary to cover a wider range of experimental conditions.

The experimental data obtained were first correlated in terms of Equation (4). For this purpose, the viscosity and thermal conductivity data used had been computed for the average gas temperature.

Data obtained by use of helium cooled by air in a vitreous-alumina heat exchanger, having a length-diameter ratio of 60, are presented in Figure 5. The data shown refer to inlet-gas temperatures of 1450 - 2665°F. and Graetz numbers of 0.03 - 5. A group of three parallel straight lines, each for a different condition of cooling-air flow, has been obtained. The plot shows conclusively that either by reducing the velocity of the cooling air or by heating it, the trend-lines shifted in position, and a different value was obtained for the constant, K . That is to say, there is a difference in Nusselt number for any selected value of Graetz number. Since varying the velocity or increasing the inlet temperature of cooling air had the effect of varying the tube-wall temperature, it seemed obvious that a satisfactory correlation would require inclusion of the surface temperature, or of properties that are dependent upon the latter.

When the average temperature is used for the evaluation of heat transfer properties, no allowance is being made for the variation of these properties over the cross section of the flowing fluid. However, these variations influence the heat exchange within the fluid. The Seider and Tate viscosity correction takes into account variations of viscosity, but ignores the other properties. The use of a gas-to-wall temperature ratio, on the other hand, corrects for variations in the velocity profile with temperature. But, as these velocity variations are caused by changing physical properties due to temperature changes, the T_a/t_w ratio actually corrects for all changes in the physical properties with temperature. Therefore, application of the temperature-ratio corrections would be expected to result in a better correlation. Consequently, the $\frac{L}{\pi} \frac{WC}{kL}$ group was supplemented by

addition of the T_a/t_w ratio. The final form of Equation (4) thus became:

$$\frac{h_1 D}{k} = K \left(\frac{4}{\pi} \frac{WC}{kL} \right)^a \left(\frac{T_a}{t_w} \right)^b \quad (5)$$

where: $h_1 D/k$ is the Nusselt number (Nu), and WC/kL is the Graetz number (Gz).

Several runs were made holding the Graetz number constant in order to determine the extent of the dependence of Nusselt number on the temperature ratio. The results of these tests are shown in Figure 6. The average value of the exponent b, obtained by taking the slope of these curves, was found to be -0.9 for values of T_a/t_w less than approximately 3. It can be seen from Figure 6 that any further increase in the gas-to-surface temperature ratio above 3 has practically no effect on the Nusselt number.

In laminar flow, when a fluid flows isothermally the velocity profile is assumed to be parabolic, with a maximum velocity at the center axis of the pipe or tube, and zero velocity at the wall. The flow may be thought of as concentric cylindrical elements of fluid moving relative to each other with little or no mixing of the layers. If the hot stream of gas is being cooled, as in this investigation, the viscosity of the gas near the wall is lower than that of the main stream of the fluid; consequently, the fluid near the wall travels at a higher velocity than normally when the wall is not cooled. For this to happen, some of the gas from the center of the tube must flow toward the wall to maintain the increased velocity at the tube-wall. Thus, the cooling of the fluid causes a radial component of velocity that modifies the nature of the laminar flow.

Since in cooling the gas the parabolic distribution of velocity is distorted, correction should be applied. As the difference in gas and wall temperatures increases, T_a/t_w increases, it is expected that the velocity profile would tend to approximate that of a well-mixed fluid, and the properties would not vary appreciably across a section of the tube. Further increase in T_a/t_w would not be expected to change the velocity profile appreciably; the properties of the fluid would remain essentially the same across the tube section and no correction would be needed.

For values of T_a/t_w less than 3, Equation (5) can be written as:

$$\frac{h_1 D}{k} = K \left(\frac{4}{\pi} \frac{WC}{kL} \right)^a \left(\frac{T_a}{t_w} \right)^{-0.9} \quad (6)$$

This equation was rearranged into a more useful form for plotting:

$$\log \left[\frac{h_1 D}{k} \left(\frac{T_a}{t_w} \right)^{0.9} \right] = a \log \left(\frac{4}{\pi} \frac{WC}{kL} \right) + \log K \quad (7)$$

The value of constant "a" was found to be 0.86 from a plot of this equation, Figure 7, by measuring the slope of the trend-curve (a straight line) obtained by the best free fit. From the same plot, for the value of "K" 1.10 was obtained as the intercept on the ordinate at unity on the abscissa. The plotted data have been corrected for differences between the gas and wall temperatures.

Substituting the values of K, a and b into Equation (5), the following equation:

$$\frac{h_1 D}{k} = 1.10 \left(\frac{4}{\pi} \frac{WC}{kL} \right)^{0.86} \left(\frac{T_a}{t_w} \right)^{-0.9} \quad (8)$$

was obtained for values of T_a/t_w less than 3.

For values of T_a/t_w greater than 3, a plot of the experimental data based on Equation (4) gave a similar straight line (Figure 8). No correction has been applied in this plot for differences between the gas and wall temperatures for the reasons already discussed.

A better correlation of the experimental data was obtained by Equation (3) which contains the dimensionless groups associated with turbulent flow:

$$\frac{h_1 D}{k} = K \left(\frac{D V \rho}{\mu} \right)^m \left(\frac{C \mu}{k} \right)^n \left(\frac{L}{D} \right)^p \quad (3)$$

where $h_1 D/k$ is the Nusselt number (Nu), $D V \rho / \mu$ is the Reynolds number (Re), and $C \mu / k$ is the Prandtl number (Pr). However, the number of length-diameter ratios (L/D) investigated was insufficient to determine their effect on the Nusselt number; therefore, the correlations presented here are applicable only to the values of L/D investigated.

In Figure 9 the heat-transfer coefficients are correlated with other pertinent variables in terms of the Reynolds (Re), Prandtl (Pr), and Nusselt (Nu) numbers. Namely, the ratio of the Nusselt number to the cube root of the Prandtl number ($Nu Pr^{-1/3}$) was plotted against the Reynolds number (Re). Two parallel straight lines, one for a lower and one for a higher flow-rate of cooling-air, have been obtained. For computing the numerical values of these dimensionless groups for plotting, the values of viscosity, thermal conductivity, specific heat and other physical properties of the helium have been estimated at the average stream temperatures.

If corrections are incorporated for differences in helium-stream and wall temperatures, the curve in Figure 10 is obtained for values of T_a/t_w less than 3. The slope of this trend line is 0.86 and the intercept on the ordinate at $Re = 1$ is 0.028. Thus, Figure 10 represents a plot of the following equation:

$$\frac{h_1 D}{k} \left(\frac{T_a}{t_w} \right)^{0.9} \left(\frac{C \mu}{k} \right)^{-1/3} = 0.028 \left(\frac{D V \rho}{\mu} \right)^{0.86} \quad (9)$$

Transposing, Equation (10) is obtained, which adequately represents the experimental data:

$$\frac{h_1 D}{k} = 0.028 \left(\frac{D V \rho}{\mu} \right)^{0.86} \left(\frac{C \mu}{k} \right)^{1/3} \left(\frac{T_a}{t_w} \right)^{-0.9} \quad (10)$$

for values of T_a/t_w less than 3.

The heat-transfer data obtained in this work is of limited scope due to the low helium flow-rates used. The heat-transfer curves should not be extrapolated beyond the range of values plotted, as a change in the slope of the curve for Graetz numbers above 5 has been indicated in our investigations.

The gas-to-wall temperature ratio was used as a correction factor instead of the viscosity ratio correction of Sieder and Tate (19). Consequently, the gas-wall temperature correction would not be applicable to a gas whose physical properties are affected by temperature differently than those of helium. Likewise, the point at which the temperature ratio ceases to influence the heat-transfer curve would be expected to be different for other gases.

Free convection effects were neglected in this investigation since the tubes used were horizontal and were of relatively small diameters. In larger tubes, free convection would be expected to influence the heat transfer as long as laminar flow was maintained.

In view of the low flow-rates, it was assumed that end effects were negligible and that laminar flow was maintained within the test section.

Problems in the Design of Ceramic Heat Exchangers

The difficulties encountered in the design and construction of our experimental vitreous alumina exchanger indicate that several construction problems remain to be solved before a ceramic heat exchanger could be produced commercially. The greatest of these problems is that of making and maintaining several gastight seals, some of which must withstand temperatures exceeding 2500°F.

These seals must be made with some type of cementing material, which when dried and fired will have a coefficient of expansion similar to that of the materials joined. As much of the piping and auxiliary apparatus used with the exchanger is metallic, it is necessary to join materials with greatly different coefficients of expansion. No satisfactory solution to this problem has yet been found.

In our experimental work the most effective joints, both ceramic-to-ceramic and ceramic-to-metal, were obtained by using a mixture of 60-70% fine grain (ball-milled for 16 hours) pure alumina plus 30-40% commercial sodium silicate solution. After the cement had air-dried, the joints were fired at temperatures above 2200°F. Several successive coatings of this cement were applied, and the drying-firing process was repeated. However, joints of this type have not always been satisfactory.

After approximately 1000 hours of operation, our experimental alumina heat exchanger was removed from the test circuit to test the seals for gas leaks. While some of the joints were found to be gastight at low pressures (5 p.s.i.g.) others were not. Also, after an extended period of operation at high temperatures, the alumina cement had a tendency to peel off the metal in case of metal-to-ceramic joints.

The difficulty of constructing effective ceramic seals was also realized under actual operating conditions. In all tests enough helium was supplied to the cycling system to maintain a slightly positive pressure in the test loop. With higher pressure drops, caused by attempts to increase the helium flow rates in the system, it became necessary to increase the helium makeup to maintain the pressure. The makeup rate (helium loss) eventually became so great that it was no longer practical to continue to increase the gas cycling rate. Thus, pressure drops above 16-inch w.g. could not be tolerated. At very low flow-rates, on the other hand, experiments have been continued for several days without adding any helium as makeup.

In addition, definite precautions had to be taken to prevent failure of the tubes from thermal shocks. Although, vitreous alumina has remarkably high resistance to thermal shocks compared to most ceramic materials, elaborate precautions had to be taken to avoid fracture from thermal stresses. Care was taken during heating and cooling periods to avoid large thermal gradients likely to cause tube failure.

Efforts have been made recently by several investigators (1) to predict the ability of basic components of ceramic materials to withstand thermal stresses encountered in service. Of particular interest in the investigations of Baroody and associates (2) was the high resistance to thermal fracture exhibited by thin-walled tubes such as might be used in ceramic heat exchangers.

Another problem in the design of ceramic exchangers is that of expansion. Any type of expansion joint adds to the task of maintaining a leak-proof cycling system. When providing for expansion, it should be desirable to keep the components of the exchanger in a state of compression rather than tension, as ceramics are relatively weak in tension. No special precautions were necessary for the expansion of the exchanger parts in this investigation since the outer tube was large compared to the inner tube, and the stresses encountered were considered safely below the limit.

Conclusions

Correlations for the prediction of the average inside-film coefficients of heat-transfer for the removal of heat from gases in the lower region of laminar flow, with high temperature differences prevailing, must include a correction for the variation of fluid properties up to a certain value of gas-to-wall temperature ratio. Beyond this point, any increase in this temperature ratio ceases to influence the heat transfer relationship.

Within the limits of this investigation, and for gas-to-surface temperature ratios less than 3, the experimental data for helium may be represented by the equation:

$$Nu = 0.028 (Re)^{0.86} (Pr)^{1/3} \left(\frac{T_a}{T_w} \right)^{-0.9}$$

or:

$$Nu = 1.10 \left(\frac{1}{\pi} Gz \right)^{0.86} \left(\frac{T_a}{t_w} \right)^{-0.9}$$

Ceramic heat exchangers appear to hold much promise for use in temperature ranges above those generally encountered in conventional exchangers. However, no progress is in sight in their design and construction until methods are developed to construct mechanically reliable gastight seals, and means are found to prevent high thermal stresses. Both of these problems would arise in a commercial size heat exchanger of this type under operating conditions. Ceramic heat exchangers are also limited at present to low pressures that makes their use with a light, gaseous heat-transfer medium, such as helium, impractical.

Acknowledgment

The work described was carried out as part of the A.E.C. - Bureau of Mines process-heat reactor program for the utilization of nuclear energy for coal gasification. The authors are indebted to the Atomic Energy Commission for partial support of the research conducted.

Thanks are due L. L. Hirst and R. F. Stewart for helpful suggestions made at various times during the course of the work, and to H. G. Lucas for assistance in the experimental work.

Nomenclature

A = heat transfer surface, ft.²
C = specific heat at constant pressure, B.t.u./(lb.)(°F.)
D = inside diameter of tube or pipe, ft.
h = film heat-transfer coefficient, B.t.u./(hr.)(ft.²)(°F.)
k = thermal conductivity, B.t.u./(hr.)(ft.²)(°F./ft.)
L = length, ft.
Q = heat flow, B.t.u./hr.
R = resistance to heat flow, (hr.)(ft.²)(°F.)/B.t.u.
T_i = temperature of helium at inlet, °F.
T_o = temperature of helium at outlet, °F.
T_a = average helium temperature, °F.
t_i = temperature of cooling gas at inlet, °F.
t_o = temperature of cooling gas at outlet, °F.
t₁, t₂, t₃ = wall temperatures at selected points along the tube length, °F.
t_w = average wall temperature, °F.
V = velocity, ft./hr.; or total volume, ft.³
v = specific volume, ft.³/lb.
W = weight flow rate of helium, lb./hr.
μ = viscosity, lb./(ft.)(hr.)
ρ = density, lb./ft.³
x = distance, ft.
a, m, n, p, b = constants

Dimensionless Numbers

WC/kL = Graetz number (Gz)
hD/k = Nusselt number (Nu)
C_pμ/k = Prandtl number (Pr)
DG/μ = Reynolds number (Re)

Subscripts

- i = inside of pipe or tube
- o = outside of pipe or tube
- f = film
- a = hot gas
- w = wall
- m = mean value

Literature Cited

- (1) Baroody, E. M., Duckworth, W. H., Simons, E. M., Schofield, H. Z., "Effect of Shape and Material on the Thermal Rupture of Ceramics", U. S. Atomic Energy Comm., Nat'l Sci. Foundation, AECD - 3486, 5-57 (1951).
- (2) Baroody, E. M., Simons, E. M., Duckworth, W. H., "Effect of Shape on Thermal Fracture", J. Am. Ceramic Soc., 38, (1955).
- (3) Browning, S. C., Masters Thesis, West Virginia University, Morgantown, W. Va., 1959.
- (4) Colburn, A. P., "Method of Correlating Forced Convection Heat Transfer Data and a Comparison with Fluid Friction", AIChE Trans., 29, 174 (1933).
- (5) Deissler, R. G., "Investigation of Turbulent Flow and Heat Transfer in Smooth Tubes Including the Effects of Variable Properties", ASME Trans., 73, 101 (1951).
- (6) Drew, T. B., "Mathematical Attacks on Forced Convection Problems: A Review", AIChE Trans., 26, 26 (1931).
- (7) Drew, T. B., Hogan, J. J., McAdams, W. H., "Heat Transfer in Streamline Flow", Trans. AIChE, 26, 32 (1931).
- (8) Groeber, H., Erk, S., Grigull, U., Die Grundgesetz der Wärmeübertragung, Springer Verlag, Berlin, Germany, 3rd ed., 1955.
- (9) Hilsenrath, J., Touloukian, Y. S., "The Viscosity, Thermal Conductivity and Prandtl Number for Air, O₂, N₂, NO, H₂, CO, CO₂, H₂O and A", ASME Trans., 79, 967-985 (1954).
- (10) Humble, L. V., Lowdermilk, W. H., Desmond, L. G., "Measurements of Average Heat-Transfer and Friction Coefficients for Subsonic Flow of Air in Smooth Tubes at High Surface and Fluid Temperatures", NACA Report 1020, (1951).
- (11) Knudsen, J. G., Katz, D. L., "Fluid Mechanics and Heat Transfer", McGraw-Hill, New York, 1958.
- (12) Lee, J. F., Sears, F. W., "Thermodynamics", Addison Wesley, Reading, Mass., 1956.
- (13) Lyon, R. N., "Heat Transfer at High Fluxes in Confined Spaces", Chem. Engr. Progr. 47, 75 (1951).
- (14) Martinelli, R. C., "Heat Transfer to Molten Metals", ASME Trans., 69, 947 (1947).
- (15) McAdams, W. H., "Heat Transmission", McGraw-Hill, New York, 1942.
- (16) Norris, R. H., Streid, D. D., "Laminar-Flow Heat-Transfer Coefficients for Ducts", ASME Trans., 62, 525 (1940).
- (17) Ramey, H. J., Henderson, J. B., Smith, J. M., "Heat-Transfer Coefficients for Gases; Effect of Temperature Level and Radiation", Chem. Eng. Progr. 50, Sym. Ser. No. 9, 21-28, (1954).
- (18) Seban, R. A., Shimazaki, T. T., "Heat Transfer to a Fluid in a Smooth Pipe with Walls at a Constant Temperature", ASME Trans., 73, 803 (1951).
- (19) Sieder, E. N., Tate, C. E., "Heat Transfer and Pressure Drop of Liquids in Tubes", Ind. Eng. Chem., 28, 1429 (1936).
- (20) Zellnik, H. E., Churchill, S. W., "Convective Heat Transfer from High-Temperature Air Inside a Tube", Paper presented at ASME-AIChE Joint Heat Transfer Conference, (Aug. 1957).

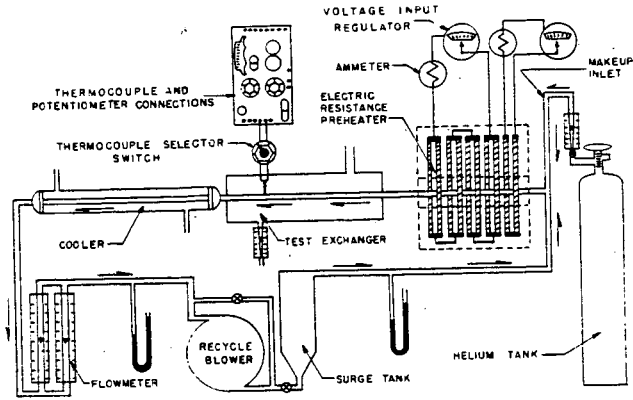


Figure 1. Flow diagram of apparatus for the study of heat transfer at high temperatures

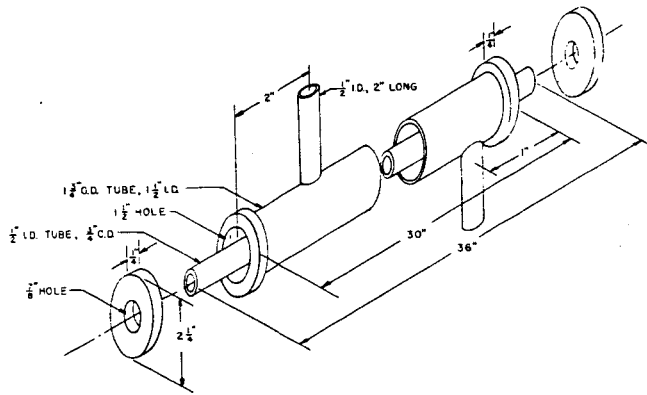


Figure 2. Construction details of vitreous alumina heat exchanger

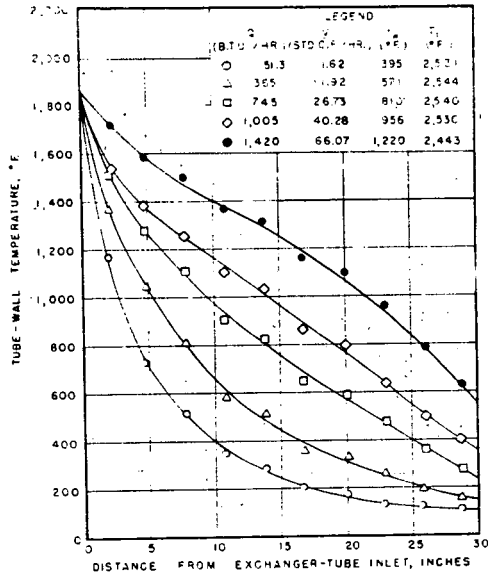


Figure 3. Distribution of tube-wall temperatures, counter flow

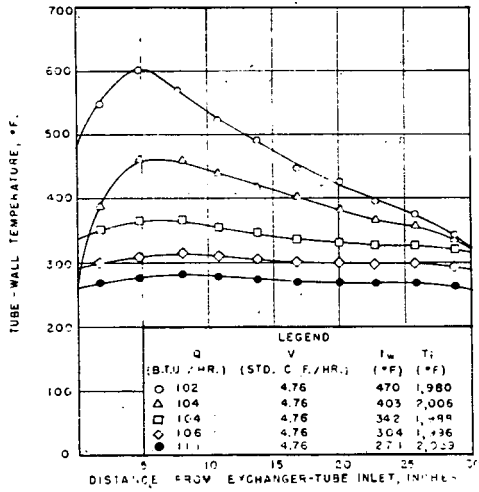


Figure 4. Distribution of tube-wall temperatures, parallel flow.

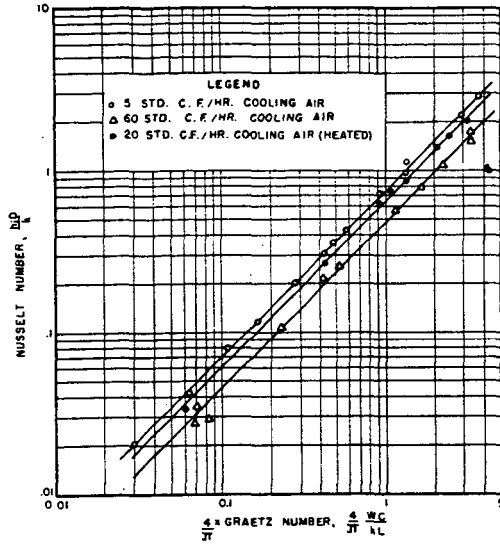


Figure 5. Correlation of heat-transfer data showing effect of cooling-air rate

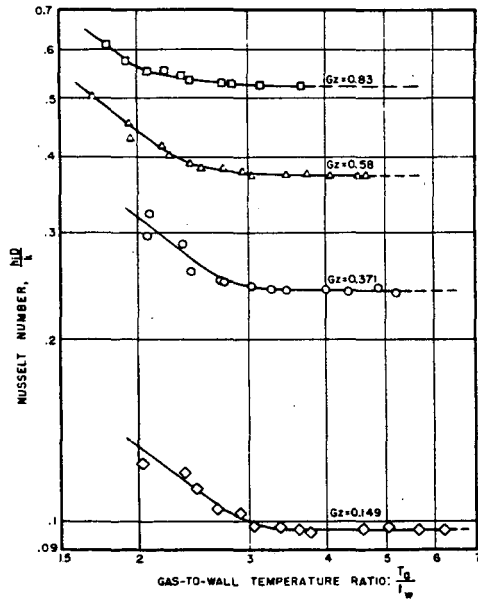


Figure 6. Effect of gas-to-wall temperature ratios on Nusselt number

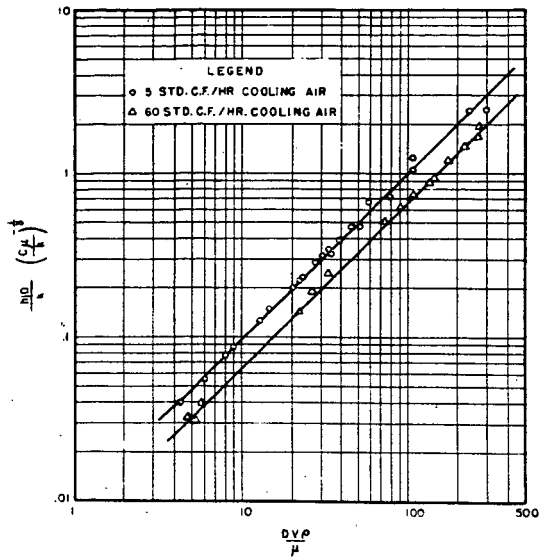


Figure 9. Correlation of heat-transfer data in terms of Reynolds number

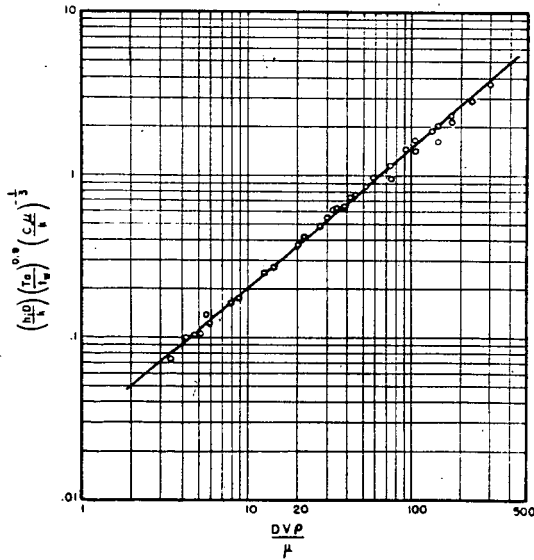


Figure 10. Correlation of heat-transfer data, corrected for temperature ratios, in terms of Reynolds number